A STUDY OF DEGRADATION OF PLATES FOR NICKEL-CADMIUM SPACECRAFT CELLS

FINAL REPORT

JPL CONTRACT NO. 953649

This work was performed for the Jet Propulsion Laboratory, California Institute of Technology, sponsored by the National Aeronautics and Space Administration under Contract NAS 7-100.

TRW
SYSTEMS GROUP

ONE SPACE PARK - REDONDO BEACH, CALIFORNIA 90278

A STUDY OF DEGRADATION OF PLATES FOR NICKEL-CADMIUM SPACECRAFT CELLS

FINAL REPORT

TRW REPORT NO. 24118-6002-RU-00

Prepared by
Dr. Willard R. Scott
Principal Investigator

JUNE 1974

JPL CONTRACT NO. 953649

This work was performed for the Jet Propulsion Laboratory, California Institute of Technology, sponsored by the National Aeronautics and Space Administration under Contract NAS 7-100.

TRW
SYSTEMS GROUP

ONE SPACE PARK - REDONDO BEACH, CALIFORNIA 90278

This report contains information prepared by TRW Systems Group under JPL subcontract. Its content is not necessarily endorsed by the Jet Propulsion Laboratory, California Institute of Technology, or the National Aeronautics and Space Administration.

ABSTRACT

The relative merits of coining and not coining of sintered nickel-oxide and cadmium plates was investigated. A survey of the industry including cell manufactures and users was made and results summarized. Sample plate materials from most commercial cell suppliers were obtained and characterized for properties that may correlate with the tendency toward physical disintegration during handling and over long periods of time in the cell. Special test methods were developed to obtain comparative data in a short time.

A wide range of physical properties and coining thicknesses was observed, resulting in a range of responses. The stronger materials resisted loss of sinter better than weaker materials whether or not coined. Coining improved handling and resistance to electrochemical cycling of weaker materials.

The mechanism of break-down of positive plate edges under cycling appears to be the same as that of thickening and blistering. Brittle, nonadherent sinter, resulting from certain impregnation processes, is the most vulnerable to degradation. It is concluded that the latter type of materials should be coined, but coining of strong materials is optional.

CONTENTS

CONTENTS (Continued)

ILLUSTRATIONS

ILLUSTRATIONS (Continued)

ILLUSTRATIONS (Continued)

ILLUSTRATIONS (Continued)

TABLES

1. INTRODUCTION

1.1 BACKGROUND

The current state of the art of sealed spacecraft nickel-cadmium cell manufacturing and quality control permits cells to be made that are essentially free from many of the defects that plagued earlier cells, such as bent plates and leaky seals. As a result, the ultimate life of currently produced cells is becoming more and more limited only by the life of the electrodes in the cells.

Electrodes can fail by a variety of mechanisms ranging from shorting due to a blister or piece of detatched sinter, to gradual "fading" due to inactivation of originally active material. These processes are subtle and the underlying causes are poorly understood. Furthermore, the processes are slow and the effects are not detectable early in life by presently used screening tests. The study reported here is directed at providing better understanding and methods of control of plate performance.

1.2 SCOPE AND OBJECTIVES

This study is broadly concerned with all forms of plate degradation that may result in degradation of cell performance. However, emphasis was placed on the more obvious forms involving relatively gross changes in and/or disintegration of the sinter structure. Attention was focussed on coining and related edge treatments for controlling the edges of sintered plates.

The study was designed to identify and evaluate the potential problems of edge effects and related mechanical aspects of plates, and to define directions towards solutions, but not to perform in-depth studies in any one area. The work will investigate mechanical and electrochemical modes of degradation of plates, including a determination of the relative merits of coining versus no coining or other methods of treatment of the edges of plates for nickel-cadmium cells, in order to recommend improvements in manufacturing methods leading to increasing cell reliability for long life applications.

1.3 SUMMARY STATEMENT OF WORK

The following task statements summarize the work performed under this subcontract:

- Gather and summarize the present state of the art of plate edge finishing in terms of methods used by cell manufacturers and experience with plates both in handling and under electrical operating conditions.

- Examine possible edge finishing methods other than those currently in use, indicating their potential relative advantages, why they are not being used, and the possible impact of implementation.

- Obtain plate materials, including unimpregnated sintered plaque (when available), and plates made to existing manufacturers specifications, from a number of commercial suppliers of sealed cells. Determine relevant physical and chemical properties of these materials.

- Determine susceptibility of the edges of the plates to mechanical damage from processing and handling.

- Perform vibration testing of plates in simulated and laboratory cell configurations, and evaluate edge damage and potential shorting problems under spacecraft qualification test environment conditions.

- Evaluate accelerated methods for electrochemical testing of plates and select a method for rapid comparative testing of plates. Perform accelerated electrochemical testing on plates with different edge treatments. Correlate results with physical and chemical properties.

- Using the results from tasks above and other available information, examine the mechanism of disruption of the sinter structure and of the development of plate-to-plate shorts resulting from the breakdown of the sinter structure.

- Investigate electrochemical degradation of the plates under normal cycle conditions by performance of electrical testing of reusable cells; inspection and chemical and physical analyses of plates from these cells; and analysis of data to correlate results of materials analysis with electrical performance.

1.4 PARTICIPATING ORGANIZATIONS

Early in the program a number of U.S. cell manufacturers potentially capable of producing hermetically sealed cells were contacted to see if they wished to participate in this work by supplying sample materials and exchanging information. Of those contacted, the following indicated they were willing to participate:

- General Electric, Battery Products Section
- Gulton Battery Company
- Heliotek Division of Textron
- Marathon Battery Company
- Tyco Laboratories

Plate materials were received and tested from each of the above companies. These materials are tabulated in Section 4.2, Table 1.

2. INTRODUCTION TO PLATEMAKING TECHNOLOGY

A brief survey of certain aspects of platemaking technology is presented in this section to provide a basis for the discussion of plate processing and degradation modes to follow.

2.1 GLOSSARY OF TERMS

Certain terms unique to the area of battery cell technology are defined here as they will be used in this report.

- Sintered Plaque

  Sintered plaque, herein referred to simply as "plaque," is the form of sintered nickel type plates just after sintering and prior to impregnation.

- Impregnation

  Impregnation is the process of depositing electrochemically active materials in the pores of the plaque.

- Plate

  The term "plate" will be used to refer to impregnated plates, and usually those that have been subjected to several formation cycles. The term "plate materials," however, may include both plaque and plate.

- Coining

  Coining, as related to battery plates, is the process whereby the thickness of the plaque is reduced in a narrow border around the outside edge of the plate. On sintered-type plates, this process is normally done prior to deposition of active materials in the pores (impregnation).

- Thickness Reduction

  For the purpose of this report thickness reduction is expressed as percent of the uncoined thickness; that is, if $\bar{t}_1$ = average original uncoined thickness, and $\bar{t}_2$ = average thickness in coined areas, then

$$\text{Thickness Reduction (T.R.)} = \frac{100\ (\bar{t}_1 - \bar{t}_2)}{\bar{t}_1} \text{ percent}$$

- Edge Coating

  Edge-coating involves applying a film of material to the border and edges of plates. This film is usually deposited in the form of a solution of a solid in a volatile solvent. This process is also referred to as "cementing" or "doping."

2.2 COINING AND COINING EFFECTS

The function of coining is to compress the sinter structure, thereby making it more dense and reducing or eliminating porosity in coined areas. Increasing the density increases physical strength and rigidity; decreasing porosity reduces the amount of active materials that are deposited in the pores during impregnation and, hence, reduces the electrochemical activity of coined areas. Thus, coining reduces the capacity available from a given total area (and weight) of plate material, hence, reduces the energy density of a cell.

The capacity per unit area of coined areas is not zero, however, because some activity remains near the surface of these areas and at the cut edges. The amount of residual activity depends on the thickness reduction produced. Minimum activity is not achieved until thickness reduction approaches 50 percent.

Since the average width of the coined border is usually constant, and independent of the size of the plate, the percentage of total plate area, and hence capacity, affected by coining increases as cell size (and plate size) decreases. The area percentage is not insignificant, i.e., for an average width of 1.5 mm, which is typical, coined area amounts to 7 percent of total plate area in a 20 Ah cell and 11 percent in a 6 Ah cell. Therefore, there is a trade-off between the potential benefits of coining and the energy density obtained from a cell. This study should provide information with which cell users and suppliers may make design decisions.

The origin of coining of sintered plates is obscure. Some say that coining was done originally to control the cut ends of wires in screen grid plates. Others suggest that coining first was done to provide a thinner, more solid area to which a tab could be welded to plates cut from the

interior of the master plaque. The latter may explain why Falk and Salkind[1] state that "There is no need for coining plaques . . . provided with perforated steel sheet grids, since the tabs are welded directly to the (uncoated) steel sheet at the edges . . . ."

Currently used production methods for sintered plates for nickel-cadmium and other cells require cutting of plate material at various stages in the processes. When plates are cut, the cut edges do not behave in the same manner as the rest of the plate surface. The edges may be rough, substrate metal becomes exposed, and the sinter structure is weaker and more susceptible to damage than at areas not having an edge. Damage may occur during handling for cell assembly or from the effect of use in a completed cell.

From the cell manufacturers point of view, crumbling edges are a nuisance during handling and any resulting large particles of sinter dislodged may produce shorting of the cell during assembly should they become caught between plates. Inasmuch as the average spacing between positive and negative plates in most spacecraft cells is less than 0.2 mm (0.008 inch), any conductive particle of this dimension or larger, if it penetrates the separator layer, can produce a short and fail the cell.

Recognizing these potential problems, the cell manufacturer may do one or both of two things: coin certain edges, and/or coat one or more edges with plastic cement. Coining compacts the sinter and, when done properly, is capable of reducing crumbling of edges during cell assembly and later under cycling conditions. Coating with cement is done to improve handling during cell manufacturing. Cementing also may prolong the life of cut edges in the cell to some extent.

A review of the cell failure information from ground tests where adequate postmortem analysis has been carried out reveals a low incidence of shorting failures attributable to loose particles. On the other hand, the

[1]S. Falk and A. Salkind, "Alkaline Storage Batteries," John Wiley and Sons, Inc., p. 124.

preponderance of cells tested have had coined and/or edge-coated plates, and in many cases of shorts, the cause of the short was not found. In many cases of shorted cells, the location of shorting has been the area just under the tabs, as indicated by a burned or melted appearance of the separator. A contributing cause of this occurrence may be loosening of inadequately coined sinter material assisted by the flexing of the plates at the base of the tab during cell assembly.

Failed cells removed and torn down from synchronous orbit testing (after 4 or more years of testing at NAD, Crane) have shown blistering and loss of sinter along the tops of the positive plates. As these cells behaved normally when new, the fact of their condition at tear-down indicates that slow, cumulative deterioration of the sinter structure can occur which is a potential failure mechanism.

Recently, certain cell manufacturers have suggested that coining is unnecessary and therefore need not be done. They contend that when the uncoined edges of the plates are properly compressed by the separator layers in a cell, degradation of the uncoined edges will be controlled. No proof of this contention is offered, that is applicable to cells operating several years and longer. On the other hand, positive plates removed by TRW from a variety of cells over a year old that have experienced cycling at a depth of discharge over 60 percent have shown considerable weakening and loss of sinter along uncoined edges. These results suggest that a number of variables are involved that are not presently recognized. To maximize cell reliability for very long term missions these variables need to be identified so that they may be controlled.

3. PRESENT STATE OF THE ART OF PLATE EDGE TREATMENT

3.1 SURVEY APPROACH

A survey was made of both cell manufacturers and users of sealed nickel-cadmium cells to determine the current state of the art of plate edge treatment and experience with edge effects. Personal visits were made to General Electric, Gulton, and Heliotek. The other participating manufacturers and a number of government agencies and industrial users of cells for spacecraft applications were contacted by telephone.

The subject was covered from two points of view: one relating to cell manufacturing per se, and the other relating to cell reliability for long-life applications. The findings of the survey are presented below in a factual manner under these two point of view headings.

3.2 CELL MANUFACTURING ASPECTS

3.2.1 Methods of Coining

Two methods for coining are currently in use: 1) stamping with dies using power press machinery; and 2) pressing one edge at a time, usually on a hand press. The former method coins the entire perimeter in one stroke and is used where plate material is made and impregnated in continuous strip form, and hence, where cutting follows impregnation. Coining of master plaques or individual plate-size plaques is done in a few cases by die-stamping and use of a single-stroke press.

3.2.2 Utility of Coining for Cell Manufacturing

There were considerable differences of opinion from one cell manufacturer to another on the effectiveness and need for coining plates from the point of view of manufacturing. Those making plates with a screen grid said coining was essential, primarily as a means of controlling the sharp ends of the screen wires produced by cutting, as well as to provide a base for welding the tabs, as mentioned above. Those manufacturers making plates with perforated sheet grids and slurry coating were divided. Some felt

that coining was necessary to facilitate platemaking and cell assembly; others felt that coining was not important for manufacturing. Investigation revealed that these differences of opinion were associated with differences in details of processing plate material and/or differences in the design and properties of the materials.

The aspects of the process that may affect the value of coining during cell manufacturing include:

a) Whether or not plates are cut (from master plaques or strip);

b) The amount of thickness reduction produced in coined areas;

c) Whether or not automatic machinery is used for cutting (blanking) plates;

d) Storage and handling practices after cutting and during cell assembly;

e) Whether or not edge-coating is used;

f) The compression, electrolyte concentration, and charge/discharge parameters used during open-cell formation cycling; and

g) Requirements for inspection of plates after formation cycling.

Additional comments of the above points are discussed in the following paragraphs.

Although sintered plaque prior to impregnation is much more ductile than after impregnation, cutting of uncompressed plaque usually results in cracking along the cut edge. This form of cracking is considered by manufacturers as normal and acceptable for further processing.

When cut plaque with such cracks is impregnated the active material absorbed acts as a cement, filling in cracks and binding loose particles together along the edges. This results in fairly strong, relatively smooth edges that handle well during cell assembly (unless cut again after impregnation). However, such edges on positive plates are prone to damage due to electrochemical cycling.

Automatic die-cutting machinery is much less tolerant of weak and/or brittle sinter structure than is hand-cutting. Worn or dirty die cutting edges can turn out large quantities of ragged edges in a short time, thus applying pressure to use such material rather than absorb the cost or schedule impact of making new plate.

Cracked edges can be put into cells without further loosening and/or loss of sintered material if the plates are handled gently at all times and stored without plate-to-plate contact. The imposition of the necessary controls to make this practical would greatly complicate present processing methods, however.

Edge-coating is able to compensate for a certain amount of edge damage. Manufacturers using edge-coating were less concerned with the need for coining than those that did not edge coat. Such coating appears to be only a temporary "fix," however, as discussed below.

Instability of plate edges, primarily on positive plates, is accentuated by the formation cycling process as practiced by most cell manufacturers, in spite of the few cycles involved. Plates that may appear to have flawless edges prior to formation often show swollen and flaking edges afterward. Well coined edges (thickness ratio > 30 percent) appear to show a much lower incidence of such damage.

Many manufacturers trim plates to final size by cutting off longer plates. This cutting therefore must take place across mostly noncoined plate material. Because positive plates are significantly more brittle after formation than before, such trimming to size after formation causes more edge damage than when the trimming is done before formation.

Normal practice for inspection of plates after formation (plus washing and drying) involves a rapid visual inspection by the unaided eye. Most suppliers agree that this method can only detect, reliably, effects and flaws having dimensions of 0.5 mm (0.02 inch) or more, and all felt that, if required, inspection sufficient to detect edge defects down to 0.1 mm (0.005 inch) in size would require magnification, and rejection of plates having defects larger than about 0.1 mm would result in a very low yield under existing practices.

The second area of variables that appears to be responsible for differences in attitude toward coining among suppliers includes the design and properties of the plate materials per se. Those aspects that appear to have the largest effect include:

a) Strength of the sinter, both before and after impregnation.

b) Strength of adhesion of sinter to the grid.

c) Level of loading of active material in the impregnated plate, i.e., the weight of active materials per unit area.

Sinter material, whether or not impregnated, that is strong without being brittle and is strongly adherent to the grid may undergo multiple cracking along edges and elsewhere without loss of particles during plate handling and cell assembly. This is considered desirable by manufacturers, expecially when radiography (X-ray photography) is used to inspect the cell for acceptance.

The higher the loading level, the more problems are seen with damage on lightly coined and uncoined edges of positive plates, primarily after formation cycling. It is believed that the stronger the sinter the less the damage at high depth of discharge.

In summary, from the cell manufacturing point of view, there was no consensus that coining was necessary. However, there was agreement that coining is desirable in that it improves handling qualities and increases the yield of defect-free edges throughout the cell manufacturing process.

3.2.3 Edge Coating

Again, from the point of view of cell manufacturing, there was general agreement that edge-coating improved handling qualities of plates, and hence was desirable. Some suppliers coat only positive plate edges; others coat only cut, uncoined edges but not coined edges. Some suppliers coat edges before formation; others do not coat until after formation. It appeared that coating was done where the particular product and process required it for convenience of manufacturing.

The material used for edge-coating is usually a solution of polystyrene in a volatile organic solvent. This solution is brushed or rolled on, and the result, after drying in air, is a film of polystyrene. One supplier felt that this material left something to be desired in that the deposited film was not flexible enough to do the best job. As a result, when plates with coated edges where cycled in formation, the coating often cracks and becomes loosened, allowing the underlying edge surfaces to become active and disrupted.

3.2.4 Other Edge-Finishing Methods

Manufacturers were asked if they were familiar with or had used any methods of finishing edges of plates other than those now in use. The question was focused on plates rather than plaque, and particularly on the problem of protecting the cut, uncoined edge produced by trimming plates to final size. Mechanical aspects will be presented first, followed by coating aspects.

First, all those asked felt that no further mechanical treatment is necessary if the edge can be coined prior to cutting except possibly smoothing of the edge with a fine file or other abrasive tool. Such smoothing is done by all manufacturers as standard procedure.

For noncoined edges, it was inquired whether sandblasting, shot-peening, or grinding could or had been used to level or round off and possibly strengthen the raw sintered edge. All manufacturers claimed to be unaware of the use of these methods and felt that any treatment of an uncoined edge that did not significantly increase the sinter density and reduce porosity would not be useful. Furthermore, the type of operations suggested were considered to be slow and costly. Some felt that when noncoined edges were coated (with polystyrene), no other treatment was necessary.

Other edge-coating materials and processes were suggested for comment. These included epoxy resin solutions, other thermosetting resin formulations, and dipping in hot melts. Generally, there was little comment on these as alternatives to polystyrene solution, other than an indication that little

or nothing had been done to investigate other materials. One supplier felt that most of these would be too brittle and hence would offer no improvement over polystyrene. This supplier mentioned that certain flexible rubber-based compounds had been used as edge coating in the past, but his company had not investigated the use of formulas other than polystyrene solutions. Other manufacturers appeared to be satisfied with polystyrene and claimed they were not familiar with the properties or relative merits of other coating materials.

3.3 RELIABILITY ASPECTS OF EDGE TREATMENTS

Reliability, as used here, is the probability that a cell will operate properly and deliver a large fraction of its initial power output on discharge throughout its mission. Emphasis is given to missions involving a relatively few number of cycles (less than 1000) and on utilization of energy densities of the order of 10 watt-hours per pound of cell weight for peak discharges. Thus, relatively high maximum depth of discharge is called for.

Information obtained from cell manufacturers on the effect of coining on cell reliability (as defined above) was meager. Manufacturers claimed that they were not aware of any data linking destruction of plate edges with cell failures. One supplier indicated that he had seen edge-coating remain on edges of plates that had experienced many thousands of cycles, but he admitted that the coating was also cracked and/or missing in many areas.

Cell users contacted generally had little data from tear-down analysis followed extended electrical testing, and even less relative to comparing coined with uncoined plate edges under similar conditions. They felt that coined edges are to be preferred. The original version of the NASA Interim Model Specification for High Reliability Nickel-Cadmium Spacecraft Cells (Specification No. S-716-P-23 dated 30 April 1969) called for coining of all plate (Paragraph 2.1.1.1.9), and this appeared to be the basis for the opinion of several users.

NASA Goddard Space Flight Center has found some disruption of positive plates in cells torn down after a number of years of life testing at NAD Crane. For example, plates from a 6 Ah cell which failed on test "Sync 6"

(0°C, 80 percent DOD max) showed blistering near the top edge. The actual cause of this condition and the specific cause of the cell failure have not been established to the knowledge of the writer. The cell was manufactured by General Electric and the plates were coined.

Users were divided in opinions on the efficacy of edge coating for reliability. Some felt that edge coating was desirable during cell assembly but had no knowledge that the coating contributed to cell life. Others felt that such coating was better than nothing to strengthen the edges.

4. CHARACTERIZATION OF PLATE MATERIALS

4.1 APPROACH

Plate materials were characterized by determination of selected physical and chemical properties; by photography under optical magnification and under the Scanning Electron Microscope (SEM); and by certain special tests, as described below.

4.2 PLATE MATERIALS TESTED

The plate materials supplied by participating manufacturers that were characterized and tested in this study are shown in Table 1.

Table 1. Plate Materials Investigated

Manufacturer	Positive Plaque	Positive Plate	Negative Plaque	Negative Plate
General Electric - I	X	X	X	X
General Electric - II	(Note 1)	X	(Note 1)	X
Gulton Battery Co.	X	X	X	X
Gulton - SAFT	(Note 1)	X	(Note 1)	X
Heliotek	X	X (Note 3)	(Note 2)	X (Note 3)
Marathon Battery Co.	X (Note 4)	X	(Note 6)	X
Tyco Laboratories	X (Note 5)	X (Note 3)	(Note 6)	X (Note 3)

Note 1. Not available.
Note 2. Negative plaque same as positive plaque for this manufacturer.
Note 3. Electrochemical precipitation process used for impregnation.
Note 4. Plaque made by dry powder process on nickel screen. All others made by wet slurry process.
Note 5. Nickel screen grid used.
Note 6. Not procured.

"General Electric - I" material was obtained directly from the manufacturer. "General Electric - II" material was furnished by Jet Propulsion Laboratory. Material GE-I was made in 1971 and was a special run having a higher loading than the manufacturers standard material of this type. Material GE-II was made in 1973, presumably to normal specifications. The materials labelled "Gulton - SAFT" are made by SAFT in France and used by Gulton in their standard spacecraft cell line.

Note that two representatives of the electrochemical impregnation process have been included. This was done purposely to obtain comparative data even though this new process is not yet in full-scale production.

All plate was characterized in the as-received condition, i.e., no electrochemical cycling or cleaning was done by TRW prior to the testing reported in this section.

4.3 PHYSICAL PROPERTIES TESTING

The following physical properties were determined for each plate material:

- Thickness
- Bulk Density
- Void Fraction
- Resistivity
- Compressive Strength

The methods used for these determinations are described below.

- Thickness and Bulk Density

  Samples of plate are measured at five points with a micrometer and the average calculated. The dimensions parallel to the plane of the plates are measured and used to calculate the sample area. The sample is weighed and the density calculated as the weight divided by the product of average thickness and area. The results of the physical properties tests are given below.

Thicknesses of both coined and uncoined areas of plate materials, together with the calculated thickness reductions, are shown in Tables 2 and 3. In these tables and henceforth throughout this report code letters are used in lieu of suppliers' names and varieties. This approach is used to facilitate the presentation and discussion of the data.

- Void Fraction

  The interconnected void volume is determined from the weight of water imbibed under vacuum by a sample of plate material. The ratio of void volume to total apparent sample volume, as determined for the density determination, is the void fraction.

Table 2. Positive Plate Materials - Thickness Data

Type	"Positive" Plaque (Note 1)			Positive Plate		
	Uncoined (mm)	Coined (mm)	T.R. (%)	Uncoined (mm)	Coined (mm)	T.R. (%)
A*	--	--	32 (est)	0.85	0.56	34
B	0.72	(Note 2)	--	0.67	(Note 2)	--
C	0.88	0.51	42	0.88	0.46	47
D	0.76	(Note 2)	50 (est)	0.77	0.35	55
E	0.69	0.29	58	0.69	0.26	59
F	0.75	0.29	61	0.71	0.25	65
G	--	--	--	0.69	0.62	10

Note 1. "Positive" Plaque is that plaque is used for making positive plate.
Note 2. Material was uncoined as received.

*This listing (and that in the tables to follow) is not in the same order as that in Table 1.

Table 3. Negative Plate Materials - Thickness Data

Type	"Negative" Plaque (Note 1)			Negative Plate		
	Uncoined (mm)	Coined (mm)	T.R. (%)	Uncoined (mm)	Coined (mm)	T.R. (%)
A	--	--	40 (est)	0.90	0.50	44
B	0.90	(Note 2)	--	0.83	(Note 2)	--
C	0.86	.051	40	0.86	0.43	50
D	(Note 3)	--	--	0.79	0.29	63
E	--	--	--	0.94	0.35	63
F	(Note 3)	--	--	0.85	0.54	37
G	--	--	--	0.81	0.66	18

Note 1. "Negative" Plaque is that plaque used for making negative plate.
Note 2. Material was uncoined as received.
Note 3. Same as "Positive" Plaque, Table 2.

- Resistivity

  A Kelvin Bridge technique is used, involving a four-point contractor with separate current and potential leads. A diagram of the contractor is shown in Figure 1, and a photograph of a prototype device is shown in Figure 2. Regulated direct current at 1 ampere is used for measurement, supplied by a regulated power supply and a 10-ohm 100-watt resistor as a ballast load. Samples are cut to 7 cm (2.75 inch) wide by 10 cm (4 inch) or more long, and the contractor is placed along the centerline. The voltage between the two potential contacts is read and is proportional to resistivity.

- Compressive Strength

  A compression measurement was used as an indication of the strength of the sinter in unimpregnated plaque. This measurement was also made on finished plates, although the interpretation for impregnated material is less certain.

  The measurement was made by placing the material in an Instron Testing Machine equipped with a circular ram having an area of contact with the plate of 0.155 $in.^2$ (1.00 cm^2). The crosshead of the machine was driven at a constant rate while the force applied to the ram and the crosshead displacement were recorded on an X-Y plate. Each run was continued until either a displacement of 0.01 inch was reached or the applied force reached 5000 pounds (pressure = 33,000 psi or 15,000 bars). Inherent crosshead displacement as a function of load was deducted from total displacement to get the sample penetration.

Data for density and void fraction, as defined above, are shown in Table 4 for all materials characterized.

The resistance as measured by the four-point contractor described above are given in Table 5. Assuming that the current flux was uniform throughout the cross-section of the material between the potential contacts, the equivalent resistivities may be calculated from these resistances by use of the relation

$$\rho = 0.137t \cdot r \quad ,$$

where

ρ = resistivity, in milliohm - cm

t = thickness (of uncoined area), in mm (from Tables 2 and 3)

r = resistance, in milliohms (from Tables 2 and 3)

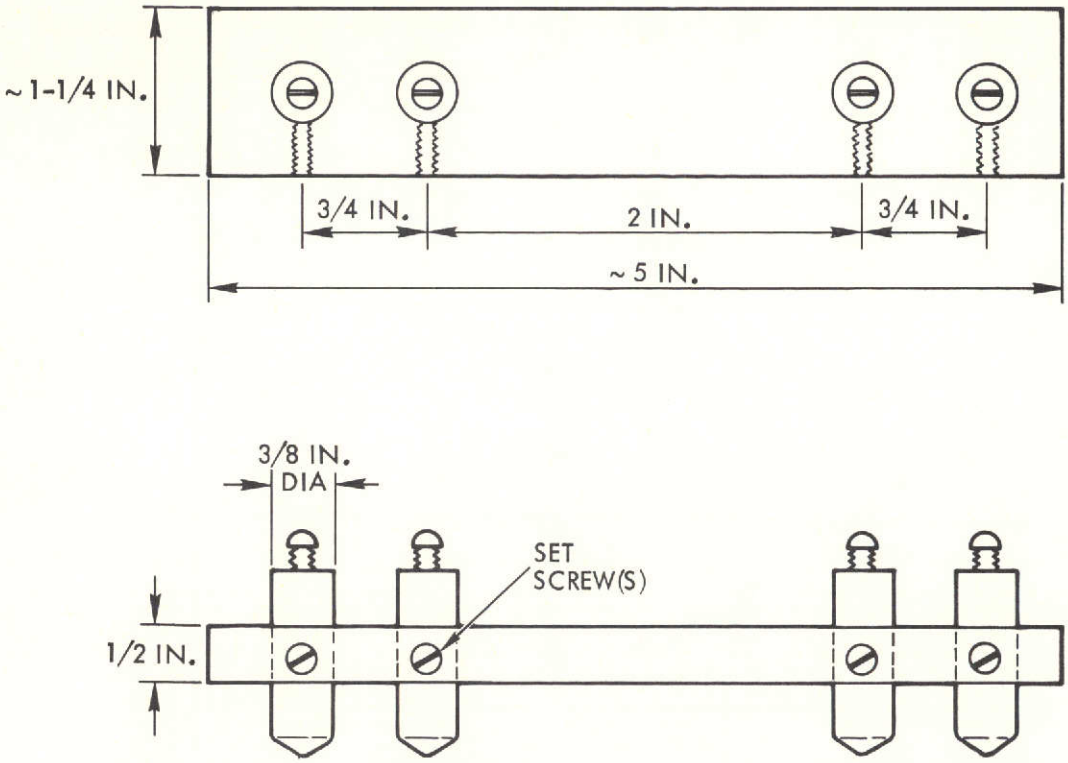

Figure 1. Four Point Contactor dimensions

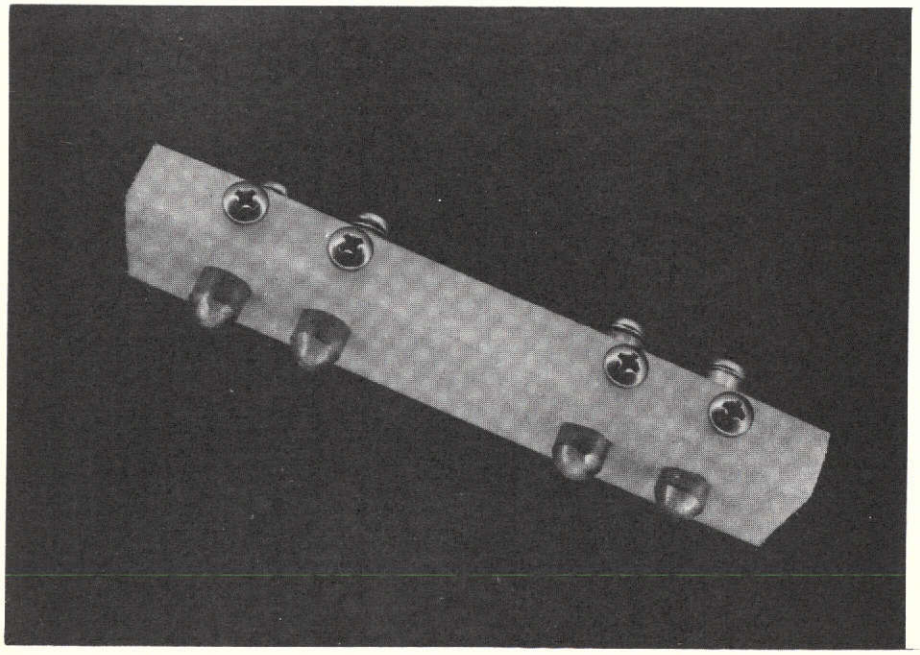

Figure 2. Four Point Contactor
(TRW Photo No. 104826-73)

Table 4. Density and Void Fraction Data for Uncoined Plate Materials

Type	Positive Plaque		Positive Plate		Negative Plaque		Negative Plate	
	Density (g/cm^3)	Void Fraction (%)	Density (g/cm^3)	Void Fraction (%)	Density (g/cm^3)	Void Fraction (%)	Density (g/cm^3)	Void Fraction (%)
A	--	--	3.64	28.8	--	--	3.94	31.6
B	2.11	67.5	3.80	24.2	1.87	73.7	4.00	33.7
C	2.08	73.2	3.55	35.2	--	--	3.88	35.7
D	2.07	67.4	3.25	39.0	(Note 1)	(Note 1)	3.15	51.2
E	1.77	75.1	3.63	27.4	--	--	3.81	30.3
F	1.95	75.0	3.11	39.0	--	--	3.31	45.7
G	--	--	3.78	25.2	--	--	3.97	34.0

Note 1. Same as positive material.

Table 5. Relative Resistances of Plate Materials

Type	"Positive" Plaque (milliohms)	Positive Plate (milliohms)	"Negative" Plaque (milliohms)	Negative Plate (milliohms)
A	--	1.06	--	1.05
B	1.10 - 1.25	1.55 - 1.80	1.34	1.25 - 1.35
C	0.75	1.03	0.75	0.85
D	1.08	1.10	1.10	0.95 - 1.15
E	2.02	2.10	--	1.43
F	2.15	2.20	--	2.40
G	--	1.41-1.75	--	1.21-1.39

Data for compressive strength are presented in the form of force vs. penetration plots, as shown in Figures 3 through 9. The plots show both the plaque and the corresponding plate material made from that plaque, when both were available. The penetration values are considered to be accurate to within 0.0005 inch.

4.4 CHEMICAL ANALYSIS

Positive (nickel oxide) plates were analyzed for nickel active material, and negative (cadmium) plates were analyzed for charged and uncharged cadmium active material. The methods used were essentially those described by Parry* except that the extracts and solutions were analyzed for nickel and cadmium by Atomic Absorption. In most cases five or six samples were analyzed to test for variation. Table 6 shows the maximum, minimum, mean, and sample standard deviation of the samples analyzed.

4.5 PHOTOGRAPHIC CHARACTERIZATION

Overall view photographs of the different plates tested in this study are shown in the as-received condition in Figures 10 through 16. All plates were the same width (2.75 ± 0.15 inches) and varied only in length. The type B plates are cut specially to give extra tab length for use in reusable cells (described below).

*Parry, J.M., "Development of Uniform and Predictable Battery Materials for Nickel-Cadmium Aerospace Cells," Contract No. NAS5-11561, Interim Annual Report, Sept. 1969 - Sept. 1970.

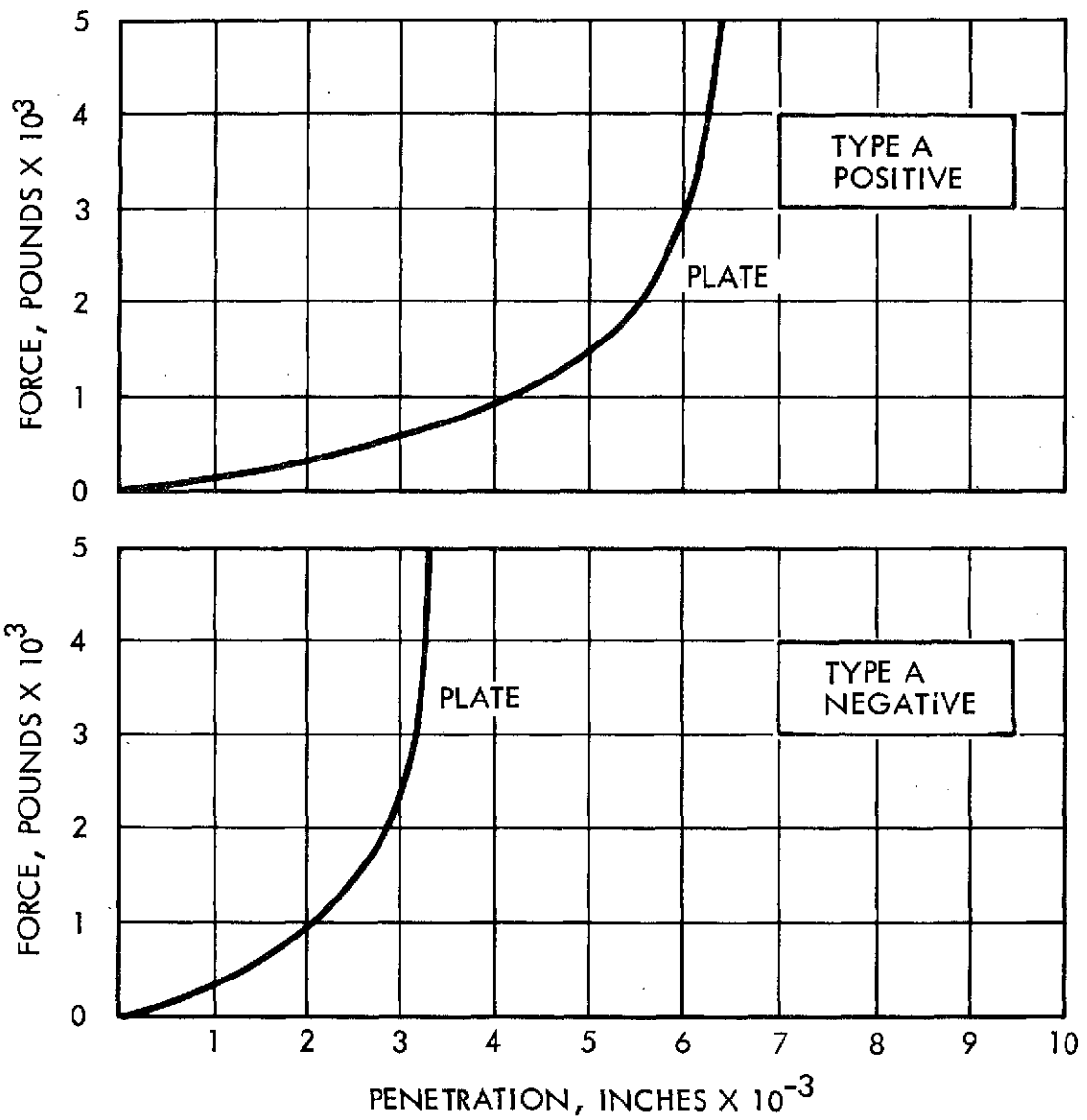

Figure 3. Compressive Strength Curves, Type A Plate

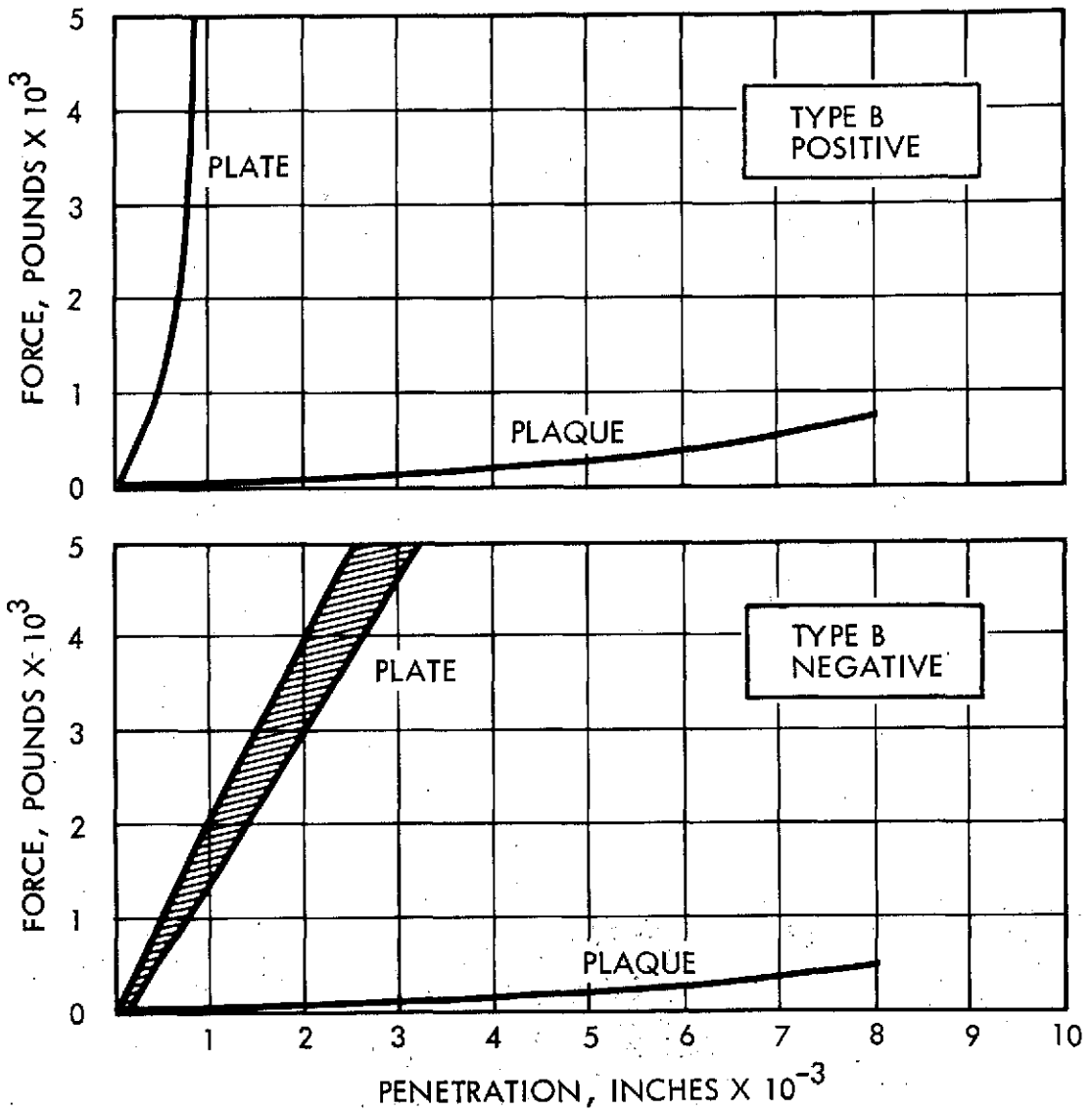

Figure 4. Compressive Strength Curves, Type B Plate

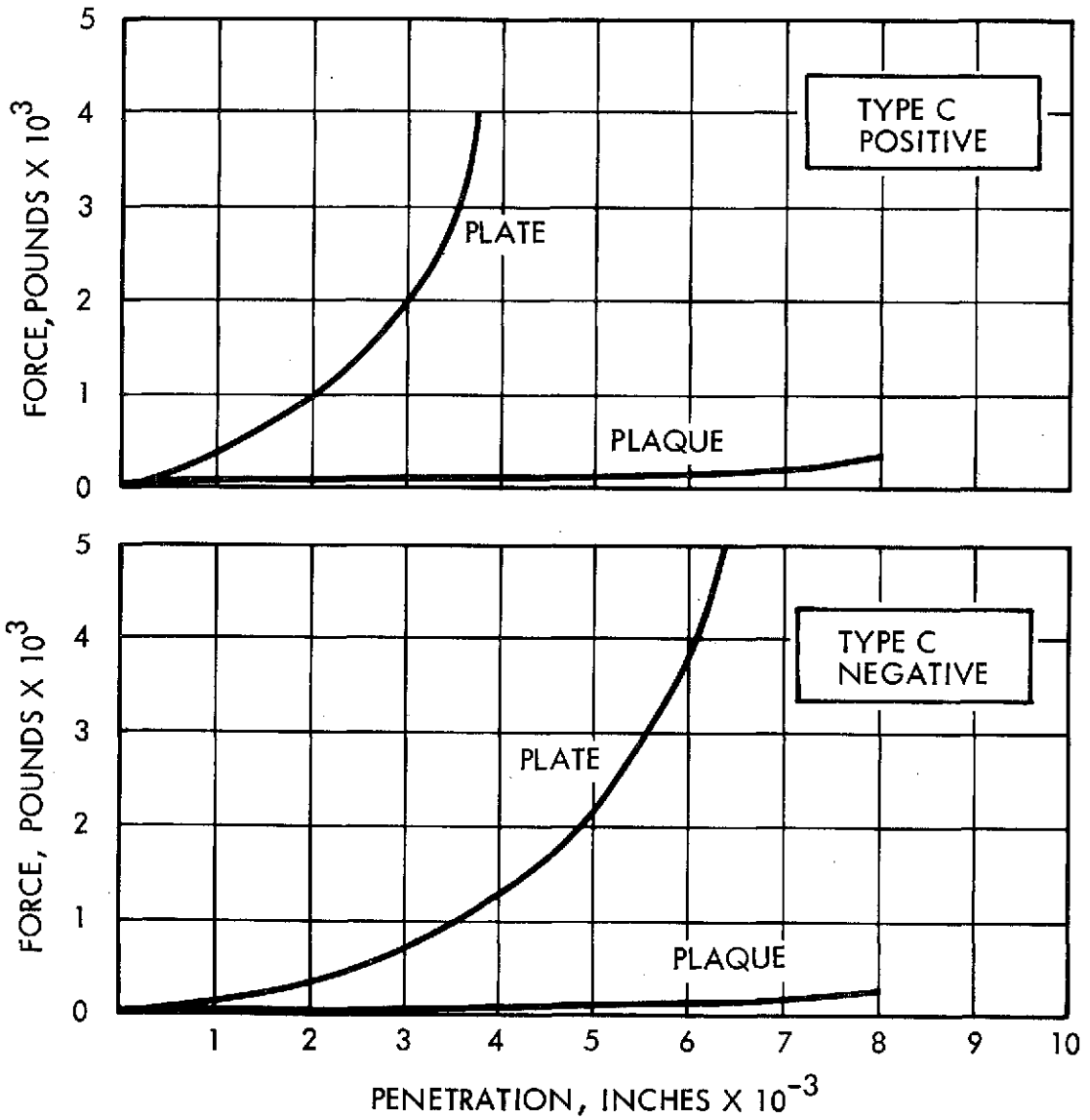

Figure 5. Compressive Strength Curves, Type C Plate

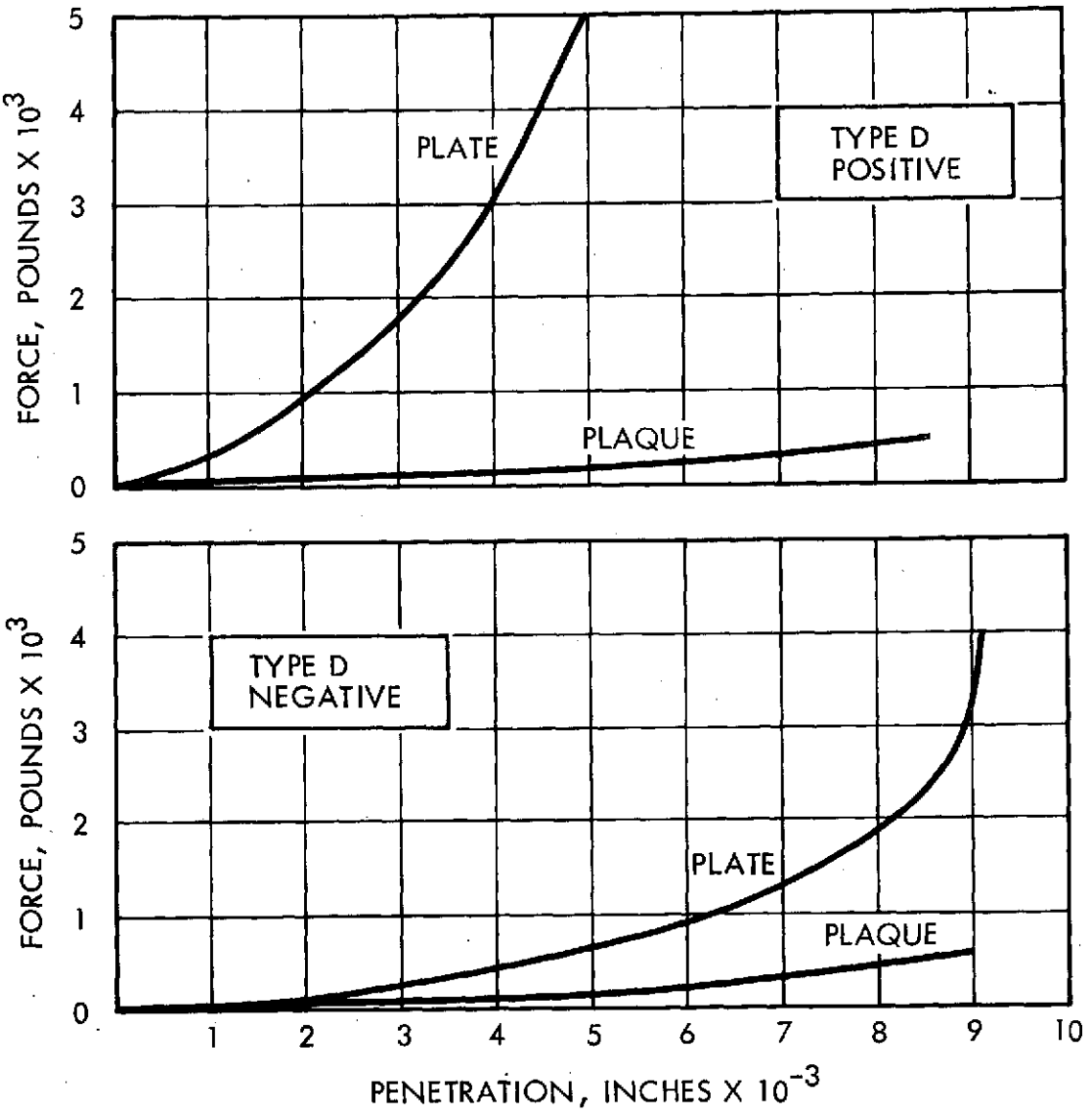

Figure 6. Compressive Strength Curves, Type D Plate

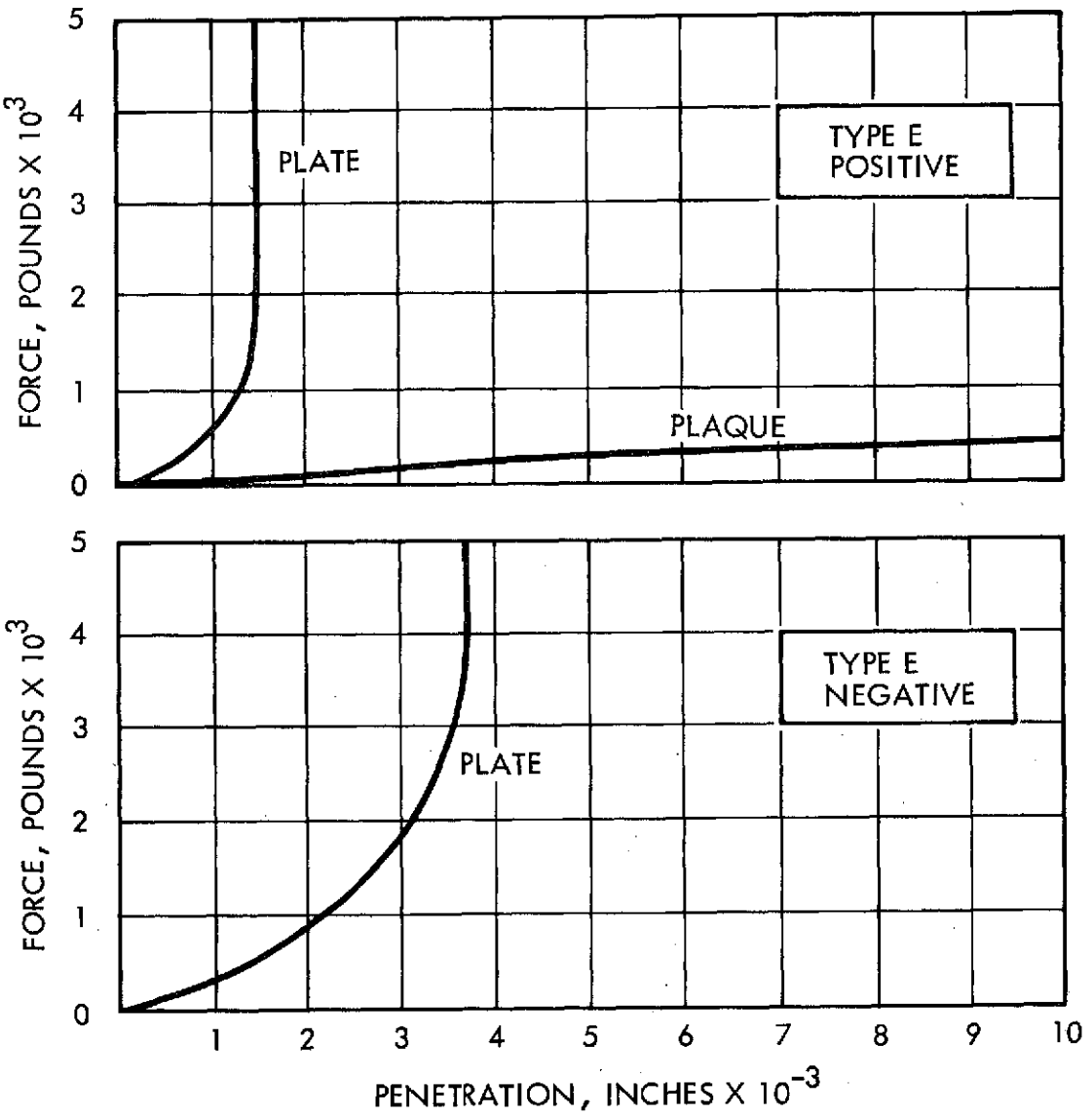

Figure 7. Compressive Strength Curves, Type E Plate

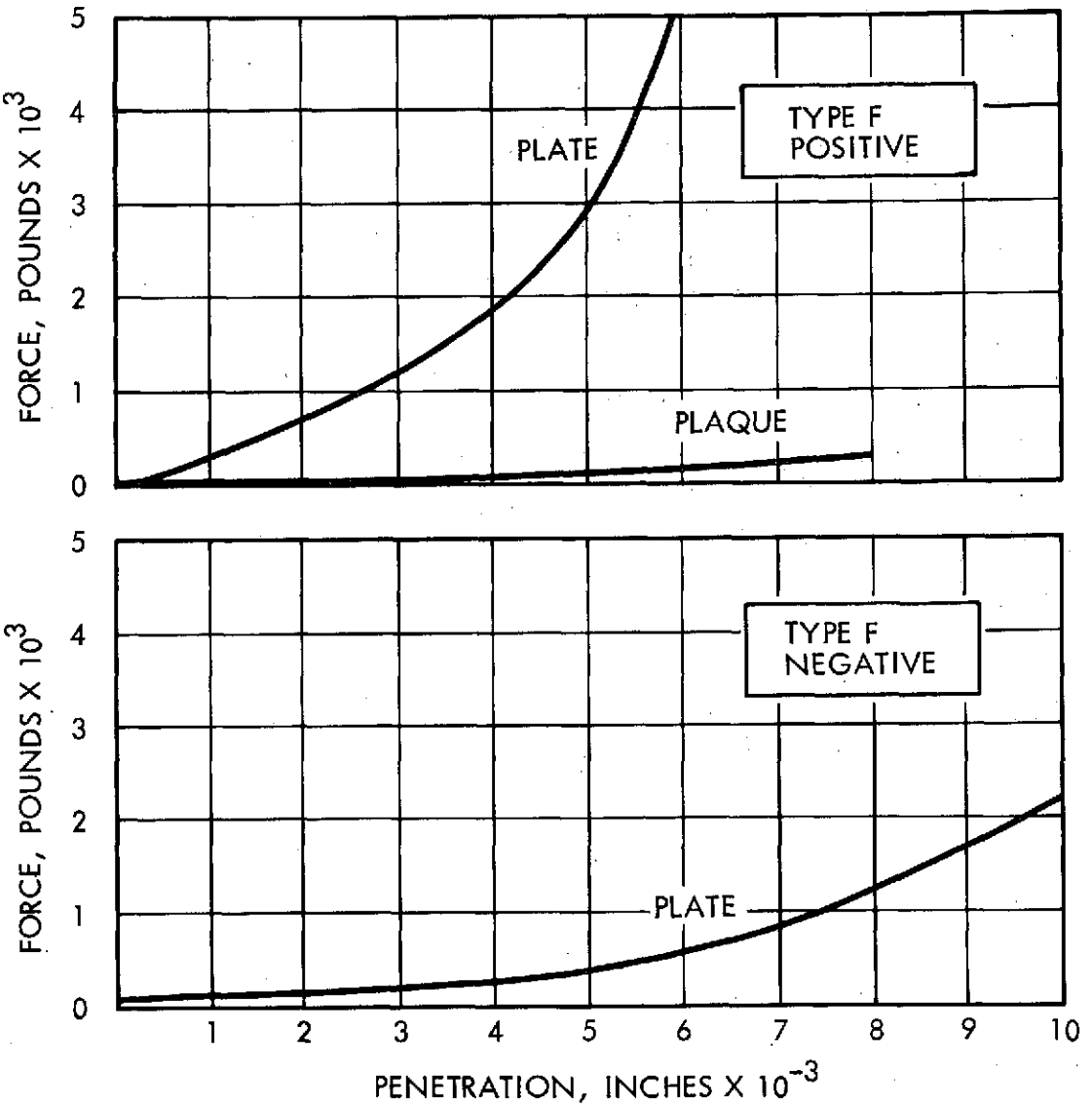

Figure 8. Compressive Strength Curves, Type F Plate

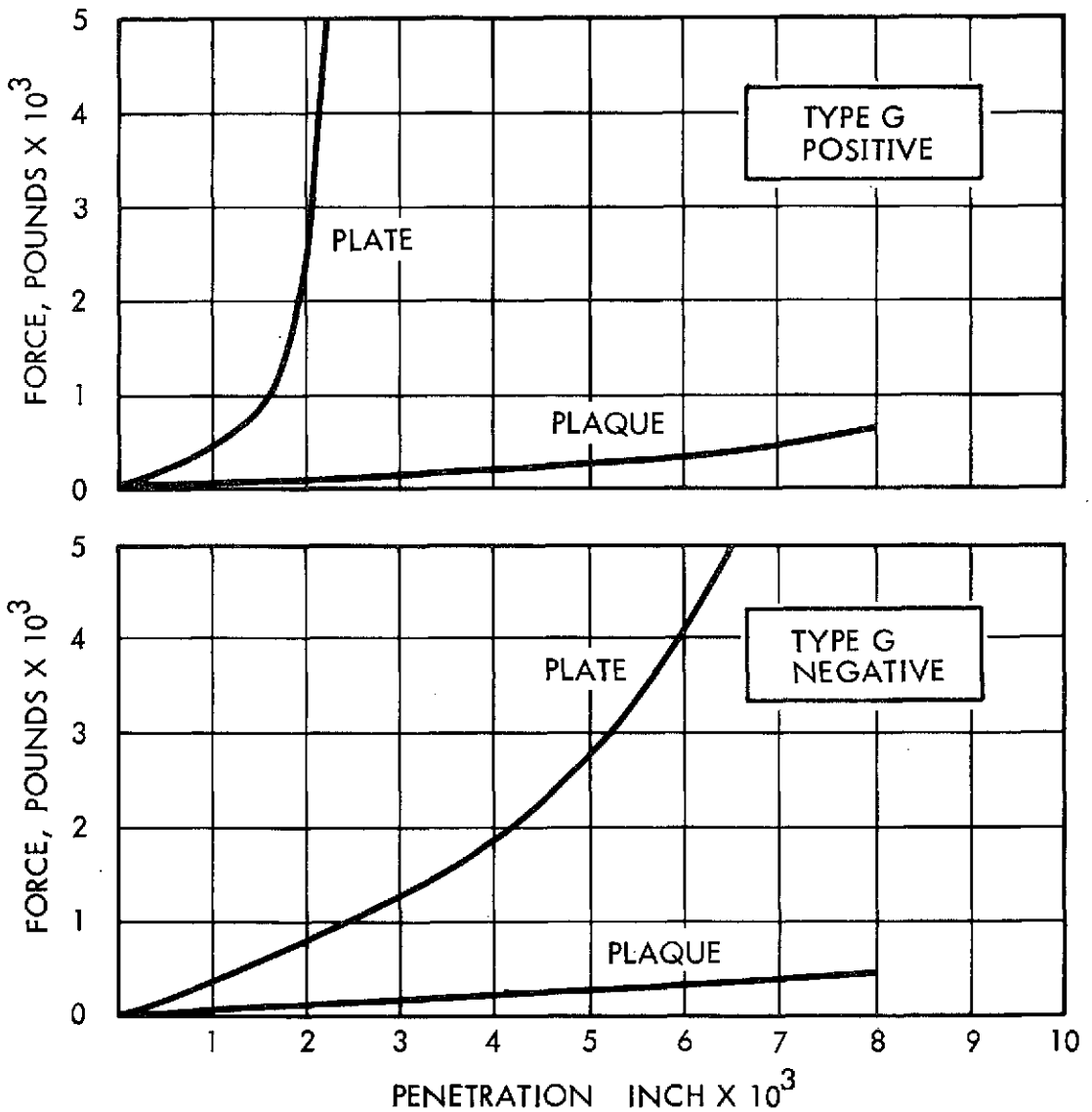

Figure 9. Compressive Strength Curves, Type G Plate

Table 6. Active Material Analysis of Plates

Type	Plate Polarity	As $Ni(OH)_2$, g/cm^2				As $Cd(OH)_2$, g/cm^2				Theoretical Capacity (Ah/dm^2) (Note 1)	
		Min.	Max.	Avg.	Std. Dev.	Min.	Max.	Avg.	Std. Dev.	Positive	Negative
A	Positive	.185	.217	.200	.012					5.75	
	Negative					.204	.234	.223	.015		8.15
B	Positive	.181	.252	.221	.025					6.30	
	Negative					.154	.183	.168	.016		6.15
C	Positive	.182	.213	.199	.013					5.70	
	Negative					.157	.190	.176	.012		6.45
D	Positive	.184	.226	.205	.020					5.90	
	Negative					.103	.116	.108	.006		3.95
E	Positive	.04	1.00	.068	.030					1.95	
	Negative					.086	.099	.093	.034		3.40
F	Positive	.037	.063	.055	.012					1.61	
	Negative					.046	.073	.059	.011		2.16
G	Positive	.143	.184	.155	.017					4.45	
	Negative					.154	.215	.192	.024		7.05

Note 1. For positive plates, calculated at 0.287 Ah/g, from average loading value. For negative plates, calculated at 0.366 Ah/g, from average loading value.

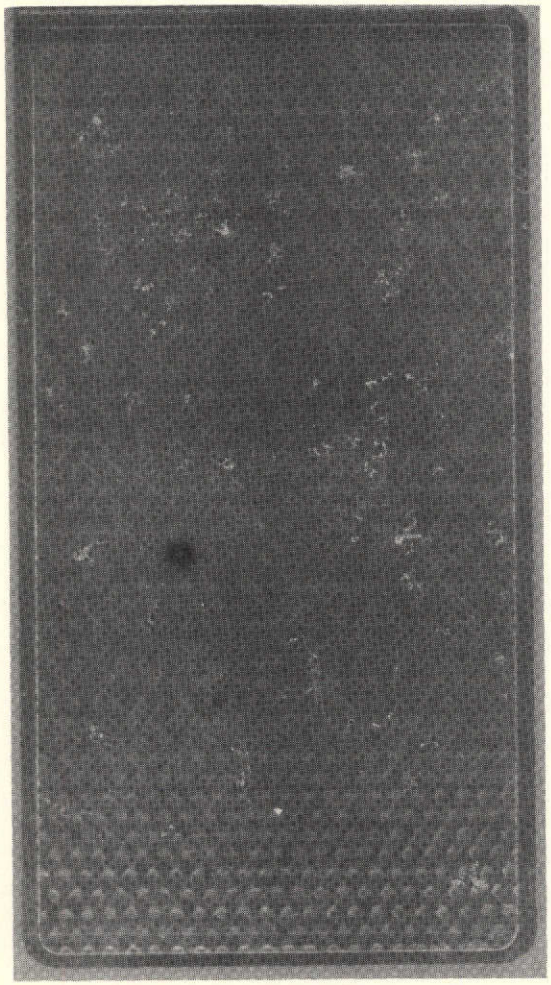

A. Positive

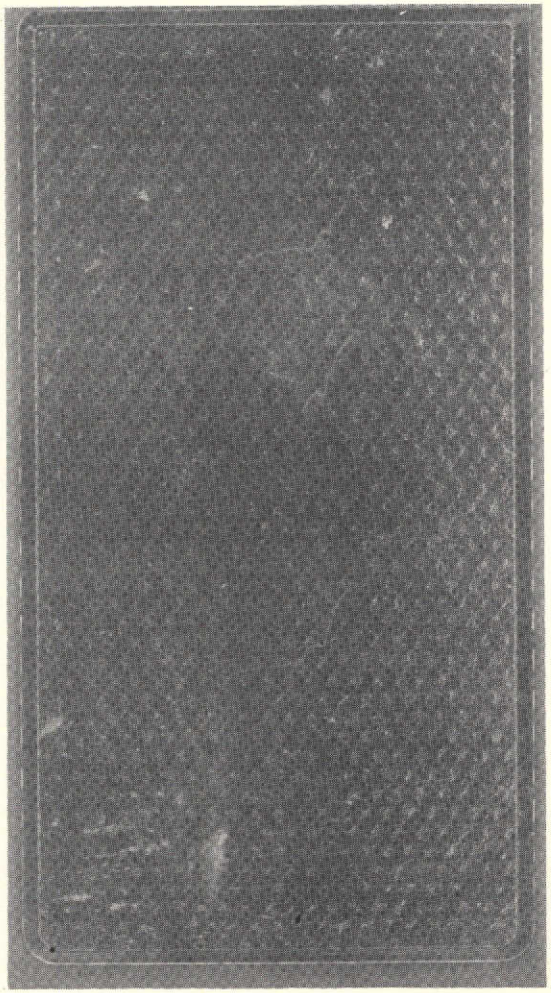

B. Negative

Figure 10. Type A Plate Photographs

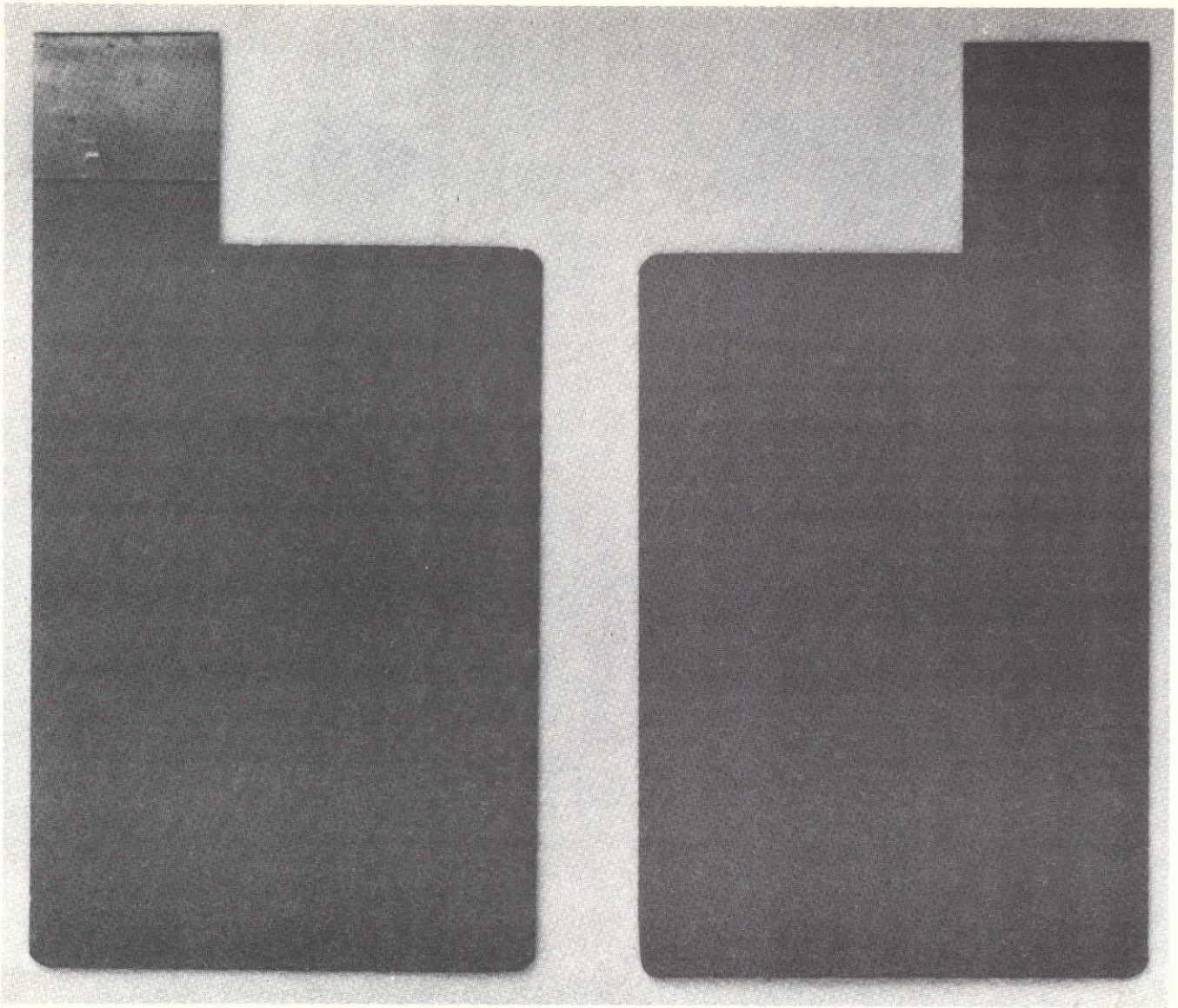

A. Positive

B. Negative

Figure 11. Type B Plate Photographs

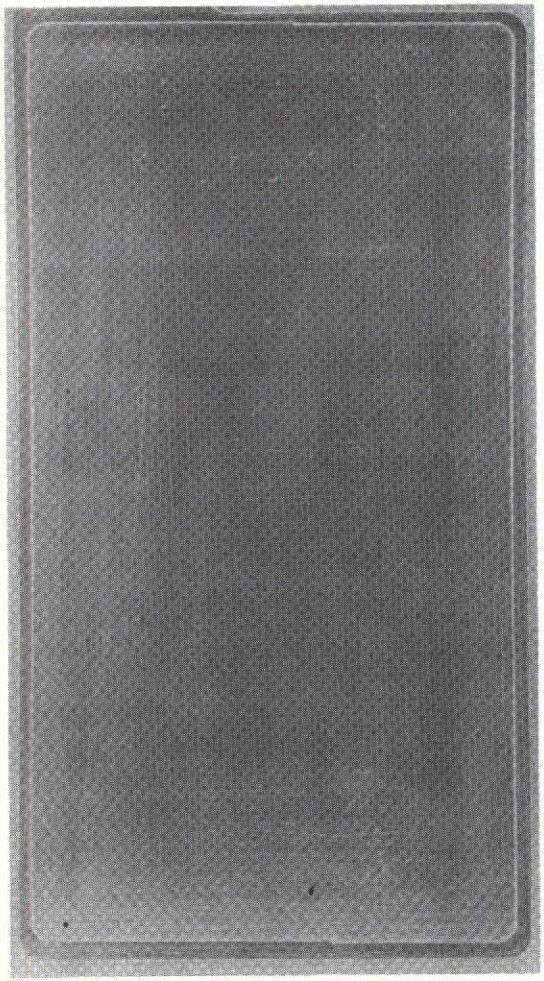

A. Positive

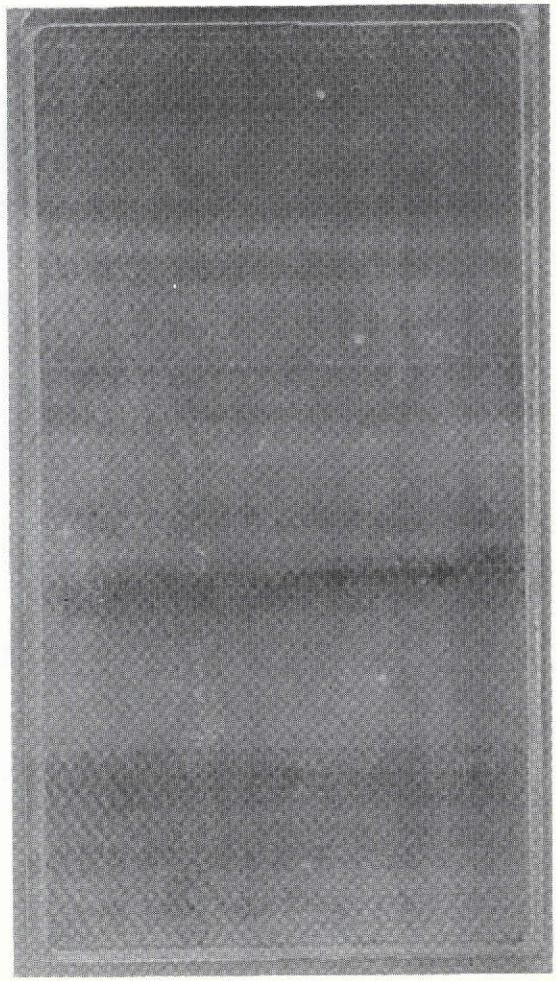

B. Negative

Figure 12. Type C Plate Photographs

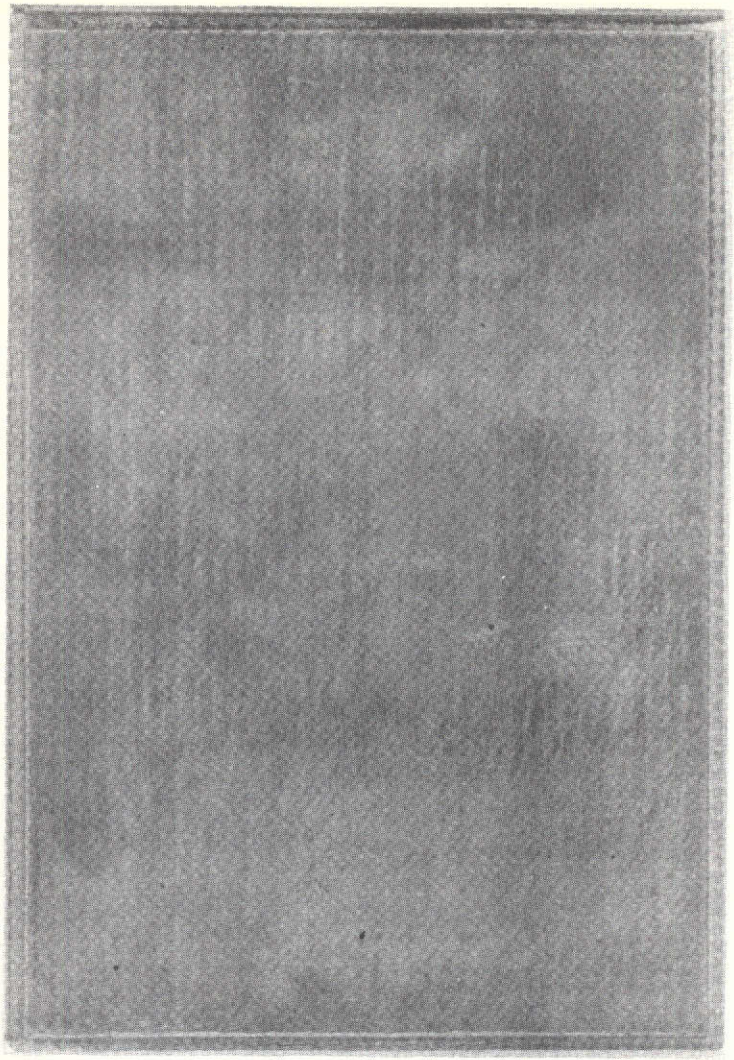

A. Positive

B. Negative

Figure 13. Type D Plate Photographs

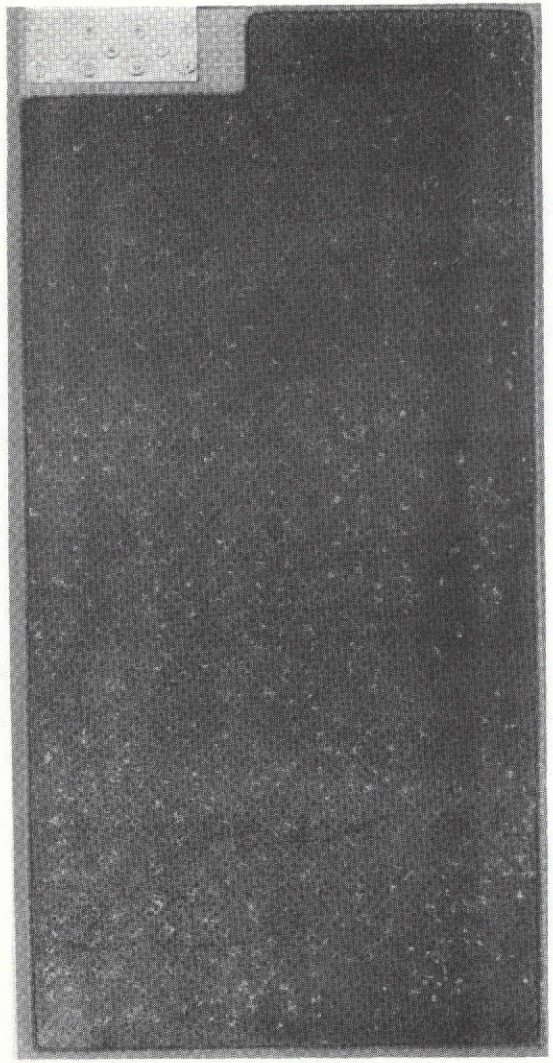

A. Positive

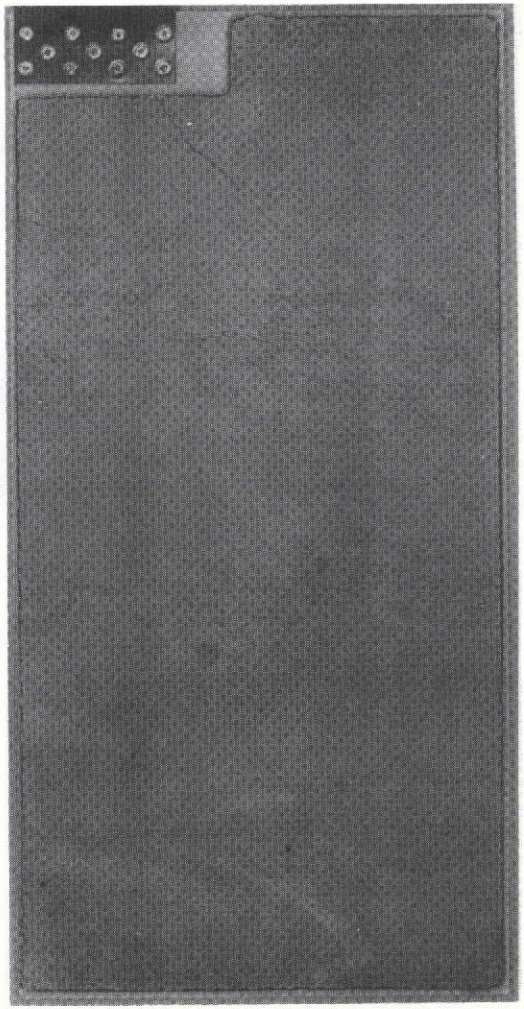

B. Negative

Figure 14. Type E Plate Photographs

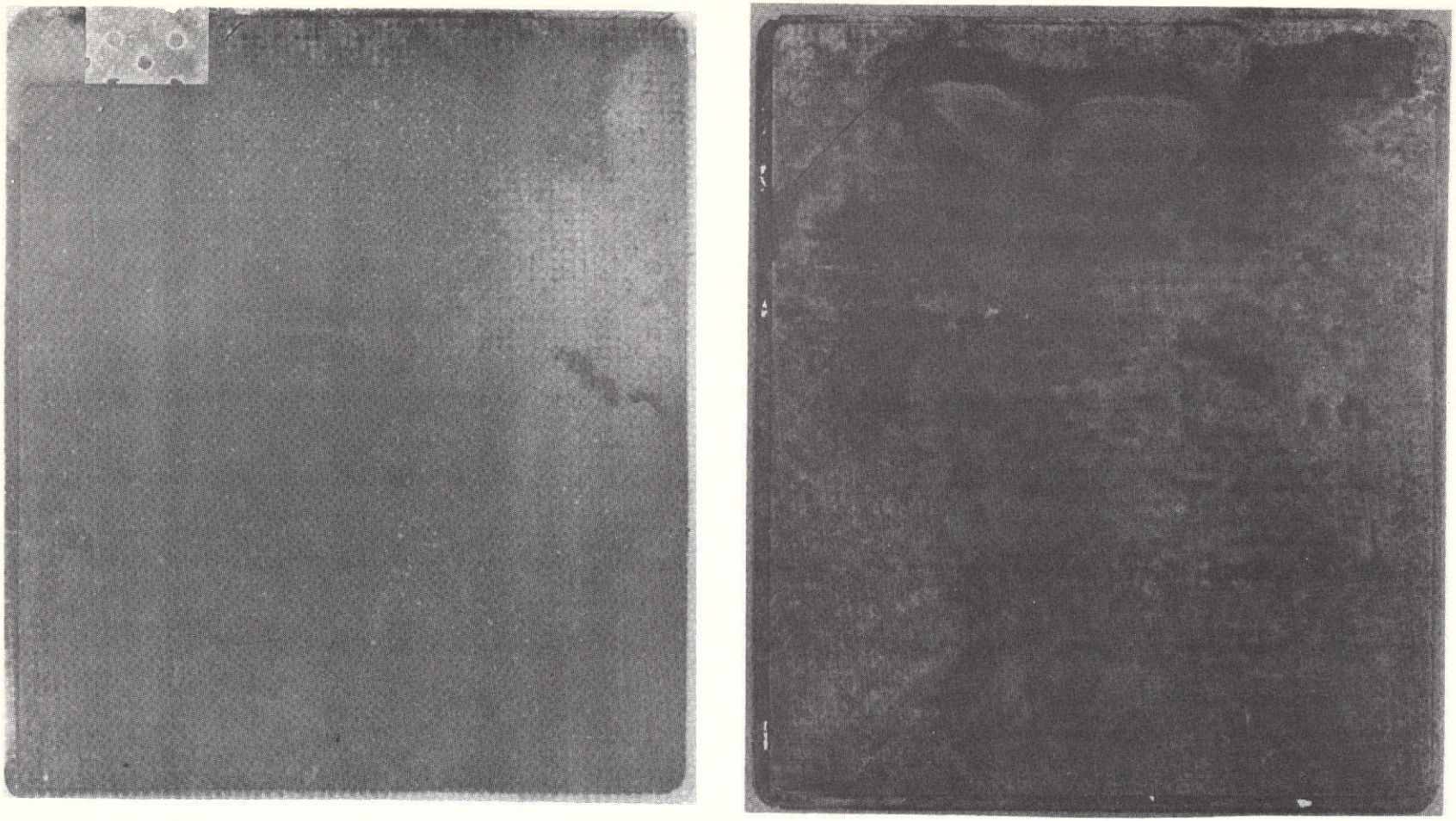

A. Positive

B. Negative

Figure 15. Type F Plate Photographs

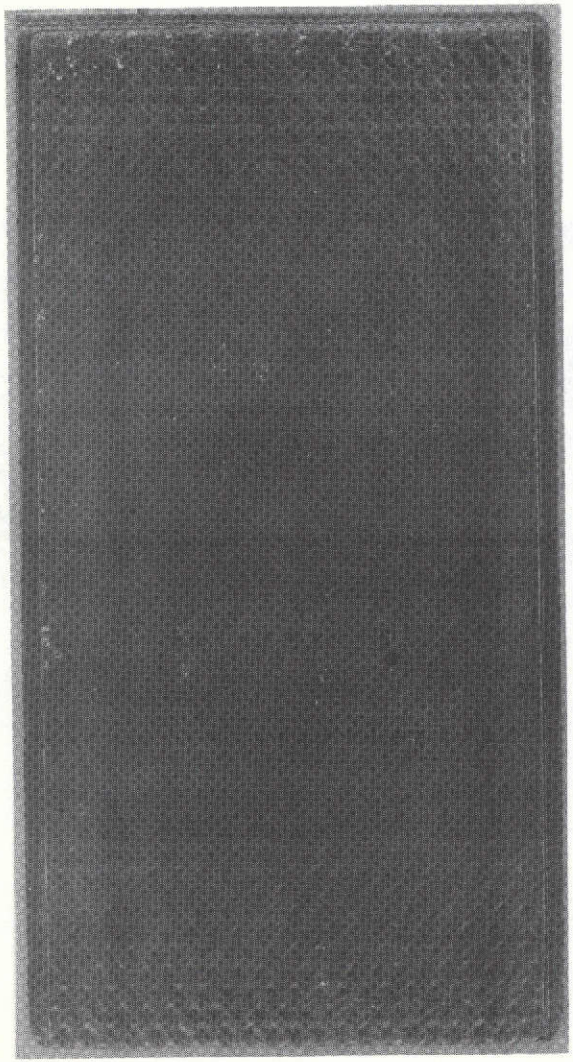

A. Positive

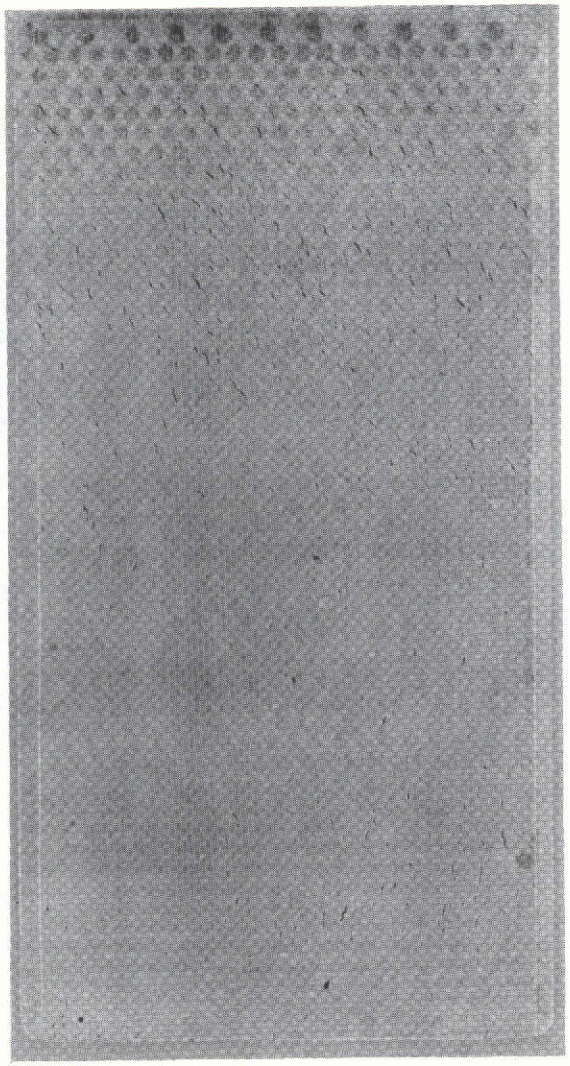

B. Negative

Figure 16. Type G Plate Photographs

The coined borders of plaques and plates from different suppliers tend to look similar to the unaided eye. However, there are in fact a wide range of variations in the materials received. These differences become apparent under magnification. Photographs of typical coined borders and edges of plaque and plate materials are shown in Figures 17 through 30. Note that when the thickness reduction is 30 percent or greater the coined border is obvious, but when the thickness reduction is only 10 percent (as with Type G, Figures 29 and 30), the coined border is hard to see in places, even under magnification.

Photographs taken under the Scanning Electron Microscope of various plate materials are shown in Figures 31 through 44. Note that separate scans were made for coined areas and for noncoined areas on some plates to try to show any apparent differences. As can be seen, the compression produced by coining does reduce the interstitial void space and pore size significantly. However, there is very little difference on the surface (as seen by the SEM) between coined and noncoined areas after impregnation.

4.6 SPECIAL MECHANICAL TESTING

4.6.1 Cutting Tests

In this study, plate materials were cut using a die-cutter and the cut edges examined under the microscope. It was noted that, using the sharpest tool available in a model-shop, only occasionally could either plaque or plate be cut without producing appreciable cracking along the cut. Figures 45 through 48 show some examples of the results. It is apparent from the photographs that some cracking along cuts is unavoidable but is more limited and controlled in coined areas than in uncoined areas.

4.6.2 Bend and Drop Testing

Various test methods were explored to characterize the brittleness of the sinter and its resistance to breakage. In one such test, plates were bent in the "long" direction (i.e., in the direction parallel to the direction of the tab) by grasping the ends and bending until the ends were at an angle of 150° (30° out of the original plane), then bending to the same extent in the opposite direction. The results are summarized as follows:

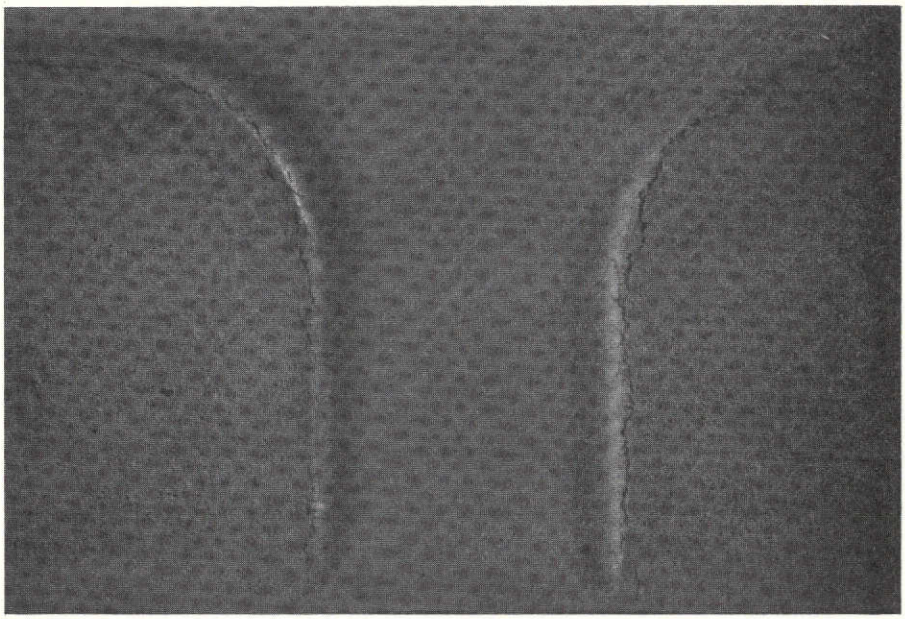

Figure 17. Type C Plaque - Coined, Prior to Cutting

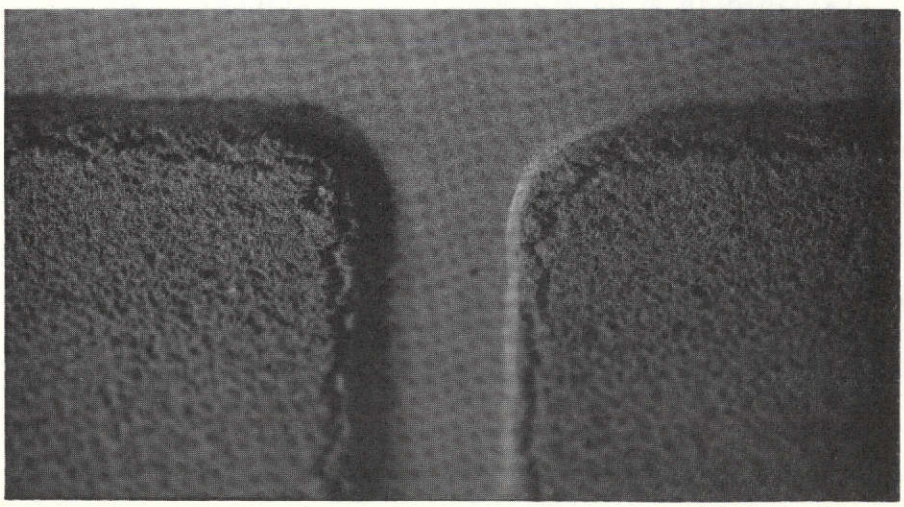

Figure 18. Type E Plaque - Coined, Prior to Cutting

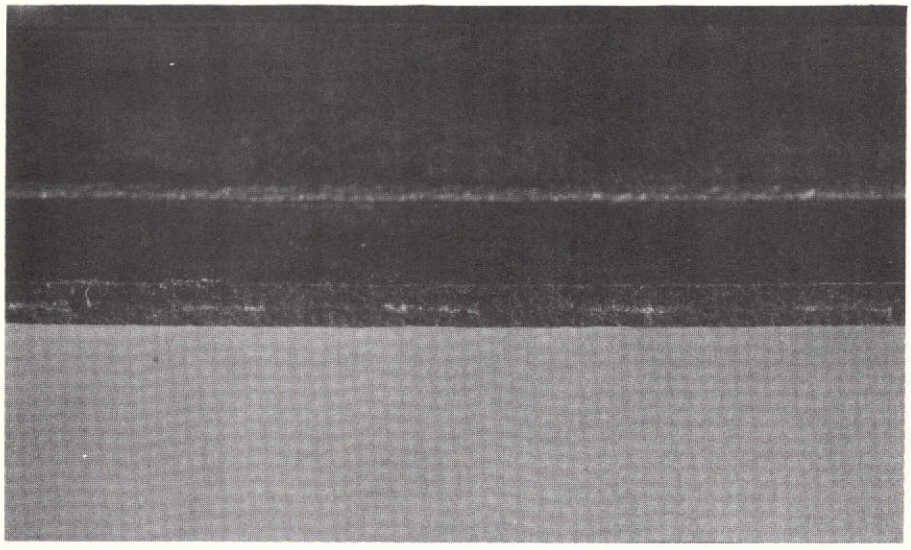

Figure 19. Type A Positive Plate - Coined and Die-Cut Edge

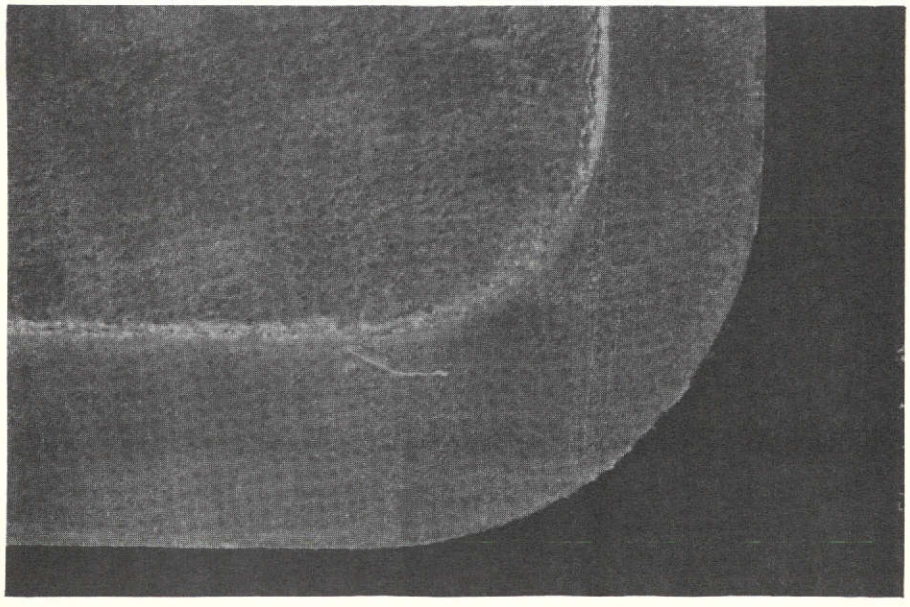

Figure 20. Type A Positive Plate - Coined and Die-Cut Corner

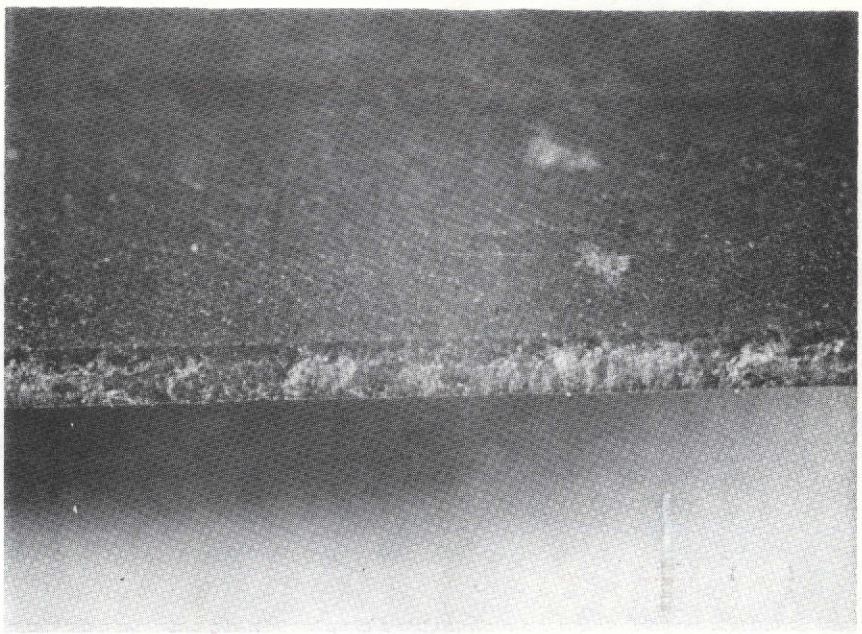

Figure 21. Type B Positive Plate - Uncoined Die-Cut Edge

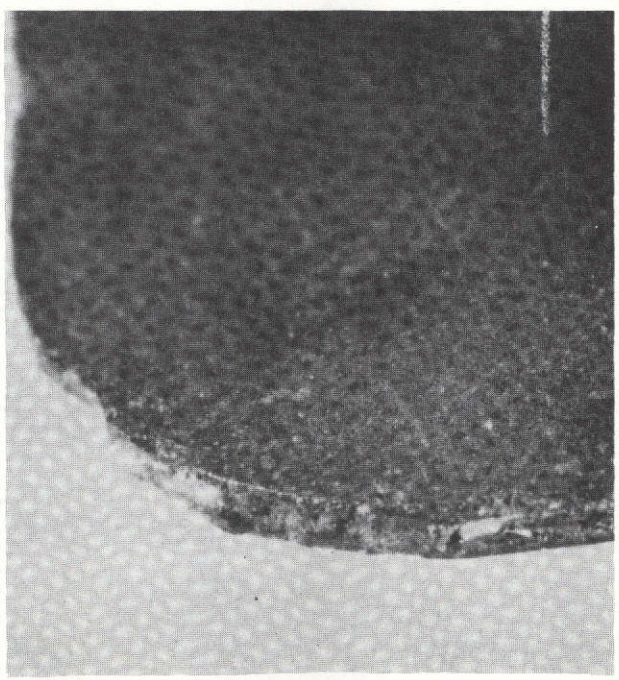

Figure 22. Type B Positive Plate - Uncoined Die-Cut Corner

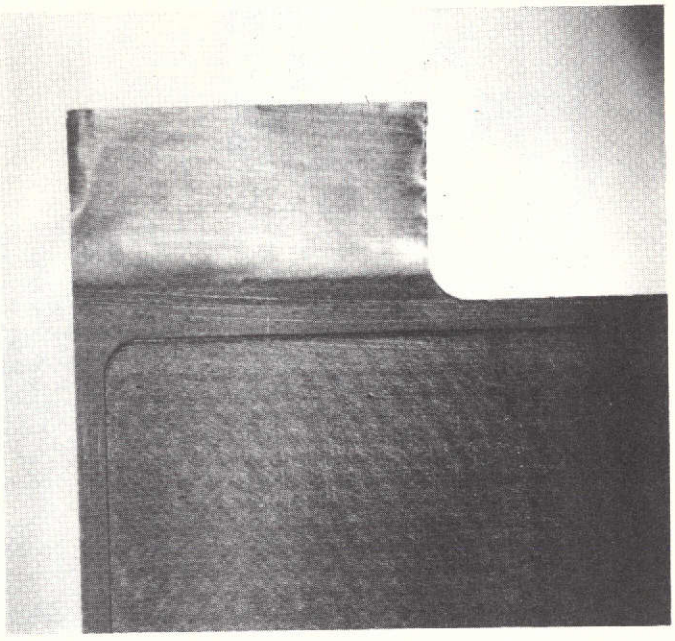

Figure 23. Type C Positive Plate - Coined Tab Area

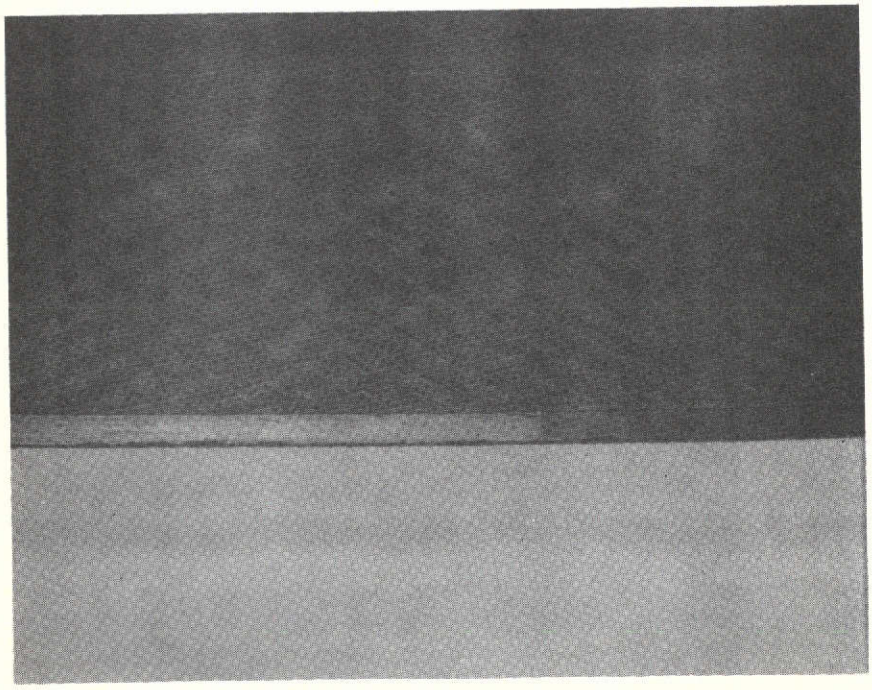

Figure 24. Type C Positive Plate - Coined and Die-Cut Edge

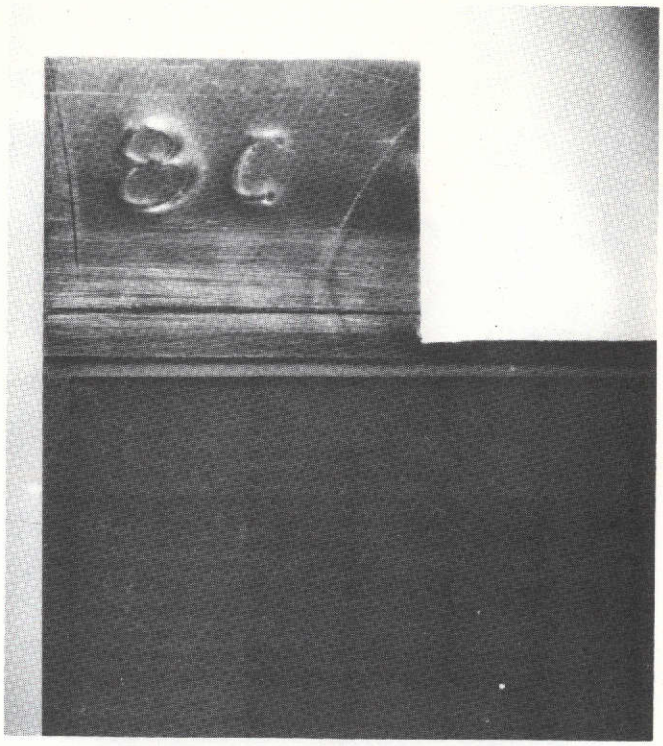

Figure 25. Type D Positive Plate - Coined Tab Area

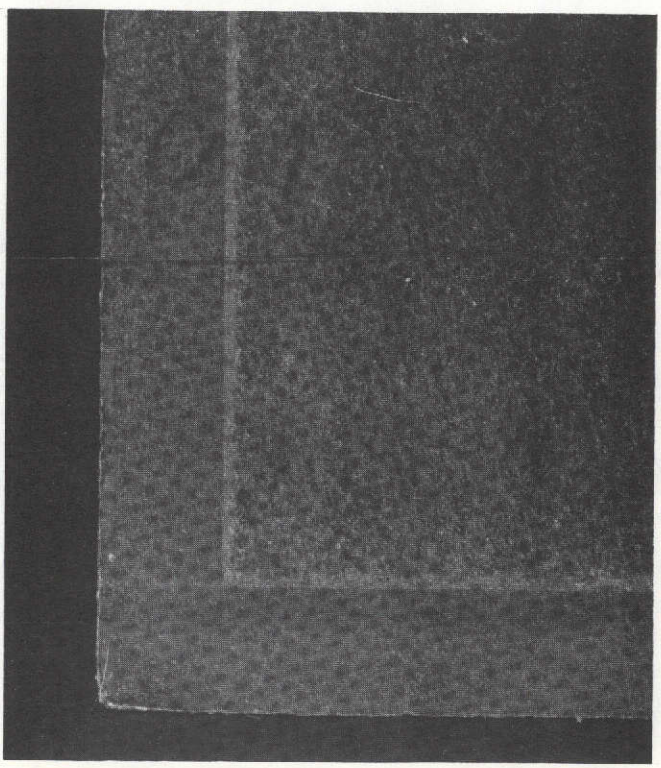

Figure 26. Type D Positive Plate - Coined Corner

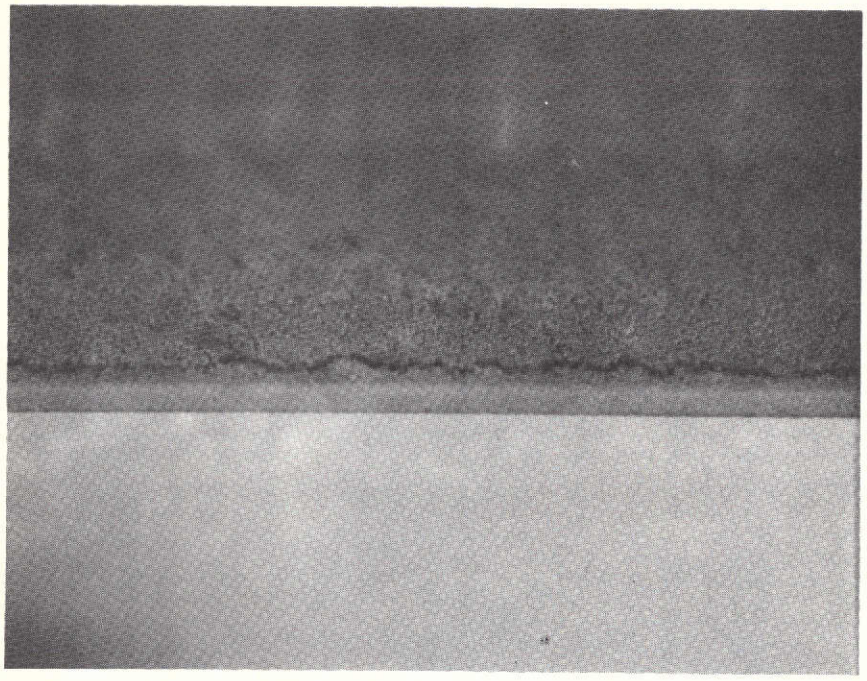

Figure 27. Type E Positive Plate - Coined Edge

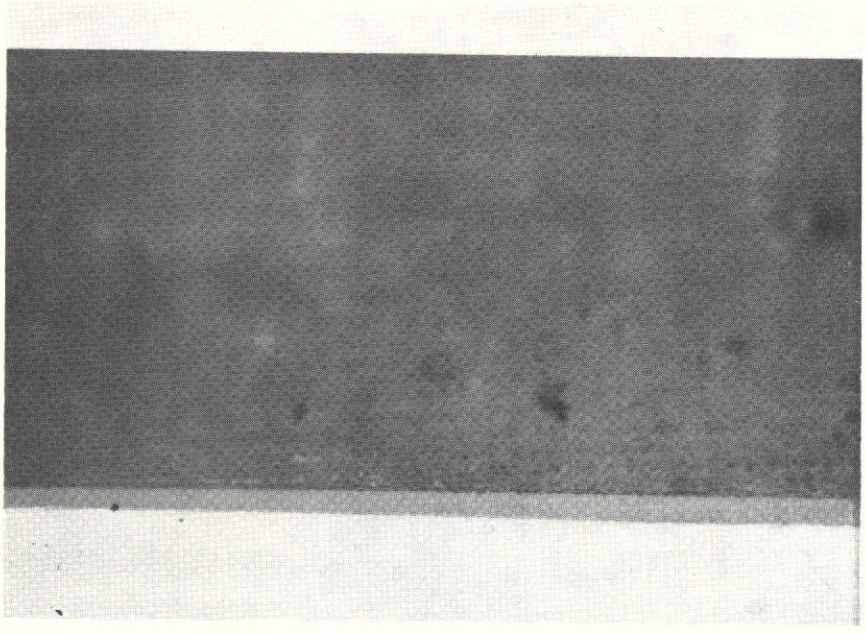

Figure 28. Type F Positive Plate - Coined Edge

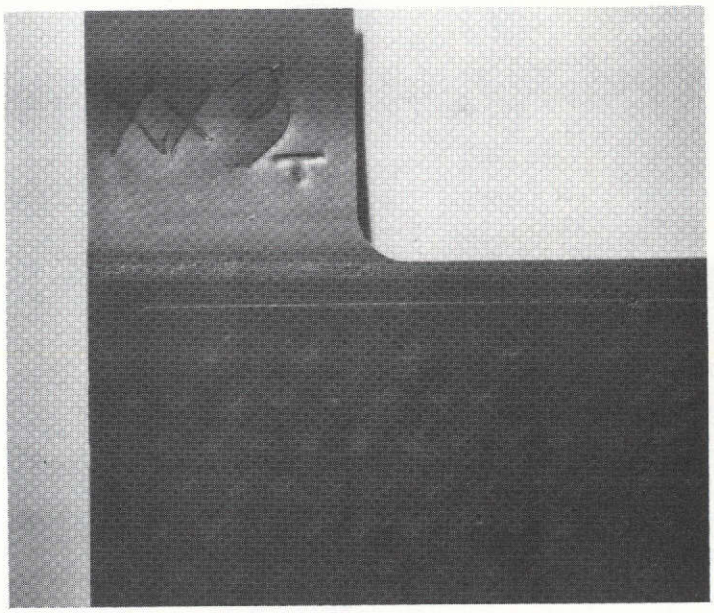

Figure 29. Type G Positive Plate - Coined Tab Area

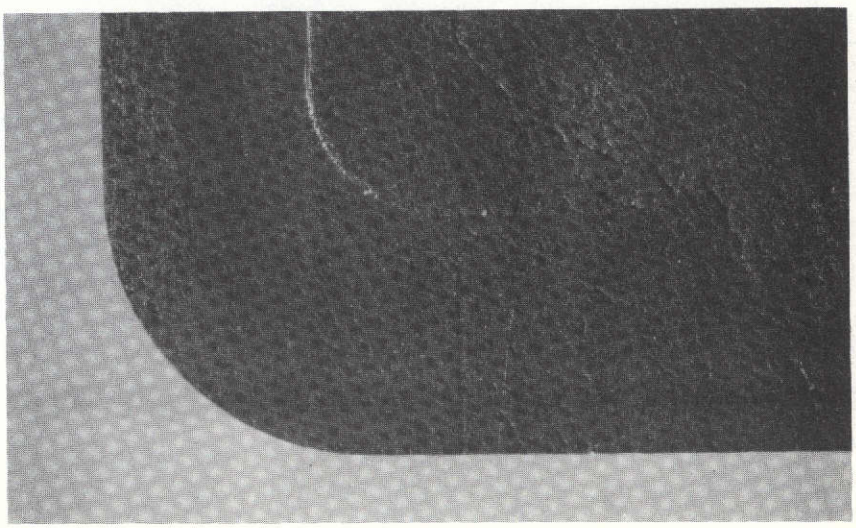

Figure 30. Type G Positive Plate - Coined and Die-Cut Corner

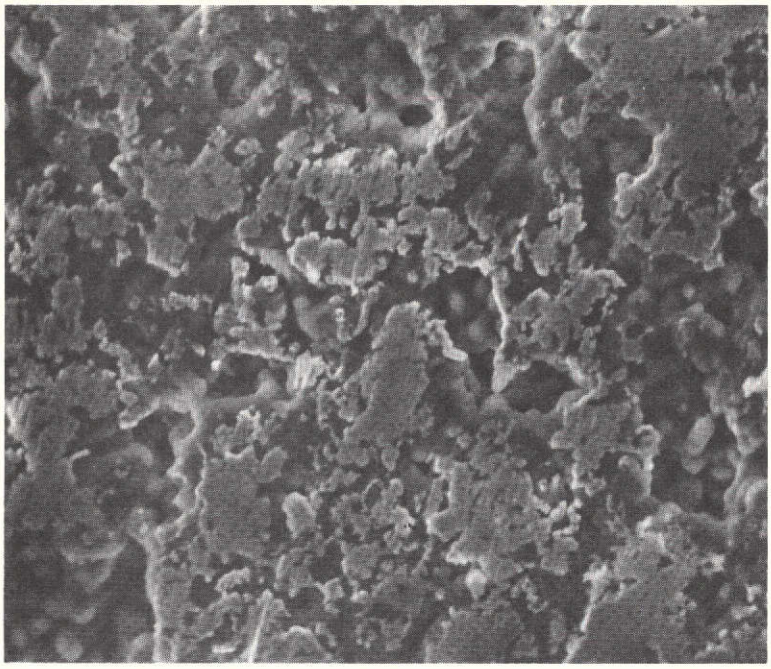

A. 500X

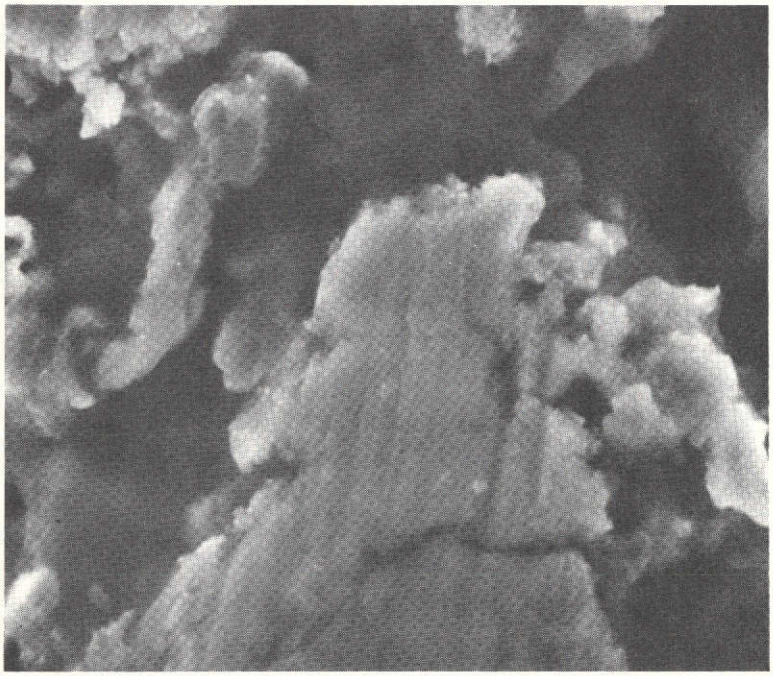

B. 3000X

Figure 31. Type A Positive Plate - Uncoined Area, SEM

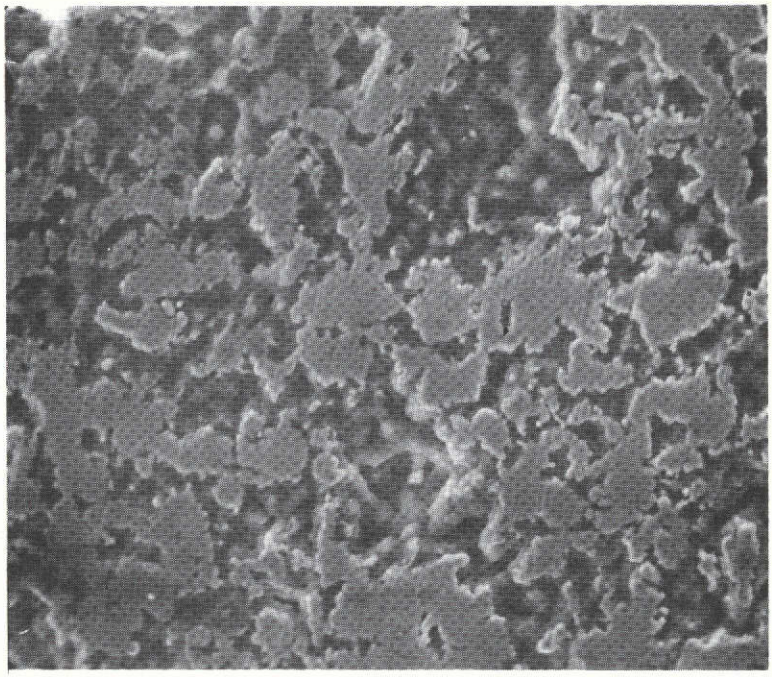

A. 500X

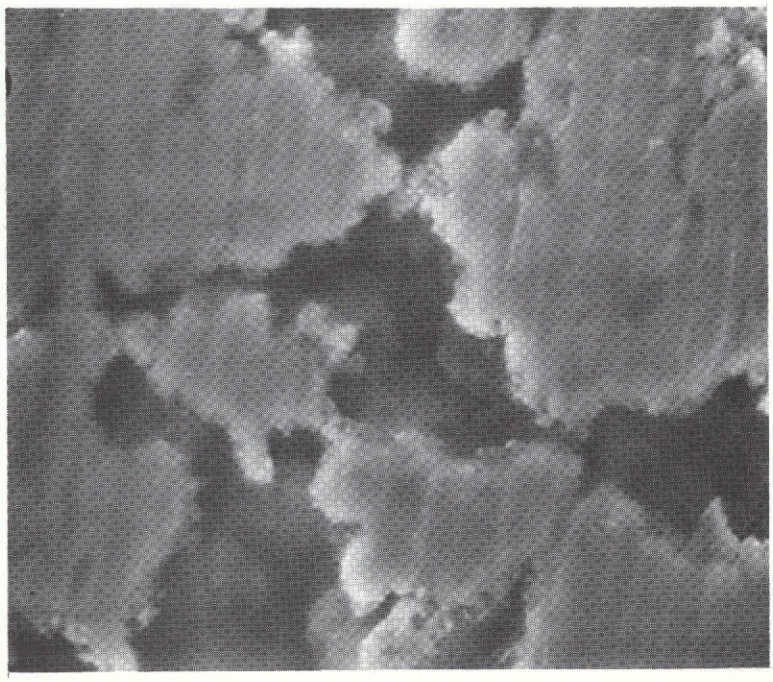

B. 3000X

Figure 32. Type A Positive Plate - Coined Border, SEM

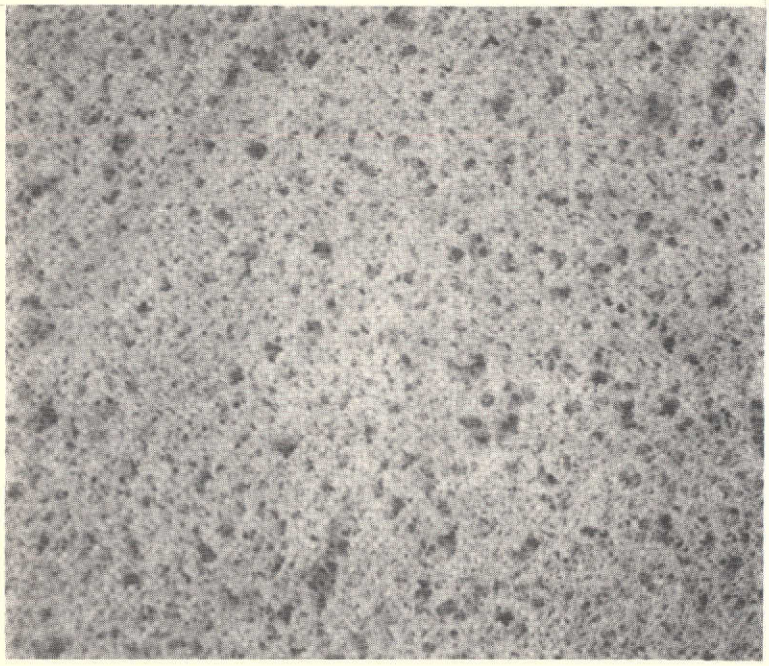

A. 100X

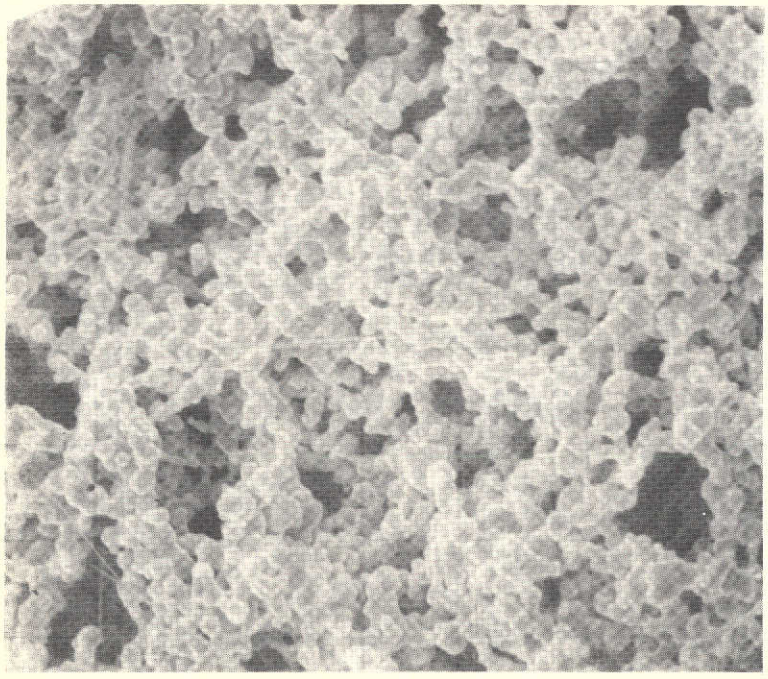

B. 1000X

Figure 33. Type B Positive Plate - Plaque - Uncoined Area, SEM

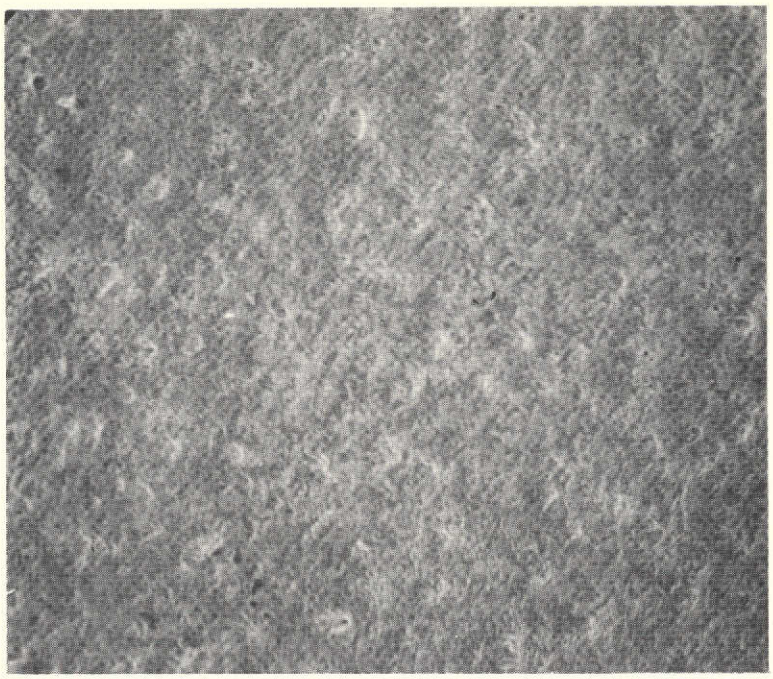

A. 100X

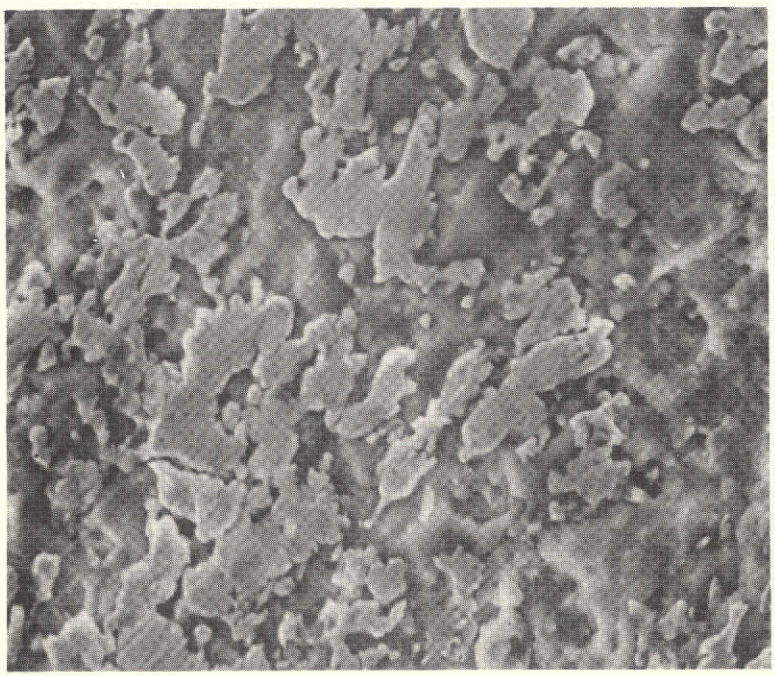

B. 1000X

Figure 34. Type B Positive Plate - Uncoined Area, SEM

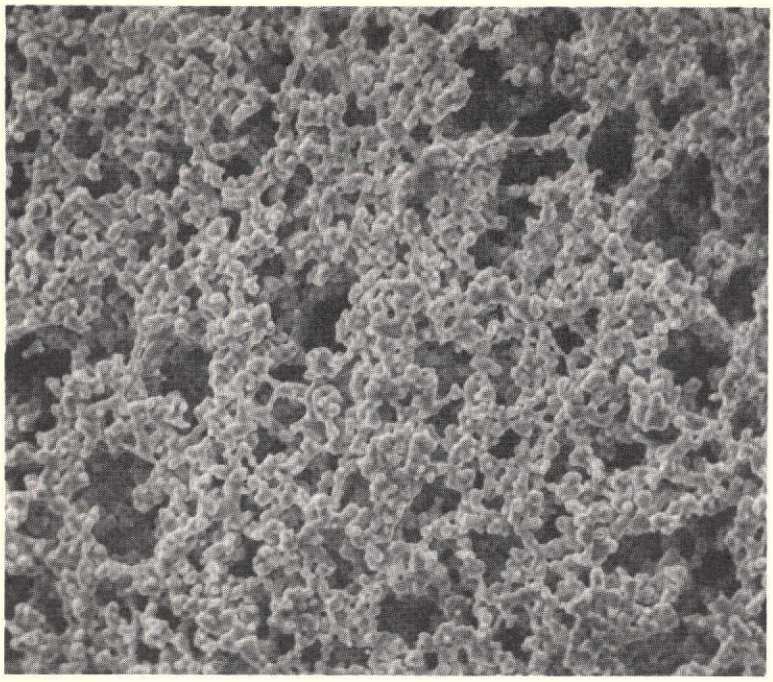

A. Uncoined

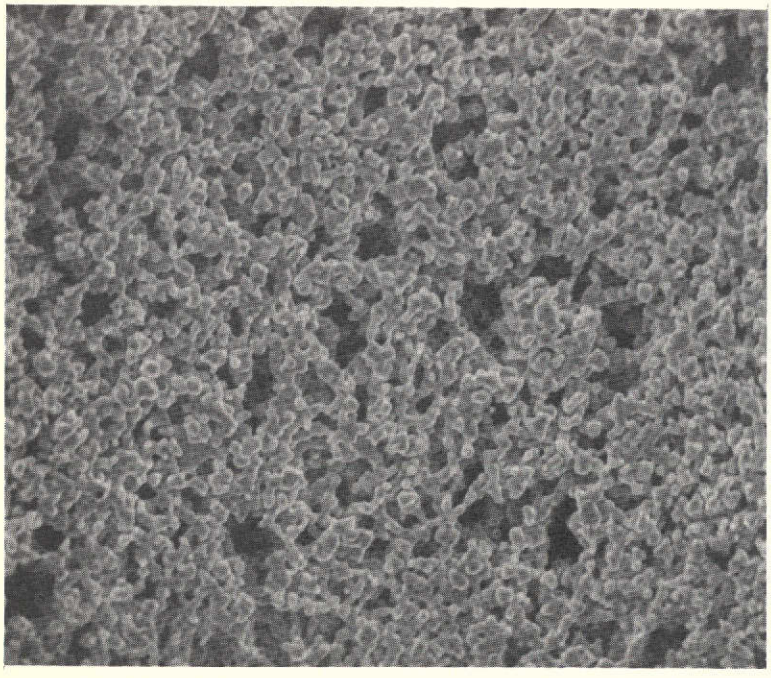

B. Coined

Figure 35. Type C Positive Plaque - SEM 500X

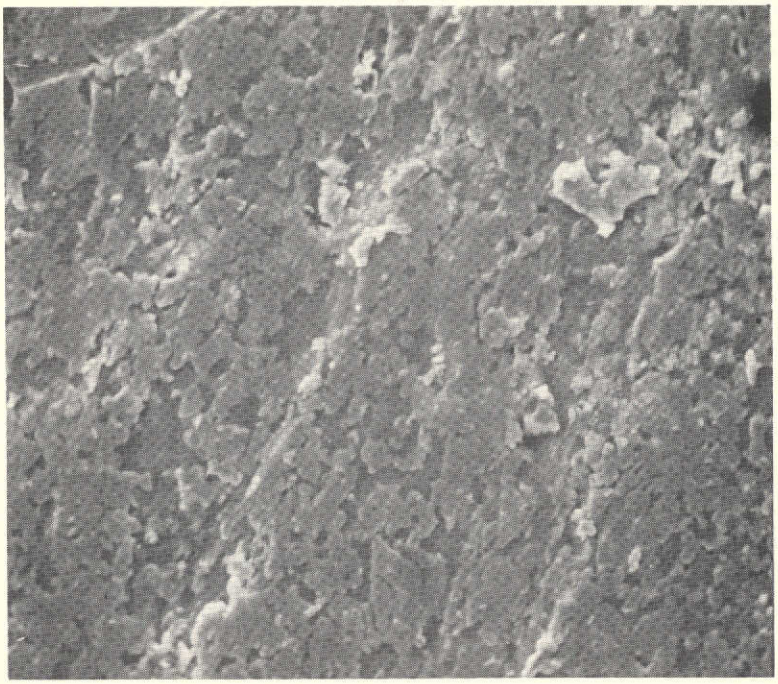

A. Positive Plate

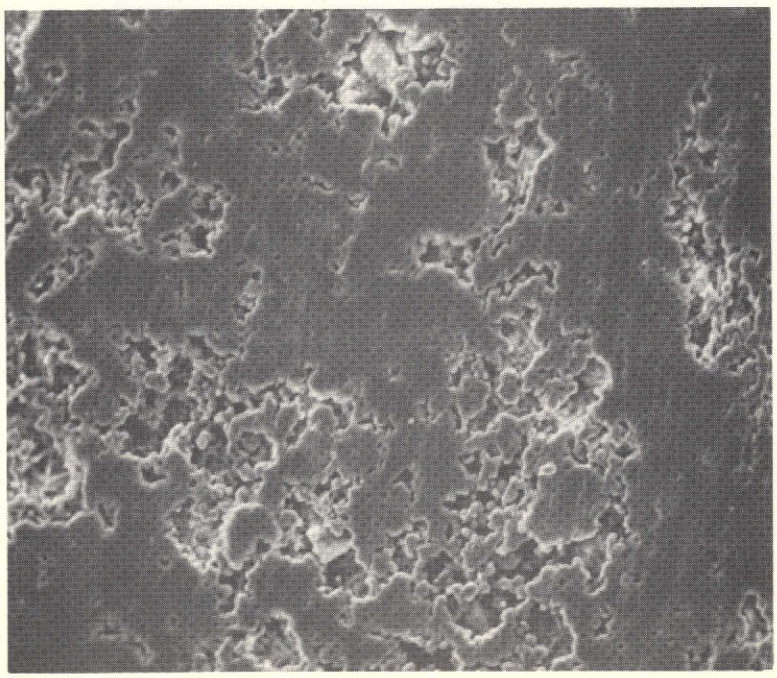

B. Negative Plate

Figure 36. Type C Plate Materials - SEM 500X

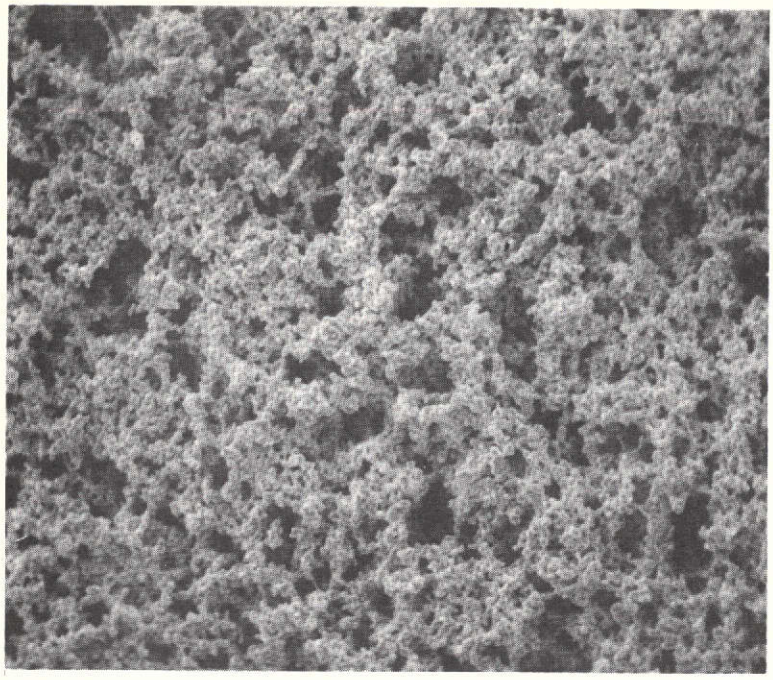

A. 250X

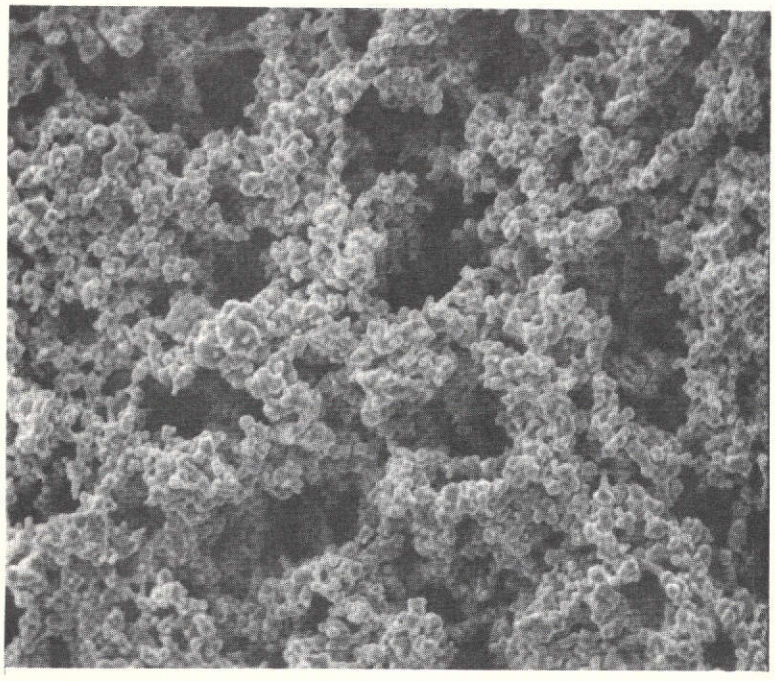

B. 500X

Figure 37. Type D Positive Plaque - Uncoined Area, SEM

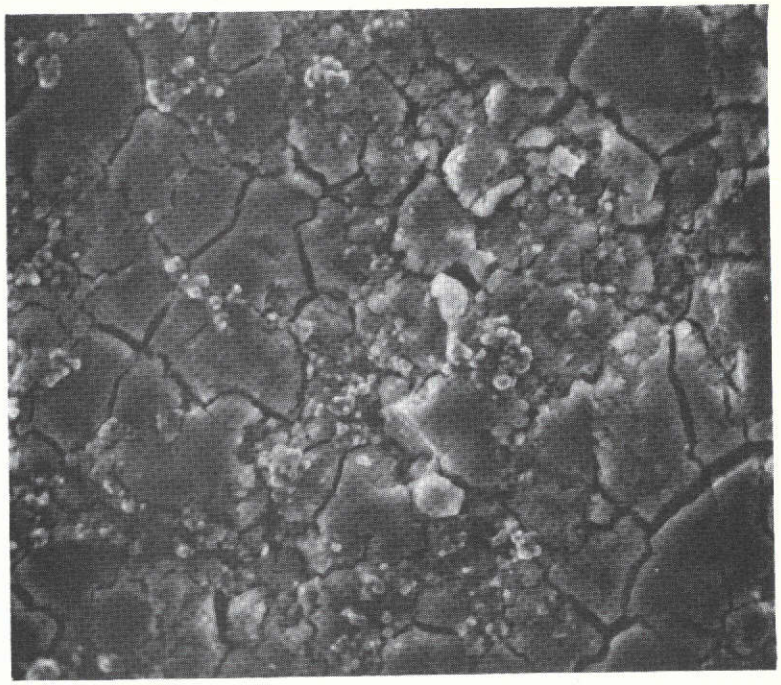

A. Positive Plate

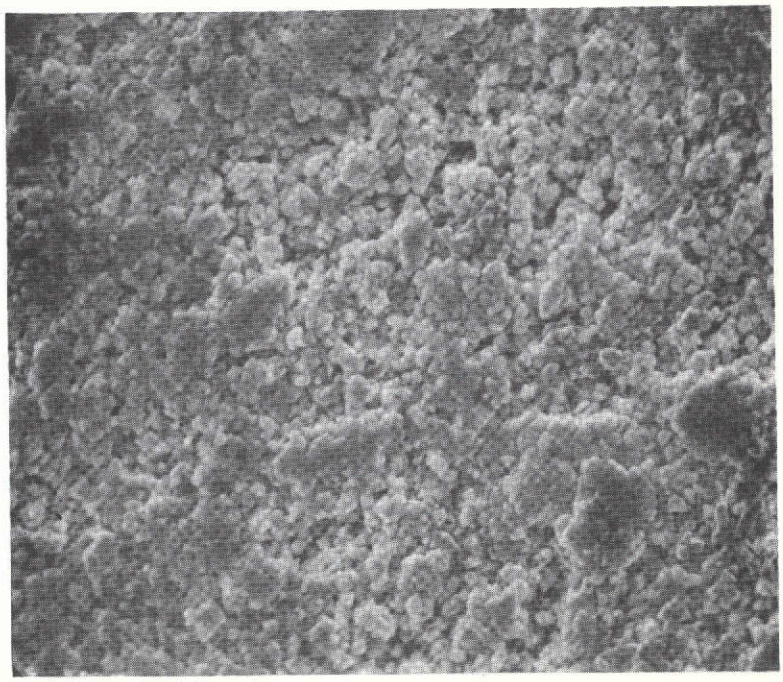

B. Negative Plate

Figure 38. Type D Plate Materials - Uncoined, SEM 500X

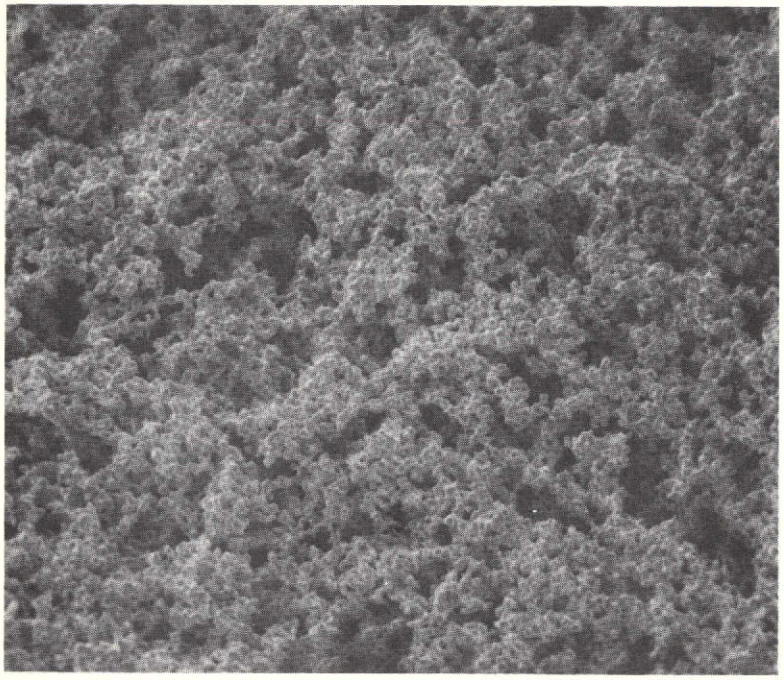

A. Uncoined

B. Coined

Figure 39. Type E Positive Plaque - SEM 300X

A. Uncoined

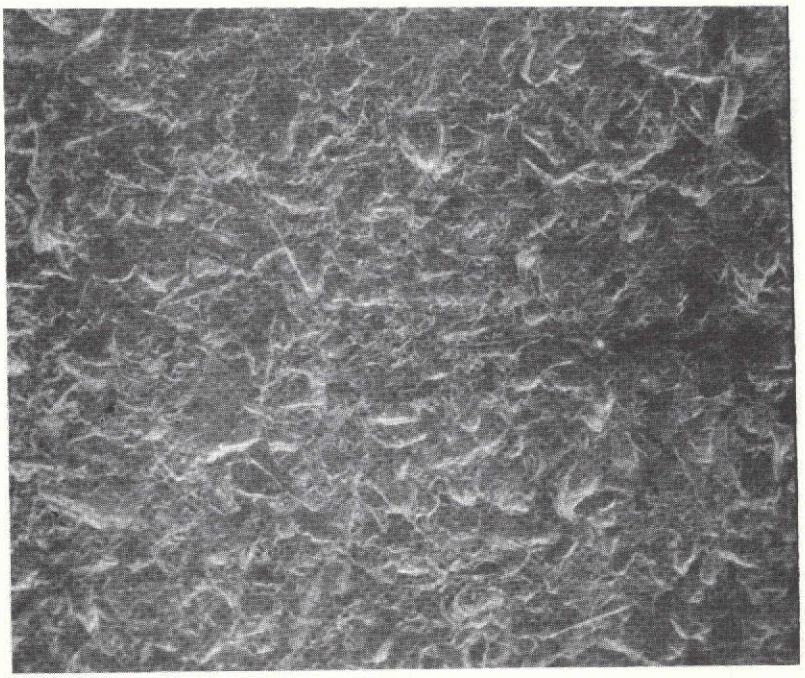

B. Coined

Figure 40. Type E Positive Plate - SEM 300X

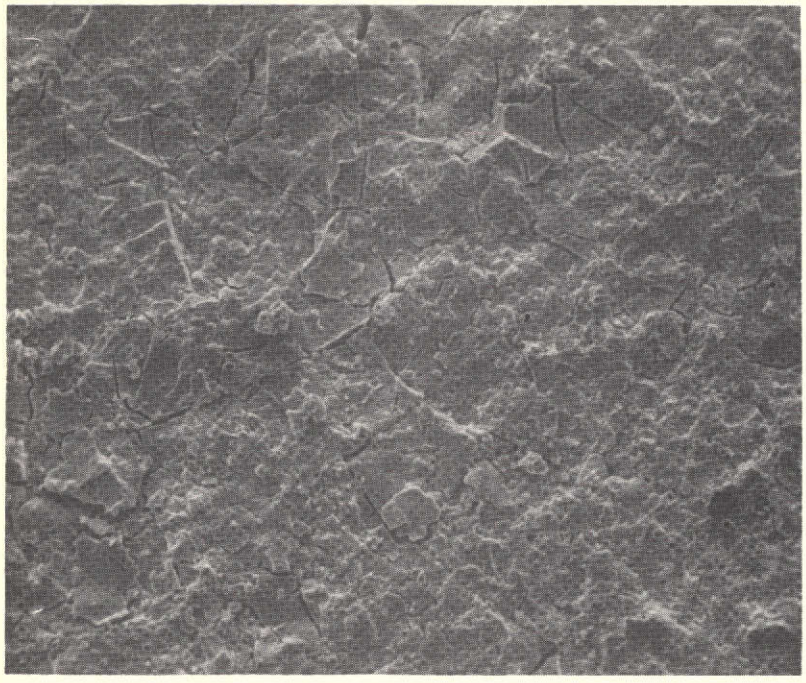

A. Uncoined

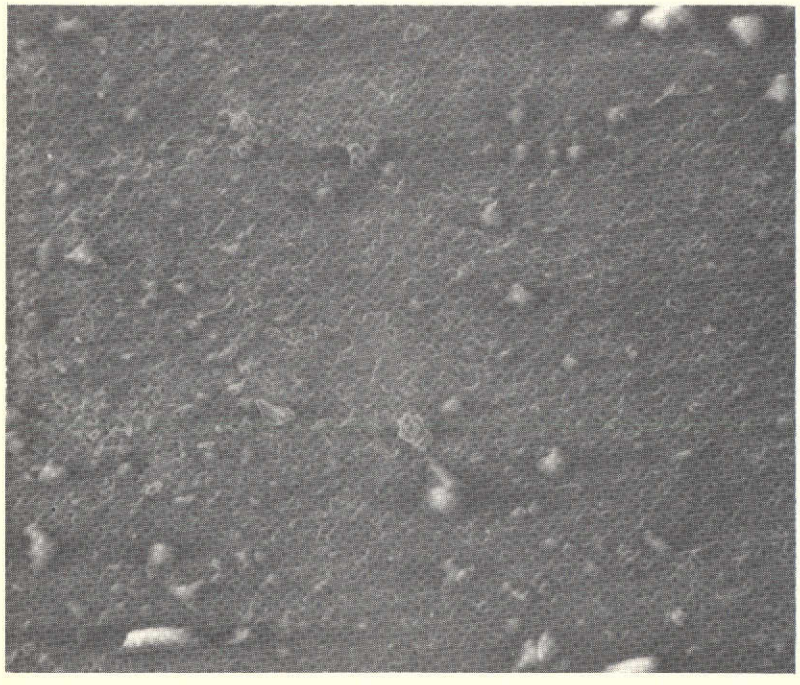

B. Coined

Figure 41. Type F Positive Plate - SEM 300X

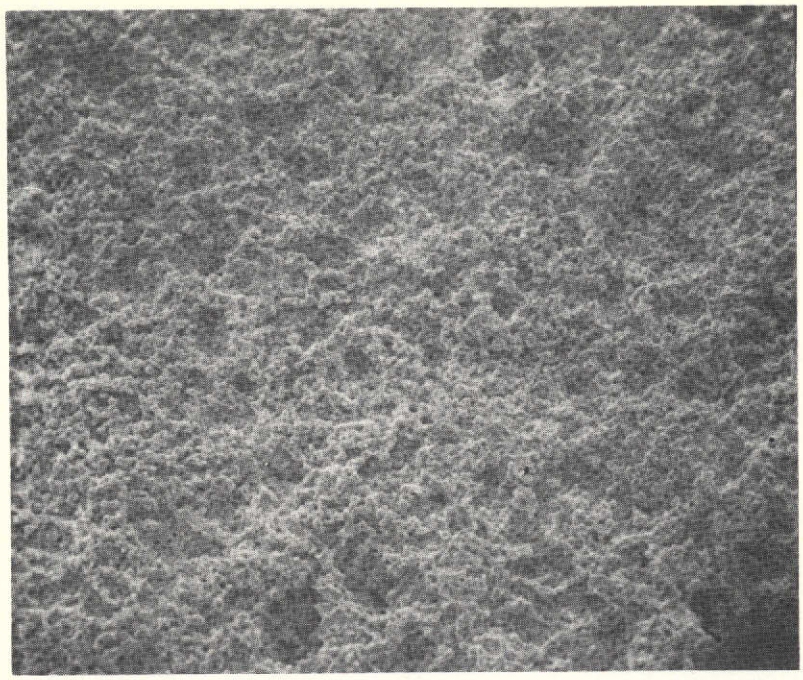

A. Uncoined

B. Coined

Figure 42. Type F Negative Plate - SEM 300X

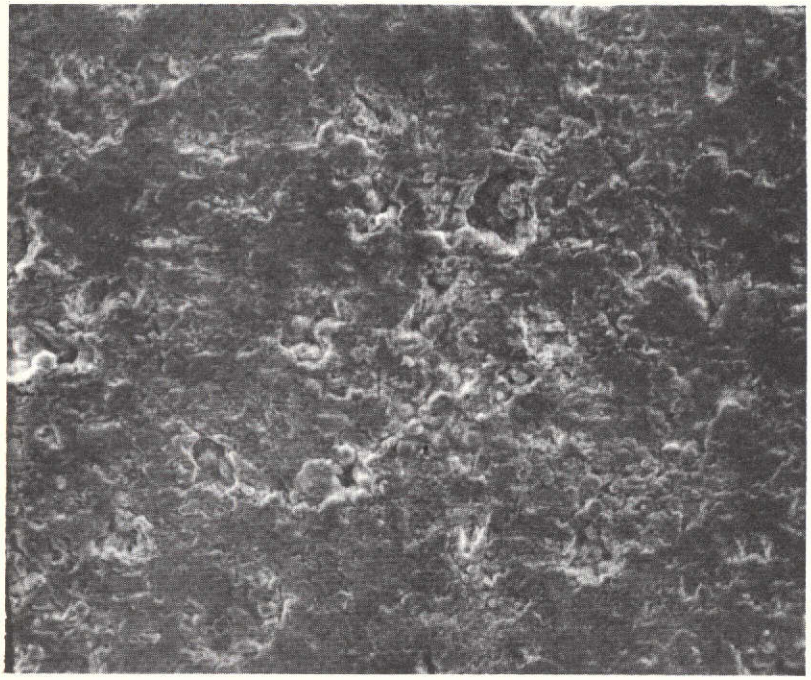

A. 300X

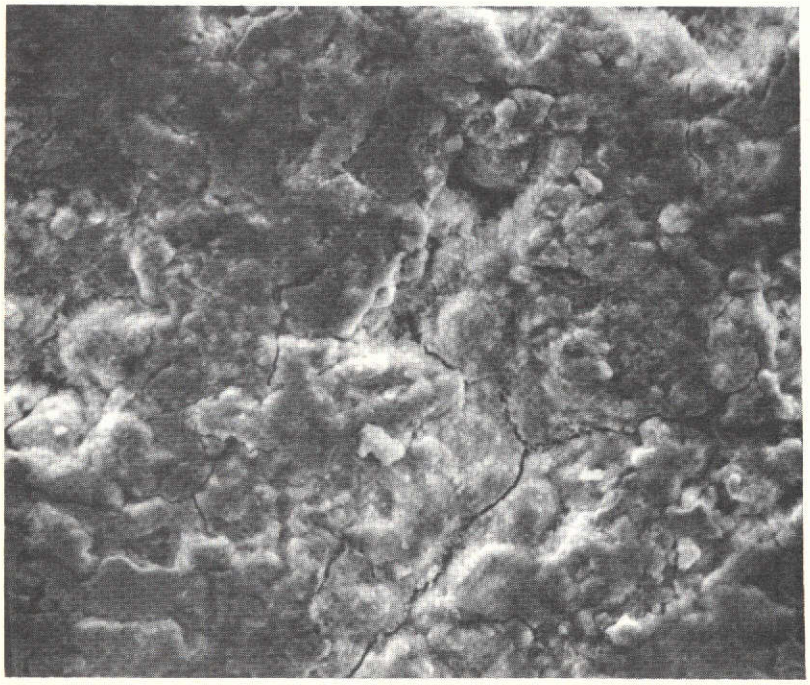

B. 1000X

Figure 43. Type G Positive Plate - Uncoined Area, SEM

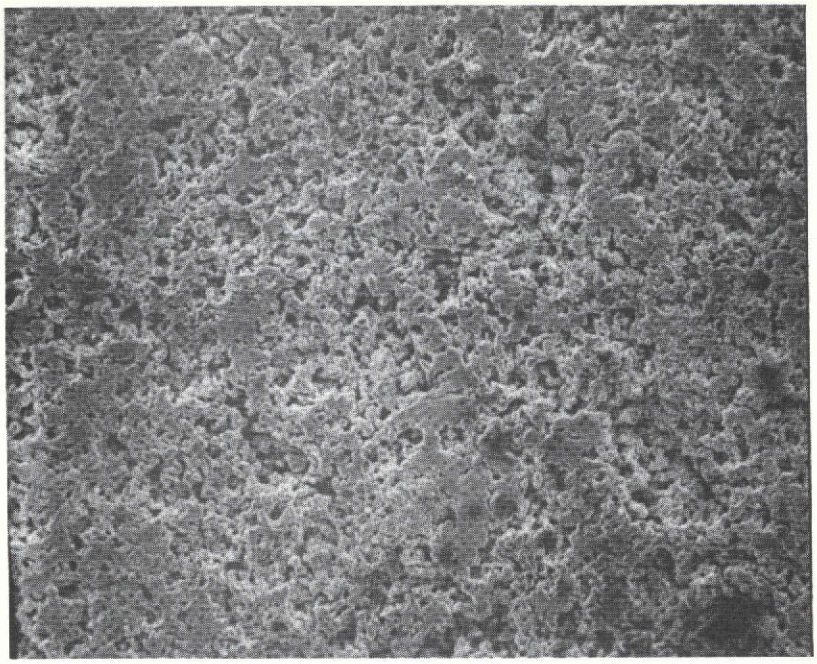

A. 300X

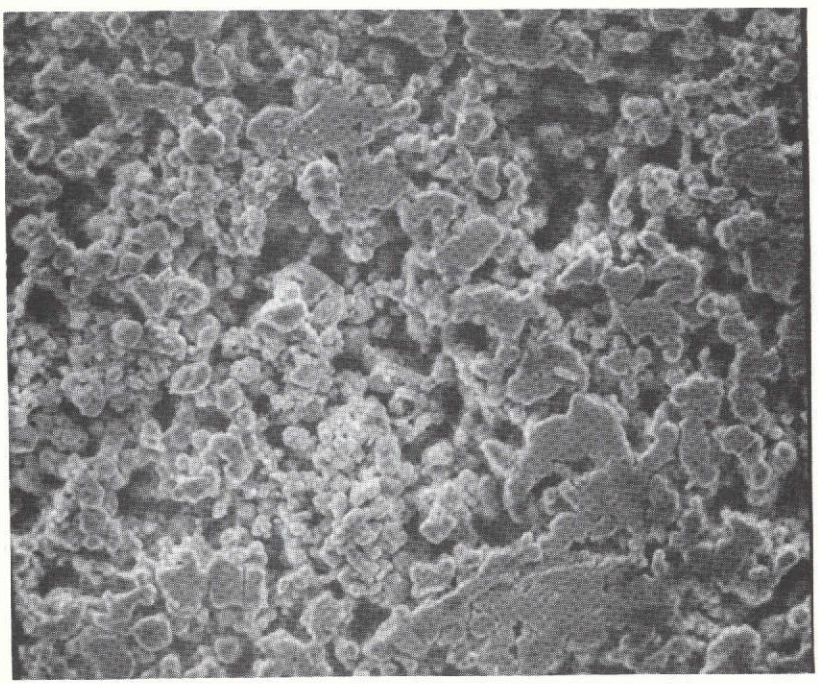

B. 1000X

Figure 44. Type G Negative Plate - Uncoined Area, SEM

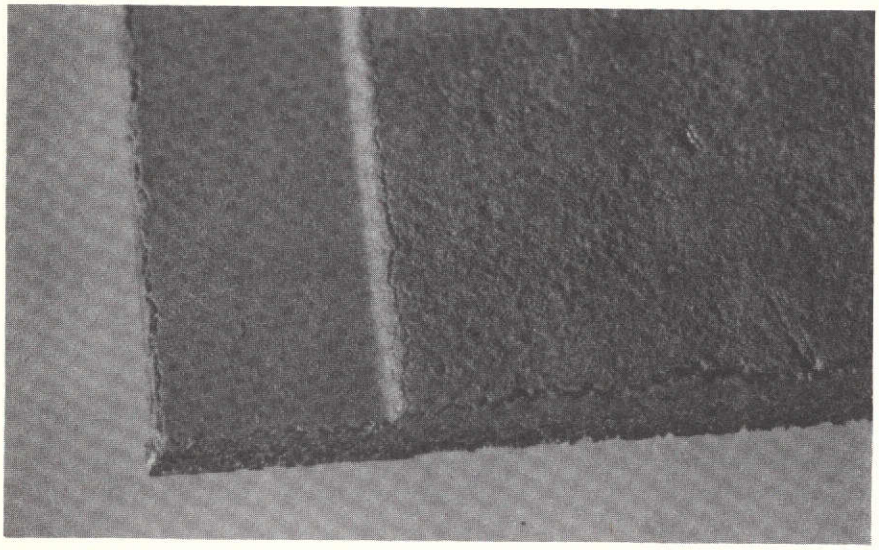

Figure 45. Type C Plaque - Cut at TRW 10X

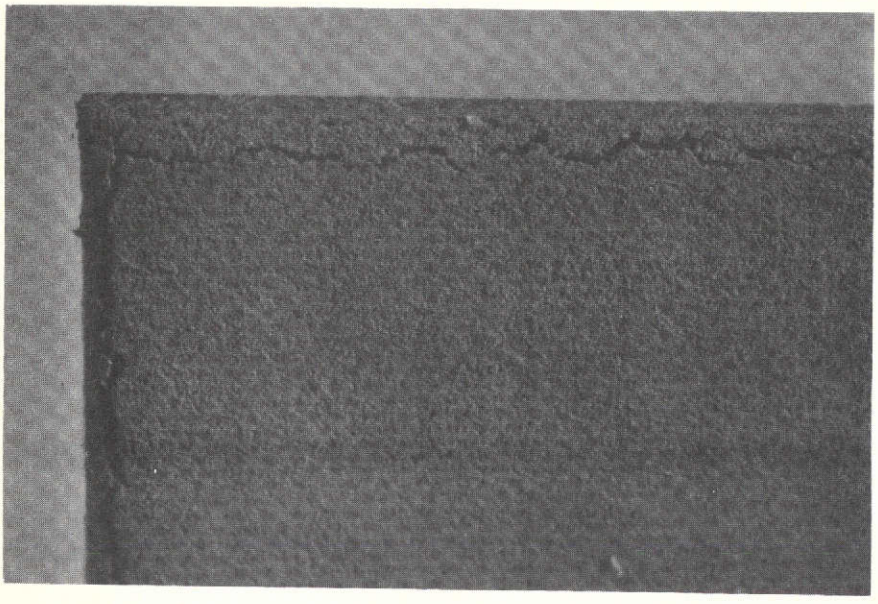

Figure 46. Type D Plaque - Cut at TRW 10X

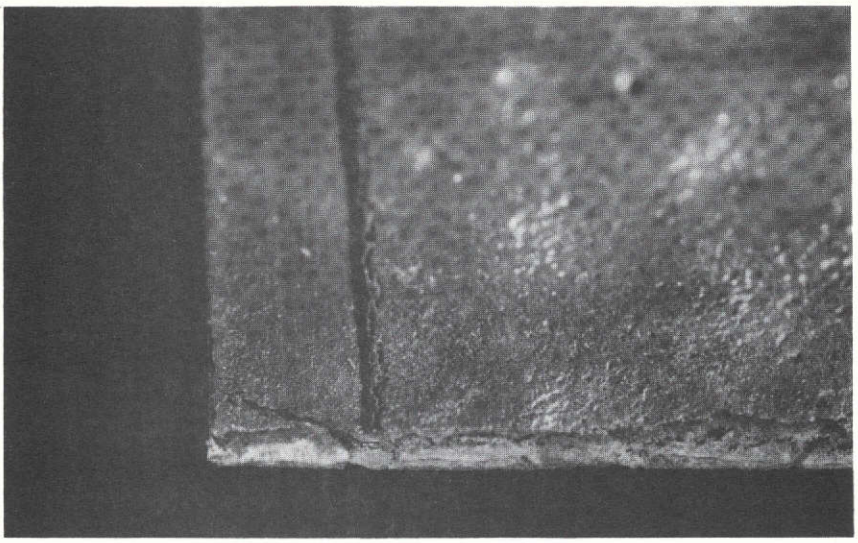

Figure 47. Type A Positive Plate - Sheared 8X

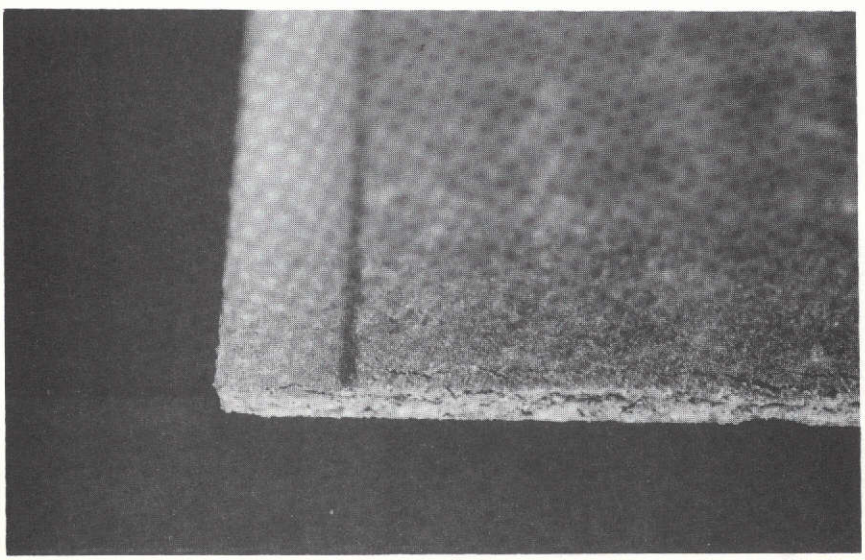

Figure 48. Type D Positive Plate - Sheared 8X

Type	Positive Plate	Negative Plate
A	Cracked at one point near middle	Cracked at several points
B	Several hair-line cracks, uniformly spaced	No visible cracking
C	No visible cracks	Several hair-line cracks
D	Cracked at one point	Cracked at one point
E	No visible cracks	Cracked at several points
F	Cracked at several points	Cracked at one point

In most cases these cracks were easily visible, particularly when the plate was flexed slightly. There was appreciably more loss of sinter at noncoined edges of these cracks than at coined edges.

Other tests involved dropping plates with coined and uncoined edges onto the bench-top from a height of 1 foot, and tapping plates on their edges on the bench-top, in a manner that might be expected during cell production. It was observed that, generally, the coined edges suffered less damage than uncoined edges. However, the results were erratic and not repeatable, and hence this type of test was not pursued further.

Another mechanical test that gave more repeatable results and that gives a good still-photographic representation was developed. This test is performed as follows: A strip 1 cm wide and 7 cm or more long is cut from the plate. This strip is then "bent" around a polished, 3/8 inch diameter stainless steel rod at intervals determined by the hole pattern in the grid. When a length of about 4 cm has been so bent, the strip is pulled back and forth against the rod many times until it appears that the condition of the piece has stabilized, i.e., no further cracking or loss of material (if any) occurs. The resulting specimen is then inspected and photographed under 2 to 3X magnification.

Photographs of specimens of plate materials, after being subjected to the above-described test, are shown in Figures 49 through 56. Figures 55 and 56 show that there is a difference in the result depending on whether the strip is cut along the machine direction (referring to the plate strip during manufacturing), i.e., at the side of the plate, or across the machine direction, i.e., along the bottom of the plate. Bending the material in the same direction it was rolled on the machine causes less damage.

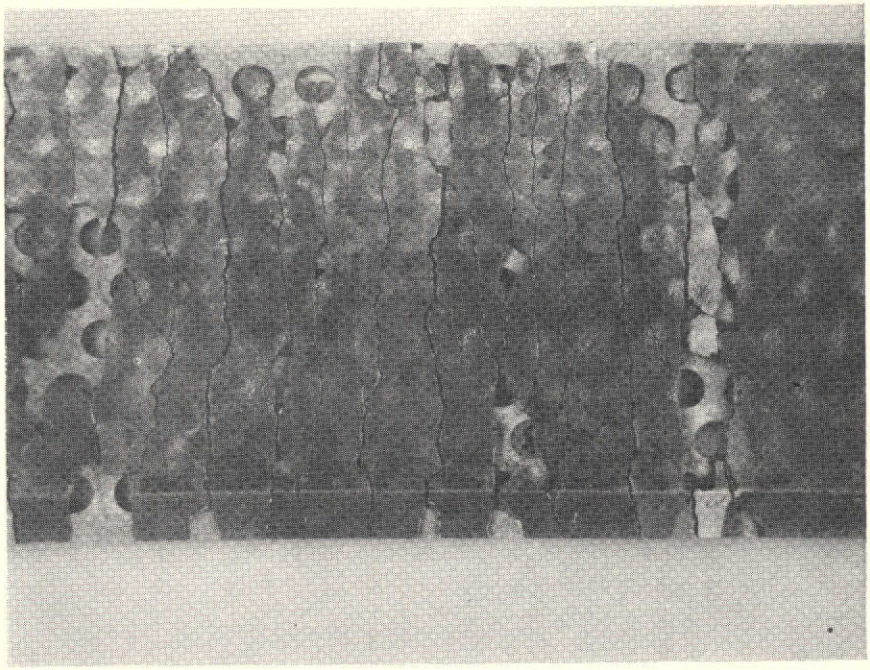

A. Positive

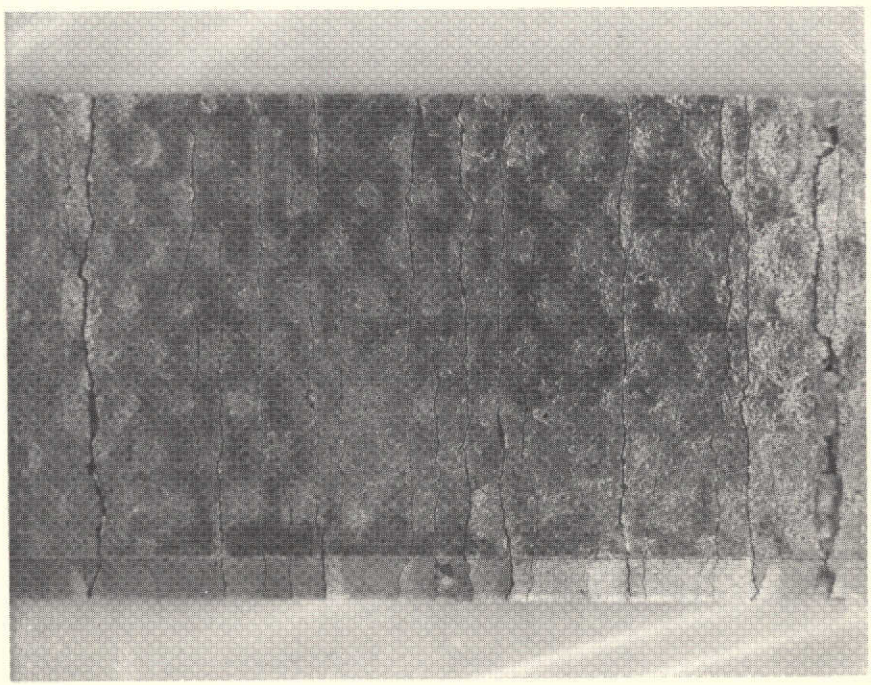

B. Negative

Figure 49. Type A Plate - Bend Test Specimens 3X

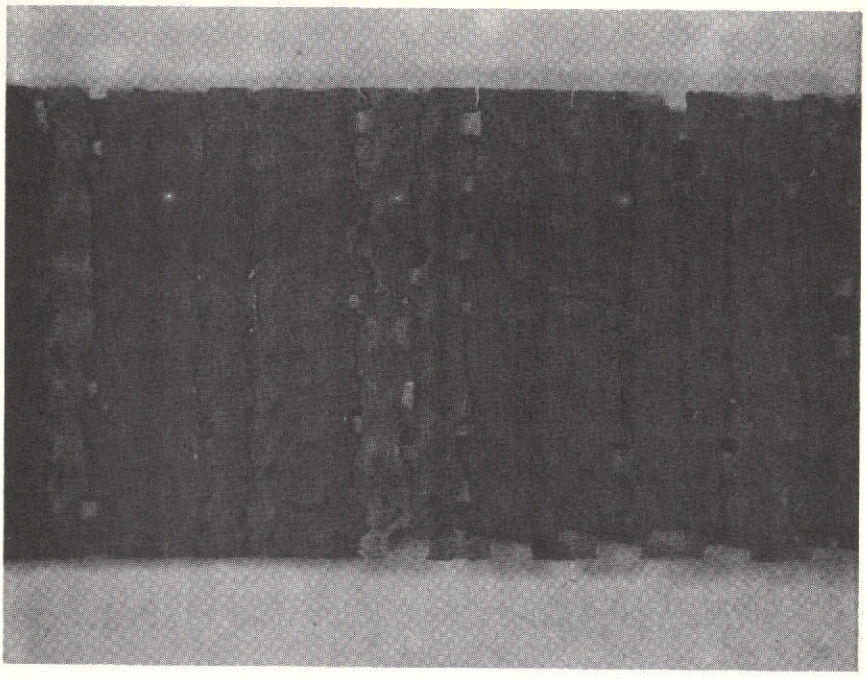

A. Positive

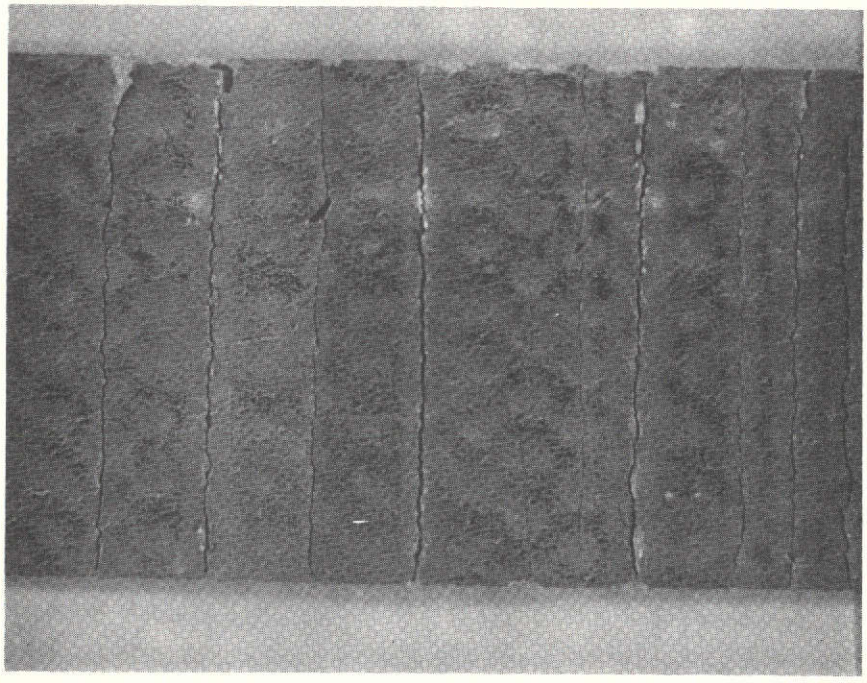

B. Negative

Figure 50. Type B Plate - Bend Test Specimens 3X

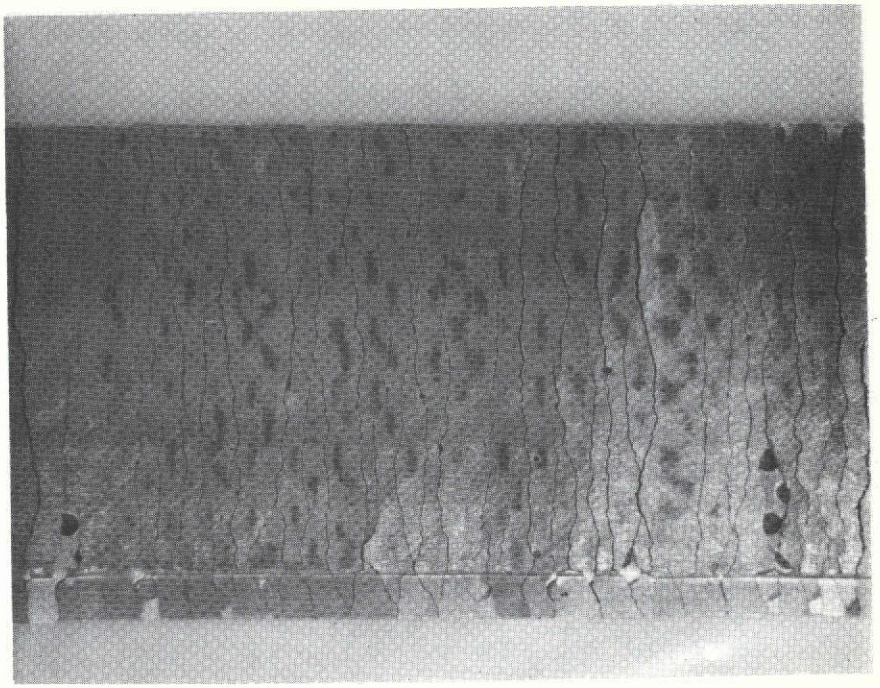

A. Positive

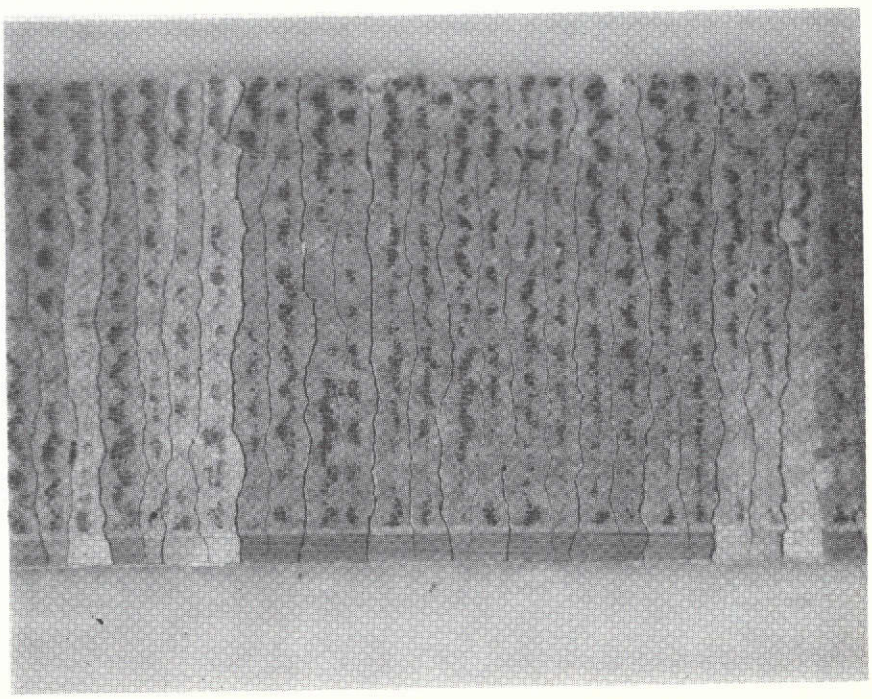

B. Negative

Figure 51. Type C Plate - Bend Test Specimens 3X

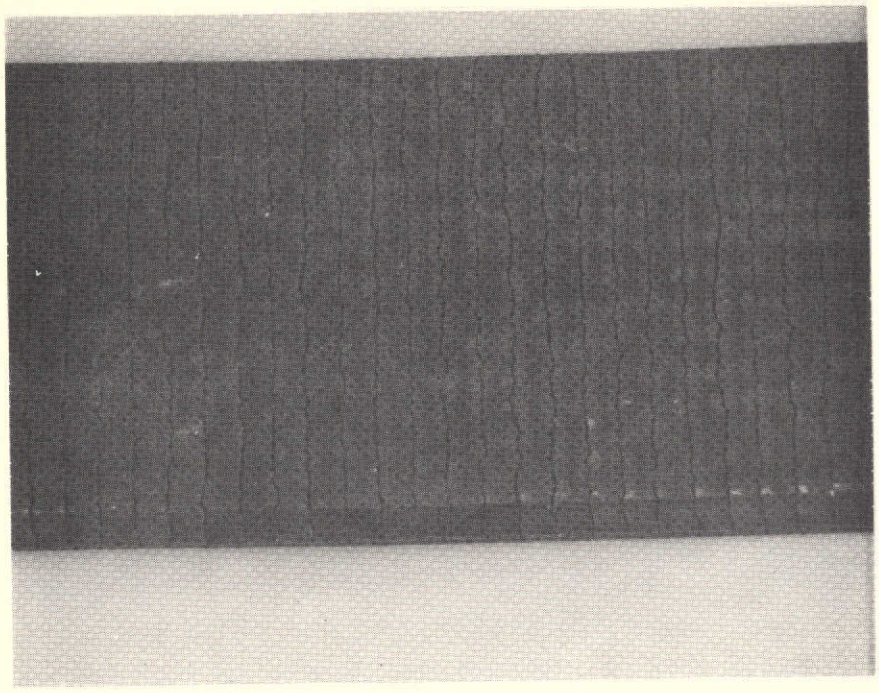

A. Positive

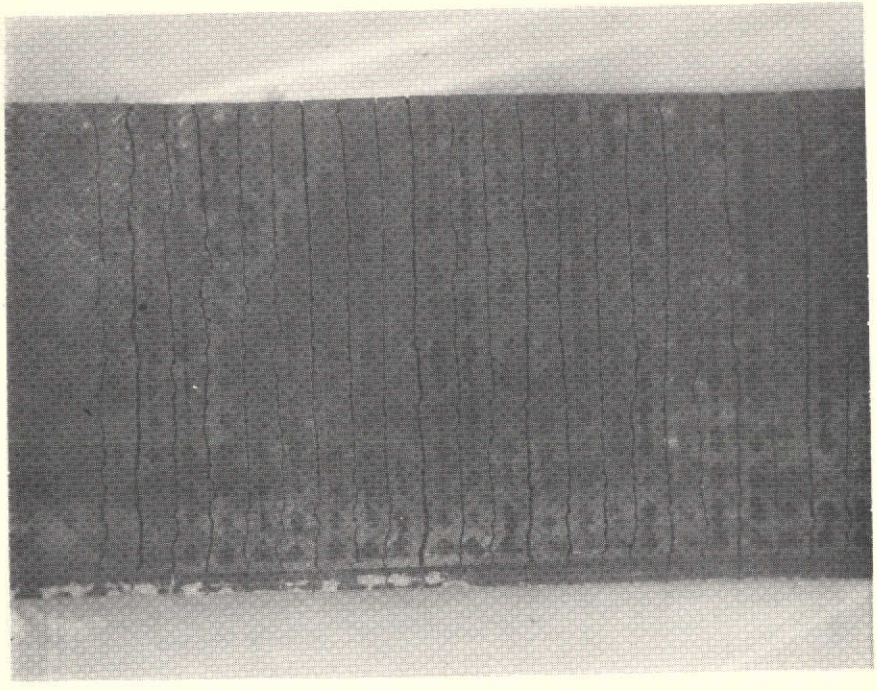

B. Negative

Figure 52. Type D Plate - Bend Test Specimens 3X

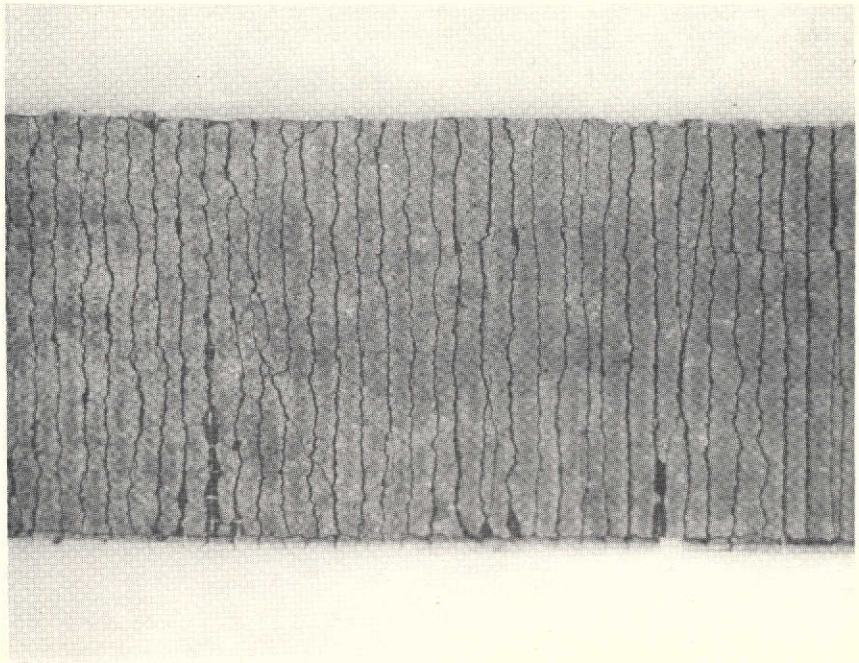

Figure 53. Type E Positive Plate - Bend Test Specimens 3X

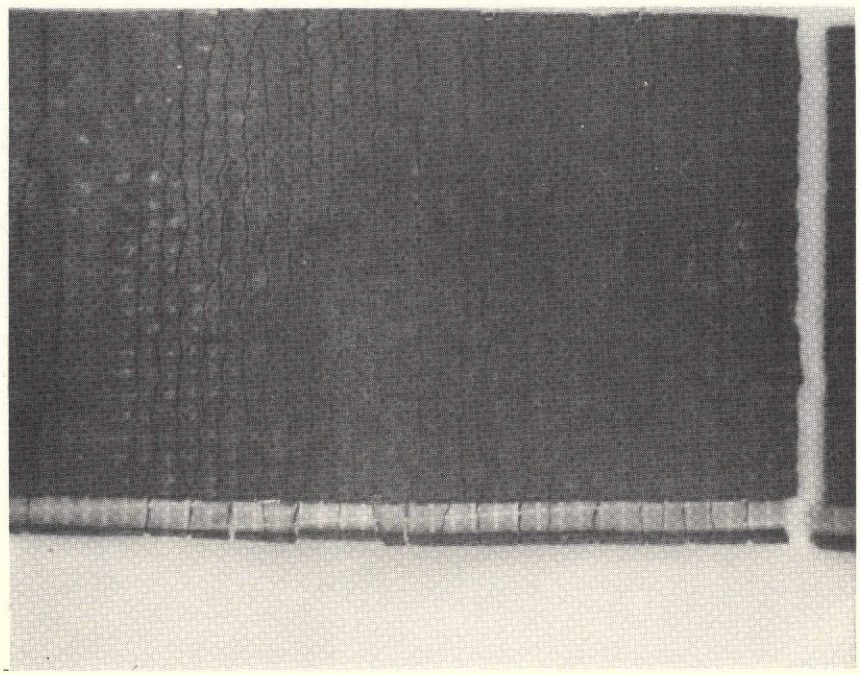

Figure 54. Type F Positive Plate - Bend Test Specimens 3X

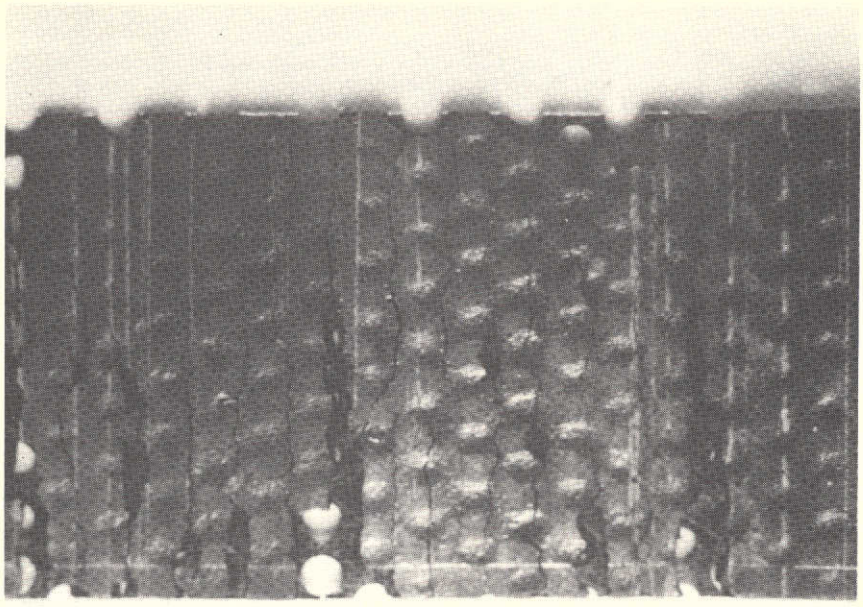

A. Side

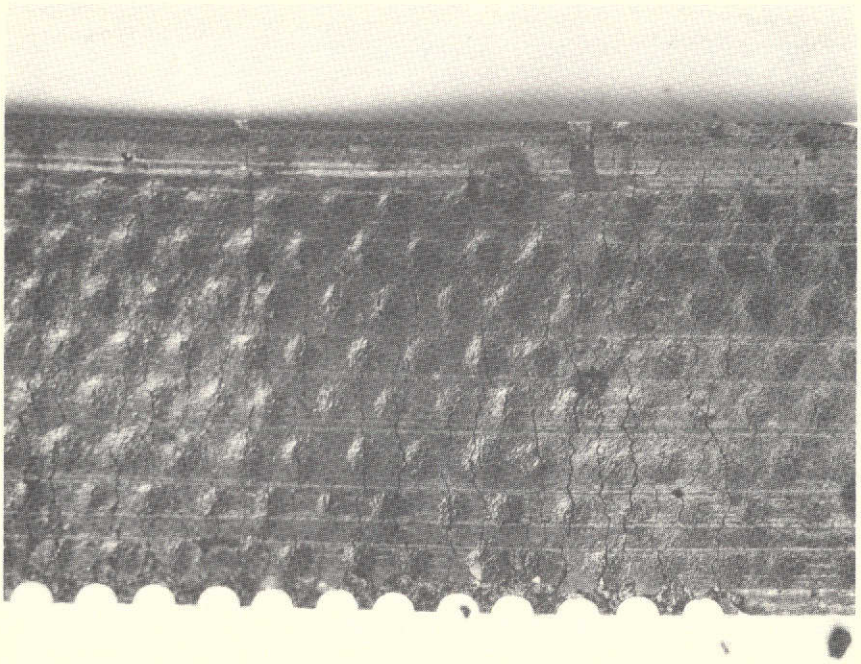

B. Bottom

Figure 55. Type G Positive Plate - Bend Test Specimens 3X

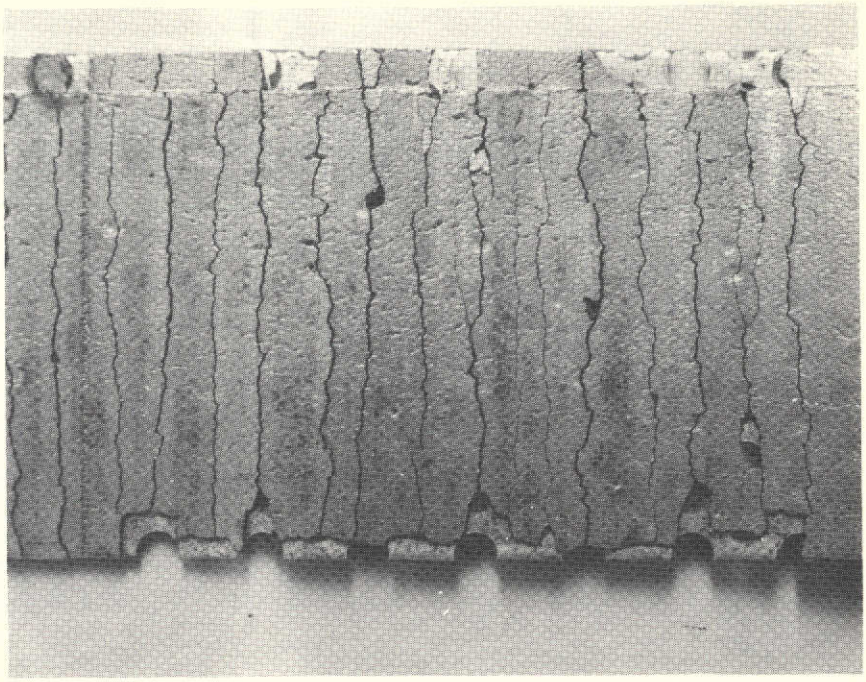

A. Side

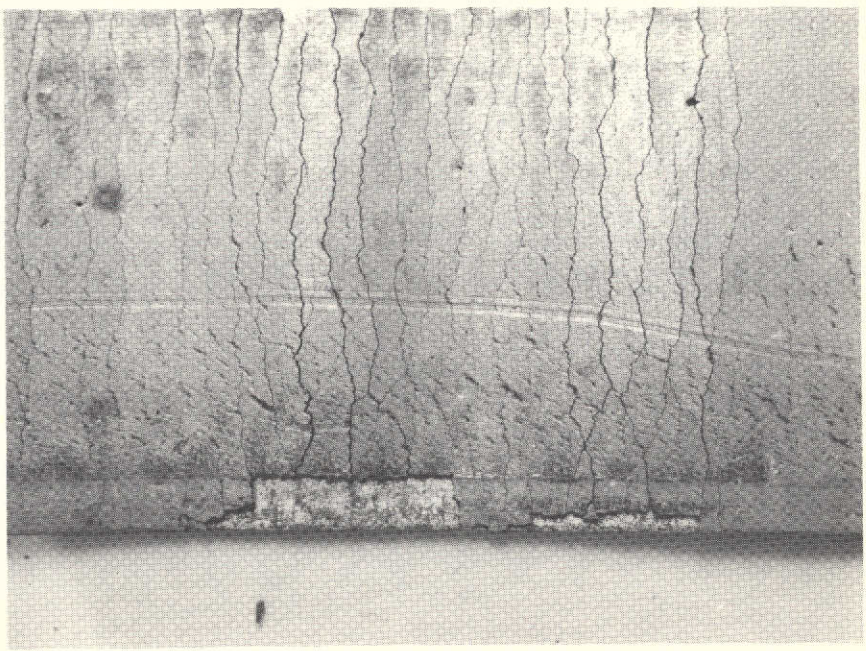

B. Bottom

Figure 56. Type G Negative Plate - Bend Test Specimens 3X

5. VIBRATION TESTING IN A SEALED CELLS CONFIGURATION

5.1 PURPOSE OF TESTING

The purpose of vibration testing in a real-cell configuration was to determine whether damage to the edges or other plate areas can be caused by the type of vibration testing seen by most spacecraft cells during cell and/or battery acceptance testing and during actual launch of a spacecraft.

5.2 APPROACH

Groups of plates from each supplier were subjected to vibration testing in a real-cell configuration. The cells used were assembled at TRW using reusable cell cases designed and fabricated by TRW for this type of work. These cells are easily disassembled for inspection of internal components.

5.3 TEST CELL CONSTRUCTION

A photograph of the internal structure of one such assembly is shown in Figure 57. The body of the cell case is made of high-density polypropylene. O-rings are used to seal the faceplates to the body. The faceplates are interchangeable, and either stainless steel or lucite faceplates may be used. Use of lucite plates allows the interior of the cell to be seen easily at all times. A gland on the side of the cell allows two additional leads to be introduced for auxiliary electrodes or thermo-sensors. The integrity of this cell and the seal used has been demonstrated by successful operation of 36 of these assemblies for 18 months with frequent pressure cycles up to 75 psig.

Seven positive and eight negative plates were put into each cell for vibration testing. Nylon separator material, Pellon Type 2505, was used for the test assemblies, as the inside thickness dimension of the case is 0.580 inch, the average interplate spacing varied from 0.006 to 0.008 inch. For the vibration testing stainless steel faceplates were used to close the cells. The completed cells appeared as shown in Figure 58, except no pressure gauge was attached during vibration.

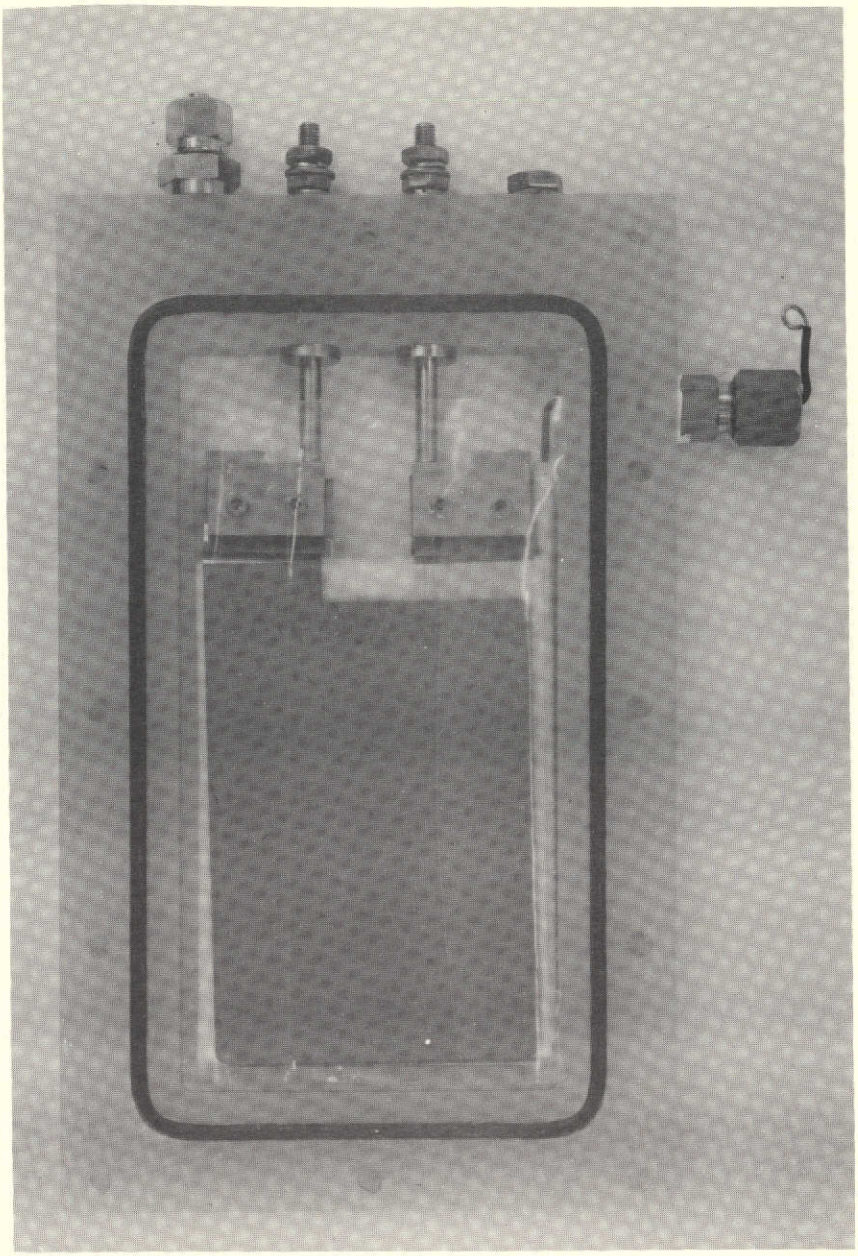

Figure 57. Internal Construction of Reusable Test Cell

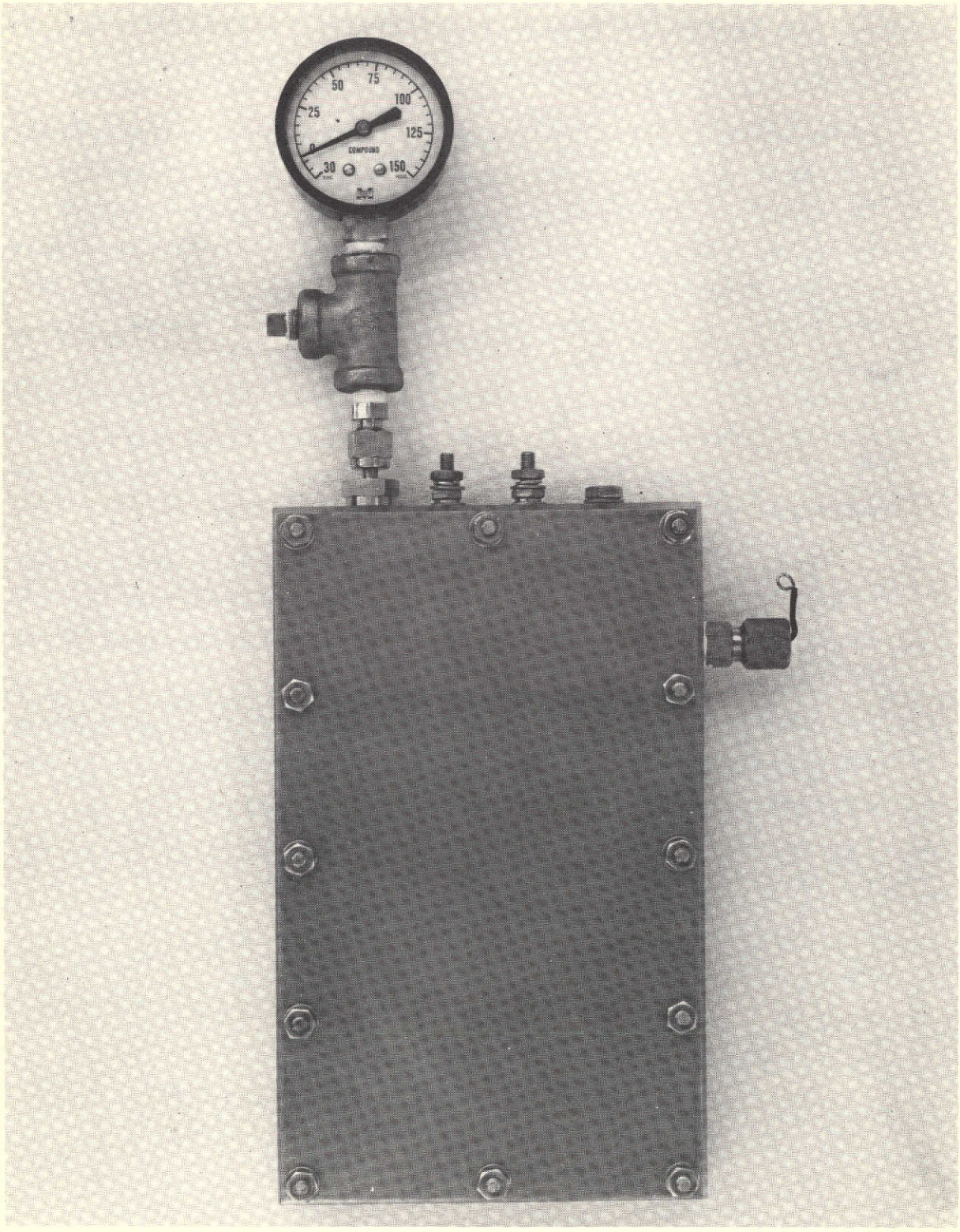

Figure 58. Reusable Cell Assembly

The contract Statement of Work calls for vibration testing to be performed using JPL Document TS 504550 Rev. A, Environmental Test Specification, Section 3.8.8.4, as a guideline. Because the designated specification would apply to a battery as a unit, and not necessarily to an individual cell, the requirements were modified by mutual agreement between TRW and JPL to correspond to the results of an analysis performed on the current V075 battery structure. This analysis showed that the sine wave spectrum shown in Figure 59 is appropriate at the cell level for all three directional axes, with the exception of a narrow peak at 300 cycles in the Y-axis. Also, the random vibration spectrum shown in Figure 60 is appropriate at the cell level for the X- and Z-axes. The orientation of these axes is shown in Figure 61. Since only movement in the X-axis would contribute to damaging the edges of the plates, testing was performed only in the X-axis direction.

Each cell was tested individually. Sinusoidal testing was conducted at a scan rate of one octave per minute, with one upsweep and one down sweep per cell. Random vibration testing was conducted at an overall wideband level of 12.16 g's rms, for five minutes per cell.

After vibration testing was completed each cell was disassembled and all plates and plate edges inspected. No signs of damage attributable to the vibration testing was seen on any of the plates.

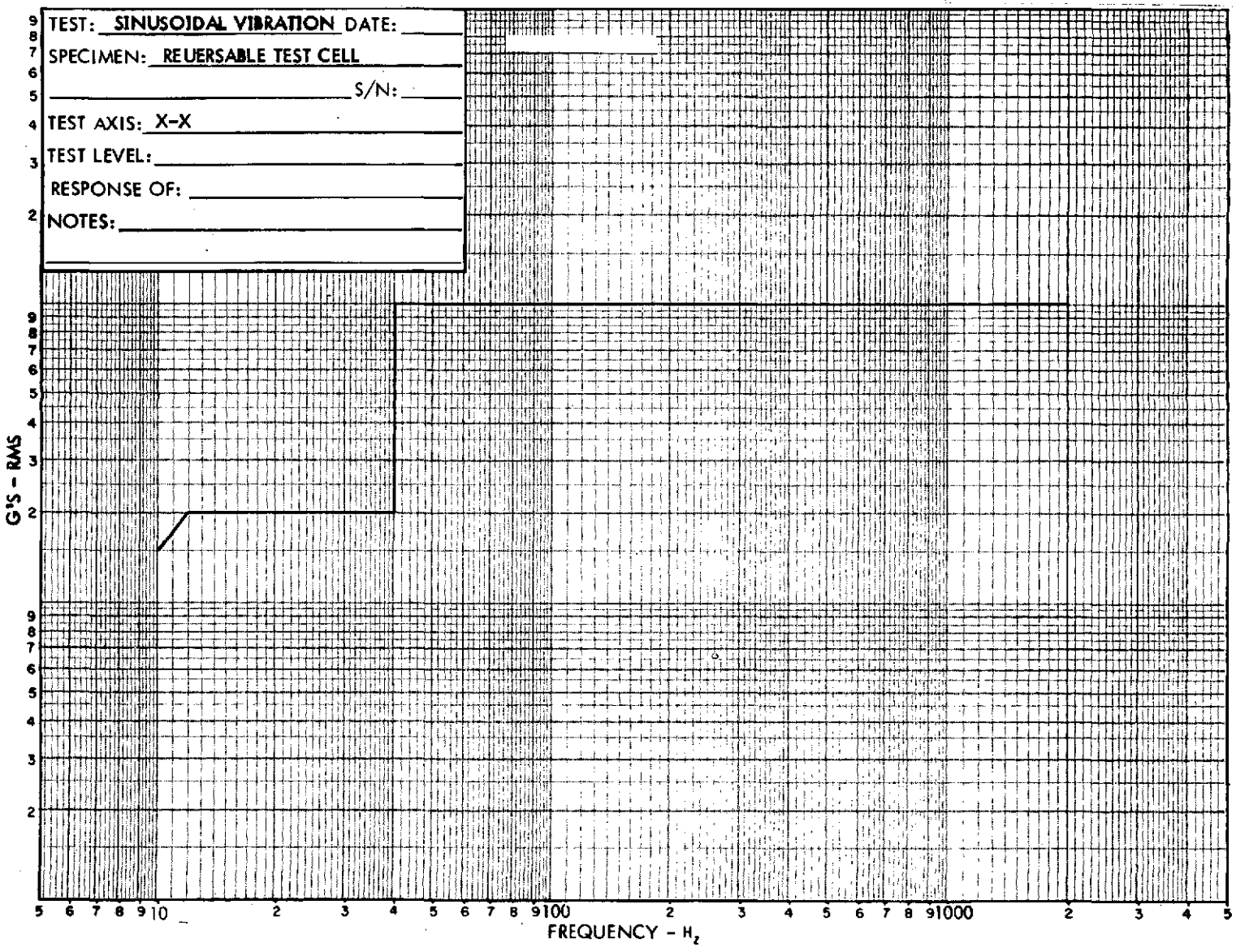

Figure 59. Sine Wave Vibration Test Spectrum

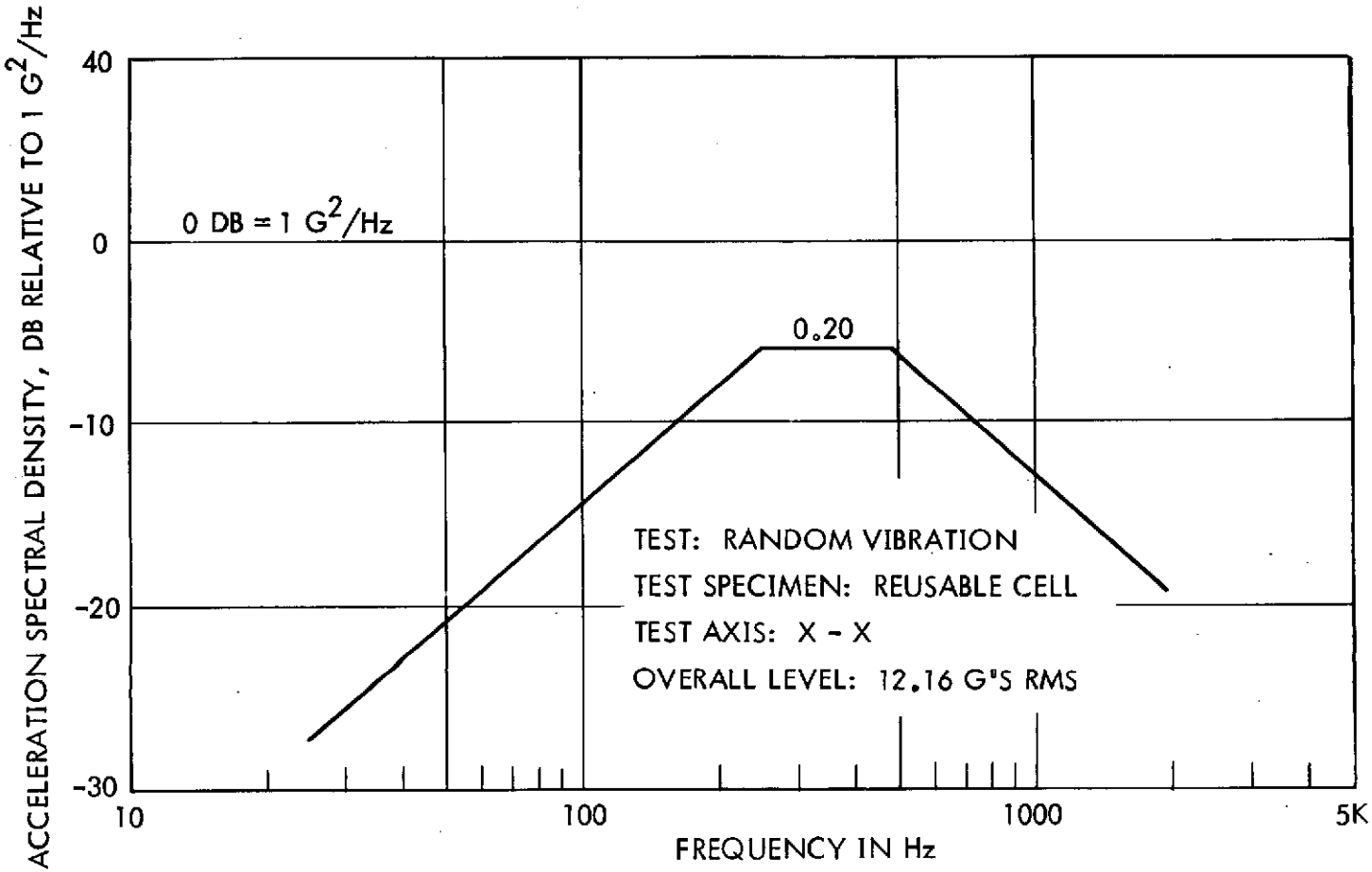

Figure 60. Random Vibration Test Spectrum

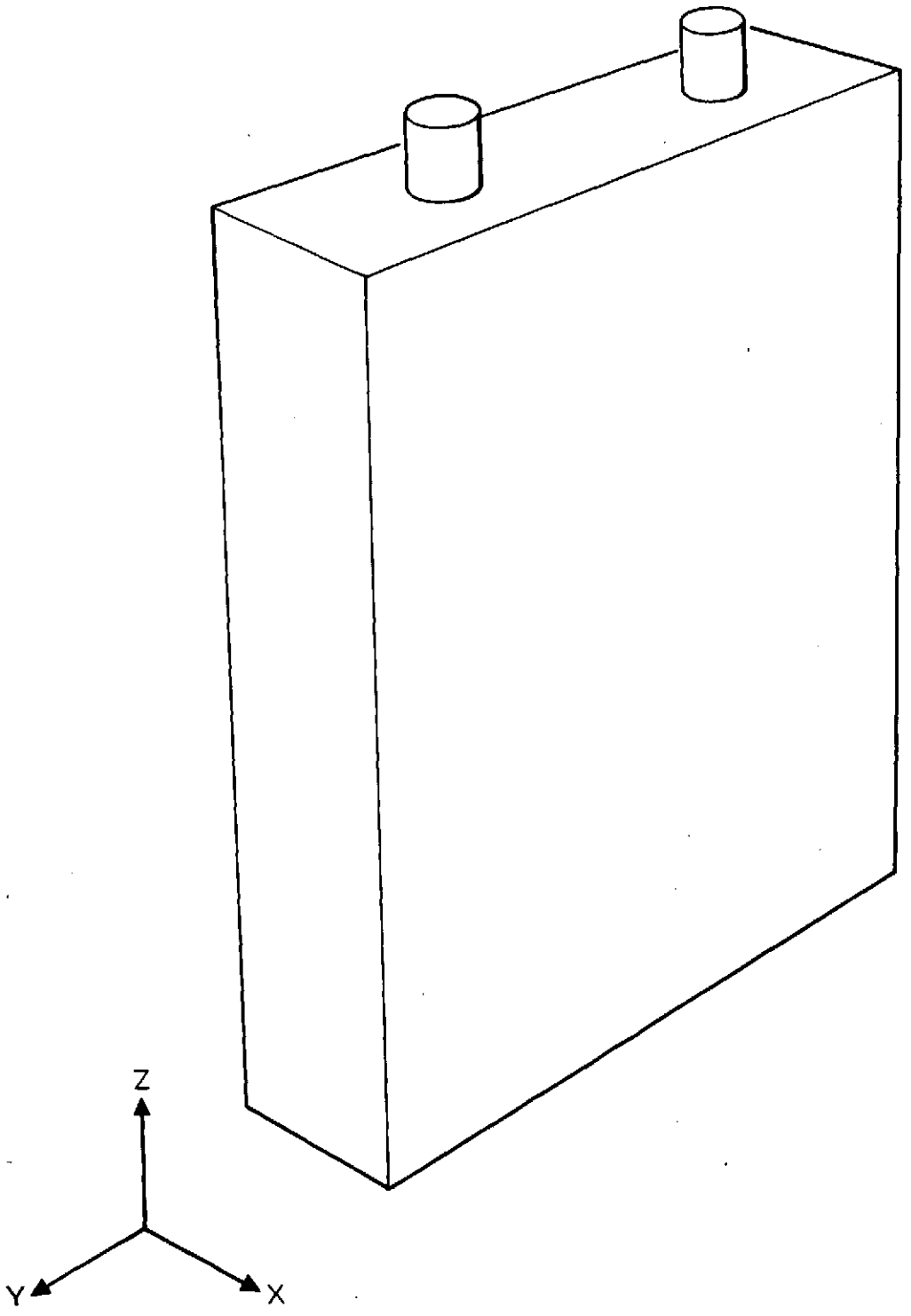

Figure 61. Vibration Axes Orientation

6. ELECTROCHEMICAL TESTING

Two types of accelerated electrochemical tests were performed in this study. One was a rapid, comparative test applicable to individual plate samples; the other involved a real cell configuration where the plates are constrained by contact with separator layers under normal compression.

6.1 ACCELERATED TESTING IN OPEN CELLS

6.1.1 Test Method Development

Because the type of test required is not standardized and had not been performed under controlled conditions previously in this laboratory, some development was necessary. The test was to take several facts into account, namely:

a) Sintered plates cycled without constraint by separators tend to swell and disintegrate more rapidly than those under constraint.

b) Repeated cycling increases the rate of swelling relative to simple continuous overcharge or overdischarge.

c) Higher KOH concentrations in the electrolyte cause more swelling of positive plates than lower concentrations.

d) Rapid gas evolution contributes to disintegration of plates.

The objectives of the development work were to arrive at a procedure that would produce the desired result in a 24-hour period, with the desired result being the generation of damage effects at edges that are clearly visible (at least under 5X magnification) and that there be a range of severity from coined to uncoined edges and from one supplier's material to another.

Exploratory tests were conducted with plates suspended freely in a large excess of electrolyte. Concentrations of KOH of 25, 34, and 40 percent were tried. Electrical procedures tried included a) charging only for 24 hours at current densities of 0.5, 1.0, and 2.0 A/dm^2 (corresponding roughly to the 0.2C, 0.4C, and 0.8C rates based on currently available positive plate loadings); and b) cycling for 24 hours at current densities up

to 3 A/dm^2 with charge and discharge times such that each plate was overcharged and overdischarged on each cycle, and hence gassing freely at the end of each half-cycle. All tests were run at room temperature (22° to 24°C).

The results of this preliminary work showed that negligible damage occurred to the plates tested after 24 hours continuous charging at $0.5A/dm^2$ at any of the KOH concentrations used. Some edge damage occurred to the more brittle positive plate materials during continuous charging at 1 A/dm^2, and more damage yet was produced at 2 A/dm^2. Results were generally the same in all three concentrations of KOH tested, but were spotty and not reproducible. No appreciable edge damage was seen on negative (cadmium) plates subjected to these conditions.

The cycling tests gave more positive results. Exploration of this test method was begun with positive plates of Types A, B, C, D, and G, using a current density of 3 A/dm^2, with current reversal every two hours. A wide range of effects were produced which were about the same in either 34 or 40 percent KOH. The appearance of those plates showing appreciable damage after completion of 24 hours cycling are shown in Figures 62, 63, and 64.

Note the curling of Type A positive plate, the large blisters near the top of one plate, and the many small blisters which formed. The coined edges along the sides of these plates remained unchanged through this test. The cut, uncoined edge at the bottom was considerably expanded and roughened, however.

As can be seen in Figure 63, the sinter structure of Type B positives was virtually destroyed on that side of each plate that faced the other plate in the cell, i.e., where current density was the greatest. Damage to the edges of these plates, which were not coined, could not be distinguished from damage to the plate surface as a whole.

Types C and D positive plates showed no visible effects of this test, except for some slight warping of Type D plates. Because these plates looked after the test as they appear in Figures 12 and 13, respectively, no photographs after testing are included here.

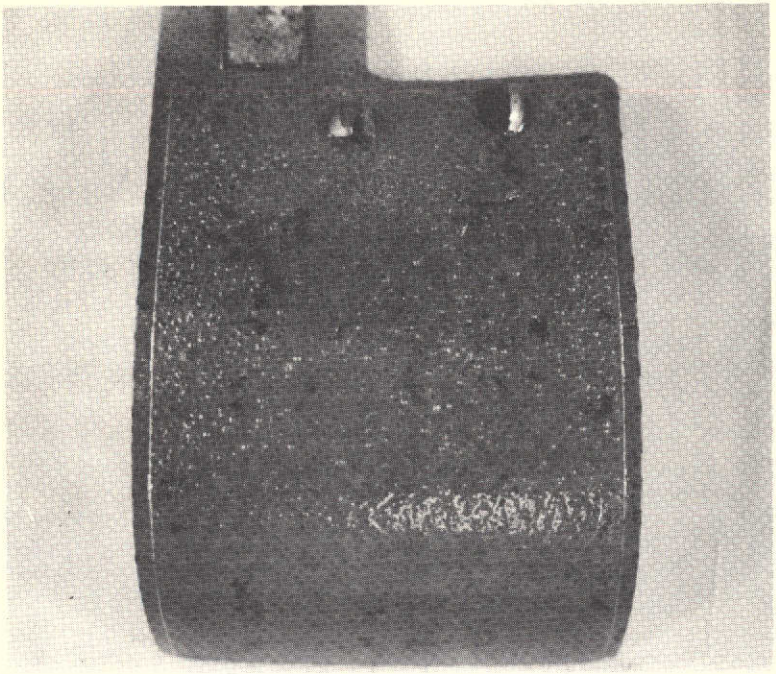

Figure 62. Type A Positive Plate - After Cycling at 3 A/dm^2

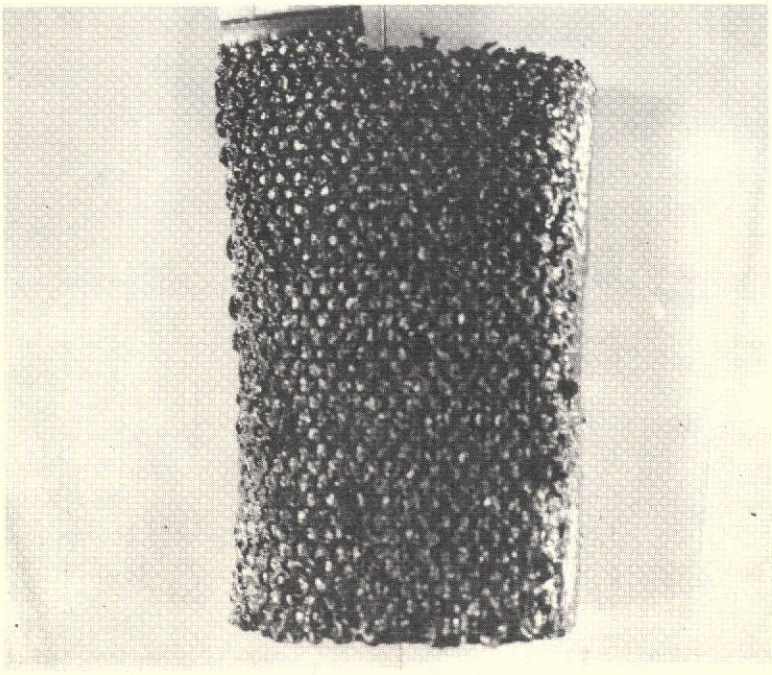

Figure 63. Type B Positive Plate - After Cycling at 3 A/dm^2

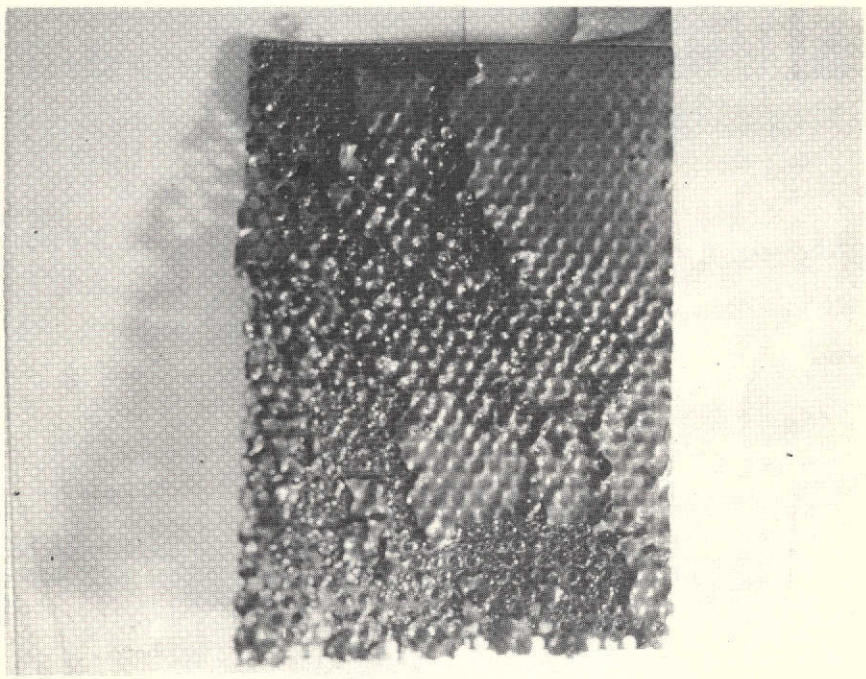

Figure 64. Type G Positive Plate - After Cycling at 3 A/dm^2

Type G positive plates showed the same type of damage that occurred to Type B material, but to a lesser extent. As seen in Figure 64, the coined border on one side of this plate largely withstood the attack, but the coined border in the other side was disintegrated. This material incorporates a thickness reduction of ten percent in coined areas of positive plates.

The severity of the damage produced by the above-described test conditions on some types of plates indicated that less severe test conditions might be adequate. Also, consultation with supplier indicated that subjecting rough-formed plate directly to such testing may produce results not typical of fully formed plate. Therefore, plates to be tested were subjected to preliminary cycling in an excess of 25 percent KOH. After an initial 24-hour charge at 0.3 A/dm^2, cycling was carried out at current densities in the range from 1.1 to 1.4 A/dm^2, with two hours of charge and two hours of discharge per cycle. The variation in current density was due to the fact that plates of different area were tested in the same series circuit. On the fifth and last cycle the discharge was allowed to continue until each cell reached 0.5 volt. The capacities per unit area of positive plate measured on this discharge were as shown in Table 7.

Table 7. Flooded Capacity Data

Type	Ah/dm^2, to 0.5 volt
A	-
B	3.90
C	3.44
D	3.84
E	2.66
F	2.54
G	3.00

After the above cycling, the plates were washed, dried in nitrogen, and inspected. No visible change in structure attributable to the cycling was seen with the exception that some outcropping of cadmium active material was seen on the surface of the Type D and Type F negative plates (both

electrochemically deposited process plates). Weight loss measurements after brushing off the surface showed that less than 5 percent of the cadmium loading had been lost. This behavior apparently is to be expected during formation cycling of this type of plate.

6.1.2 Details of the Selected Accelerated Test Method

The final outcome of the test development effort was the method described in this section.

Cells were made using two plates of the same polarity. In this study the plates were contained in open-top lucite cells made for this purpose. The inside dimensions of these cells are 3-1/4-inch wide x 1-inch deep x 7-inch high. This cell was adequate to hold a number of commercially available, aerospace-type flat plates, most of which are 2.75-inches wide and up to 6-inches long over the sintered area.

When plates that were coined on all edges were to be tested for non-coined edge effects, the coined border was sheared off along one side, usually along the bottom of the plate. Also, pieces of nickel sheet 0.005-inch thick, 0.5-inch wide, and 4-inch long were spot welded to the tabs of the as-received plates to facilitate electrical connections in the test cell.

Current was driven through the cell using a regulated power supply. A timer and switch gear was used to provide automatic cycling.

The voltage of the test cell was recorded using a strip chart recorder. The recorder was set for center zero and 5 volts full scale (±2.5 volts from center zero), as the cell voltage ranged from +1.8 volts to -1.8 volts. For individual electrode potential measurements, a low resistance Hg/HgO/KOH reference electrode was used with the open tip immersed in the electrolyte in the test cell. The test procedure as used is summarized in Table 8. Note in Table 8 that the specimen is inspected before washing and drying. This is done because it was observed that the character and visibility of many of the effects were altered considerably by drying, if not merely by rinsing the affected areas with water.

Table 8. Accelerated Cycle Test Procedure

1. Inspect plate for initial defects.
2. Shear off one coined border (optional).
3. Inspect sheared edge.
4. Spot weld auxiliary tab.
5. Weigh plate assembly (optional).
6. Perform preliminary cycling (optional).
a. Immerse and soak in 25 percent KOH solution.
b. Cycle: current 1 A/dm^2, 2 hours charge and discharge, 3 to 4 cycles.
7. Remove and inspect.
8. Immerse in 34-40 percent KOH solution.
9. Cycle: current 2 A/dm^2, 1.5 hours in each direction; 8 cycles minimum.
10. Remove and inspect.
11. Wash and dry.
12. Reweigh and calculate loss of weight (optional).

6.1.3 Results of Accelerated Electrochemical Testing

No significant effect of the accelerated test was observed on the edges or main areas of negative plates. Hence this section will deal with the results on positive plates.

The appearance of positive plates after removal from the accelerated cycle test performed as specified in Table 8 is shown in Figures 65 through 84.

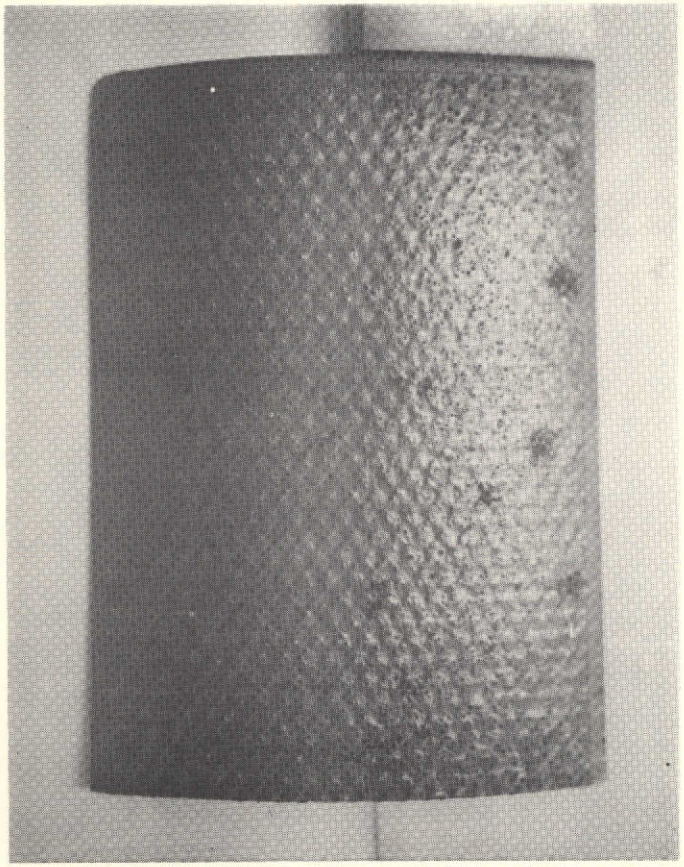

A. Plate 1

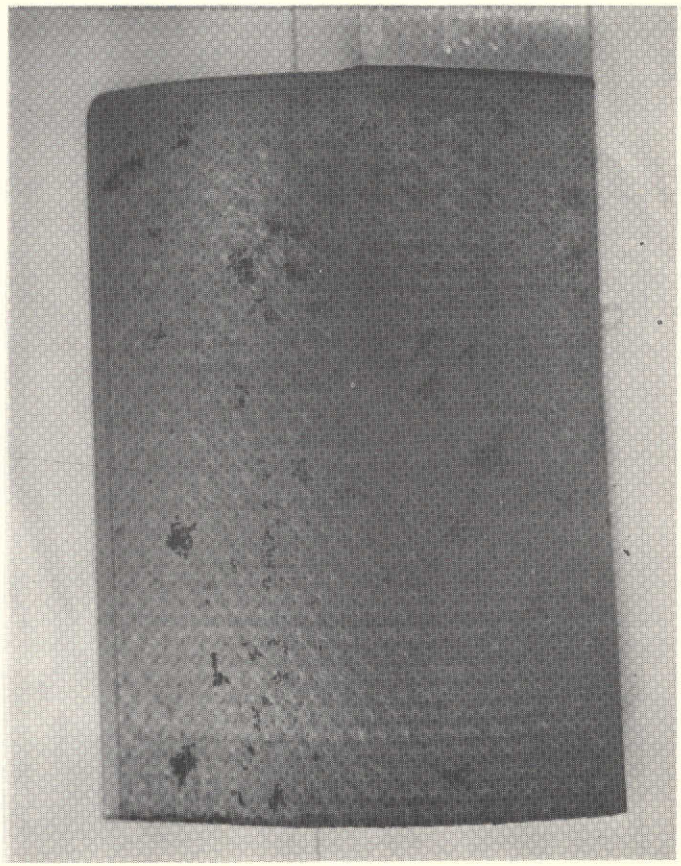

B. Plate 2

Figure 65. Type A Positive Plate After Accelerated Testing

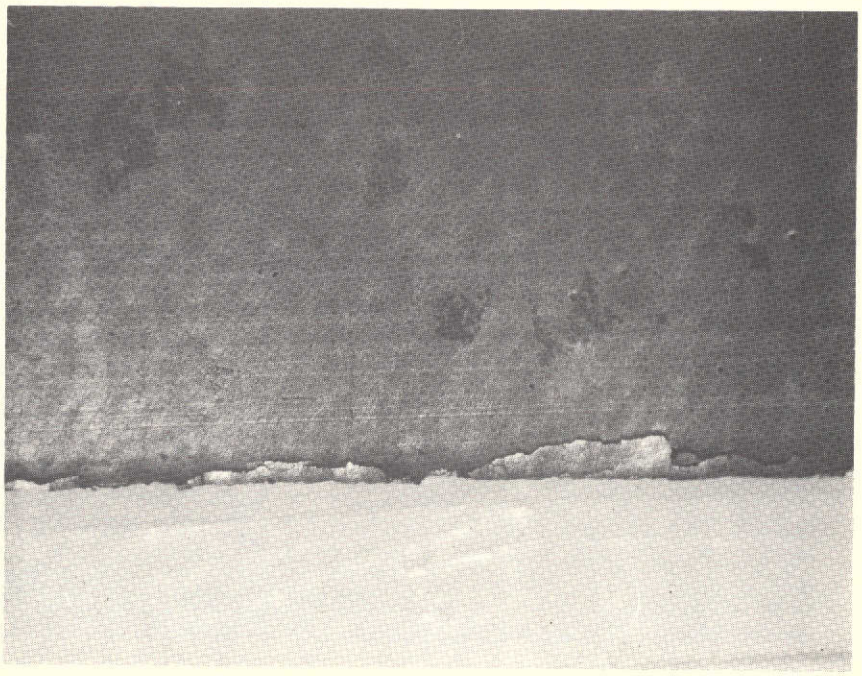

Figure 66. Type A Positive Plate - Uncoined Edge After Accelerated Testing 5X

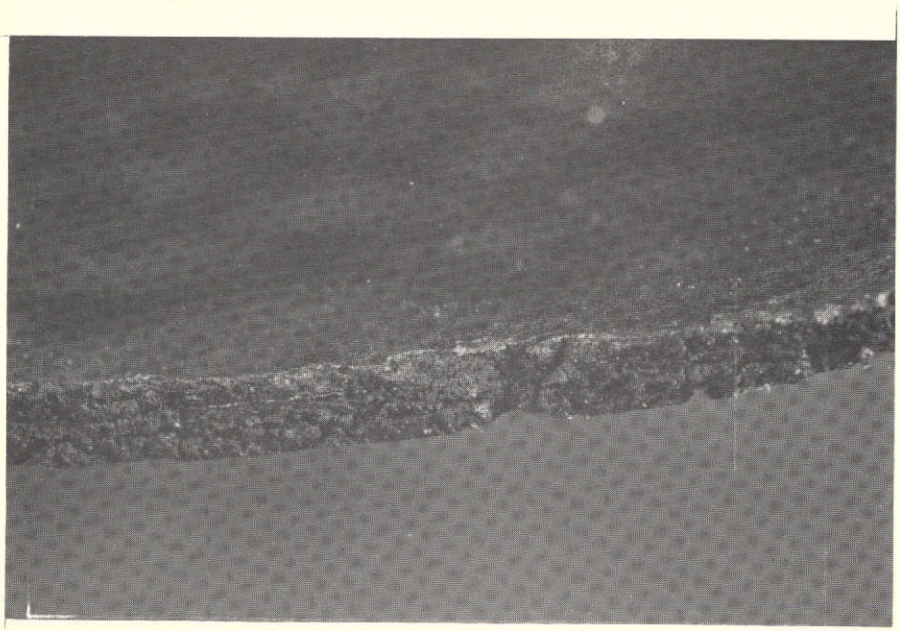

Figure 67. Type A Positive Plate - Closeup of Uncoined Edge After Accelerated Testing 10X

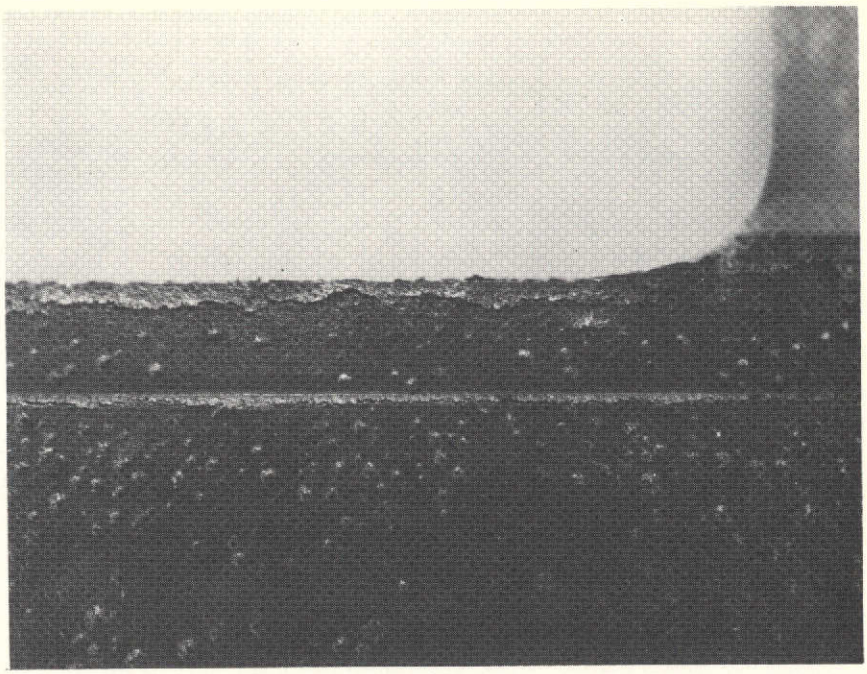

Figure 68. Type A Positive Plate - Top Edge
After Accelerated Testing 6X

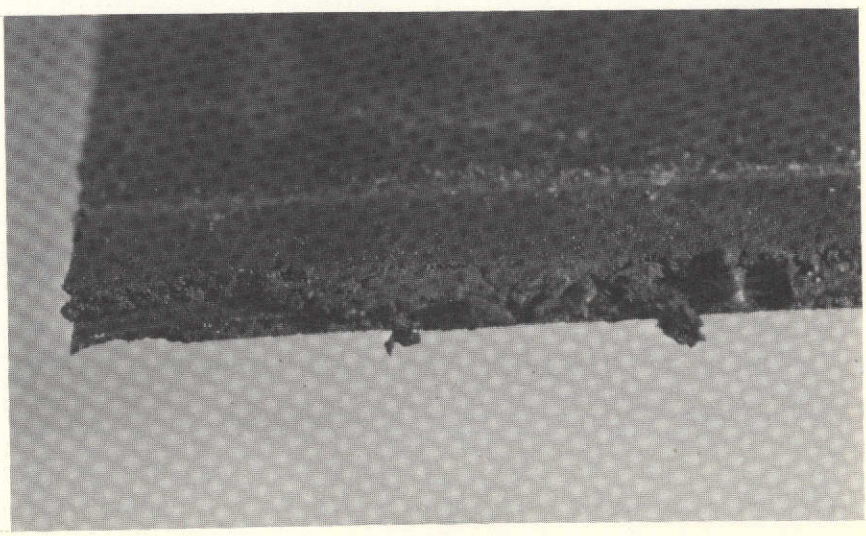

Figure 69. Type A Positive Plate - Closeup of Top Edge
After Accelerated Testing 10X

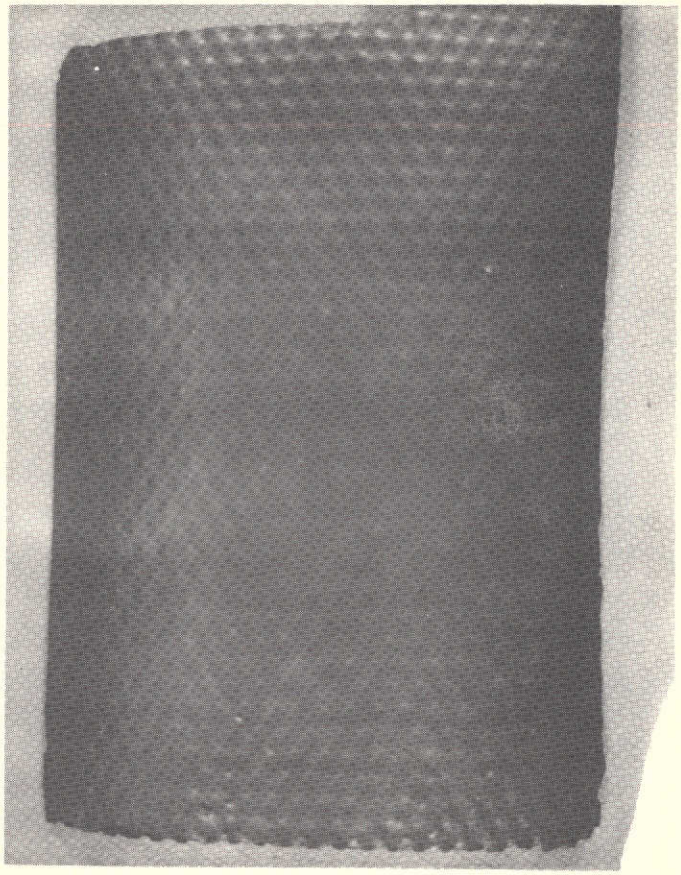

Figure 70. Type B Positive Plate After Accelerated Testing

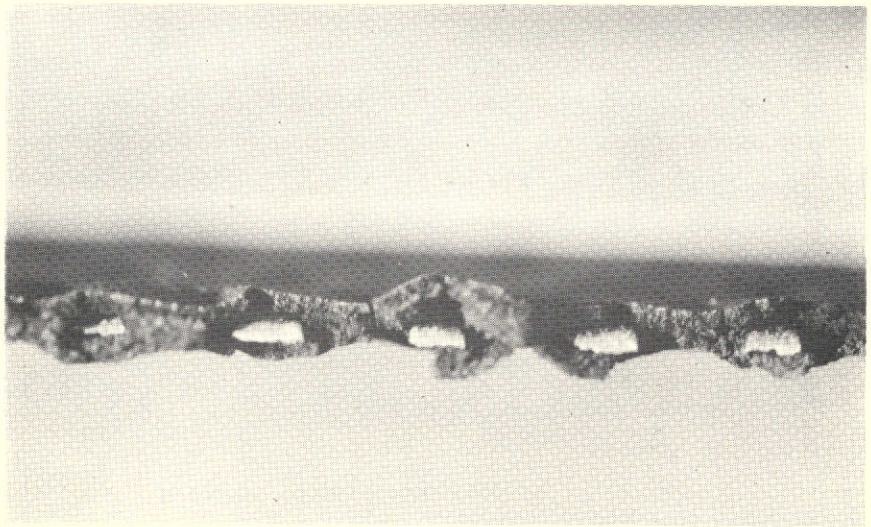

Figure 71. Type B Positive Plate - Closeup of Bottom Edge After Accelerated Testing 10X

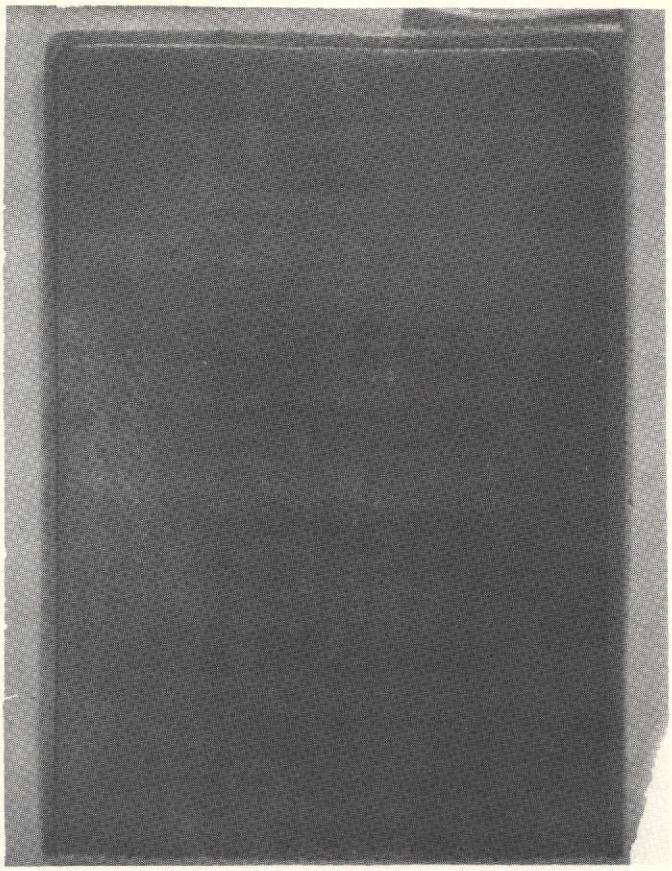

Figure 72. Type C Positive Plate After Accelerated Testing

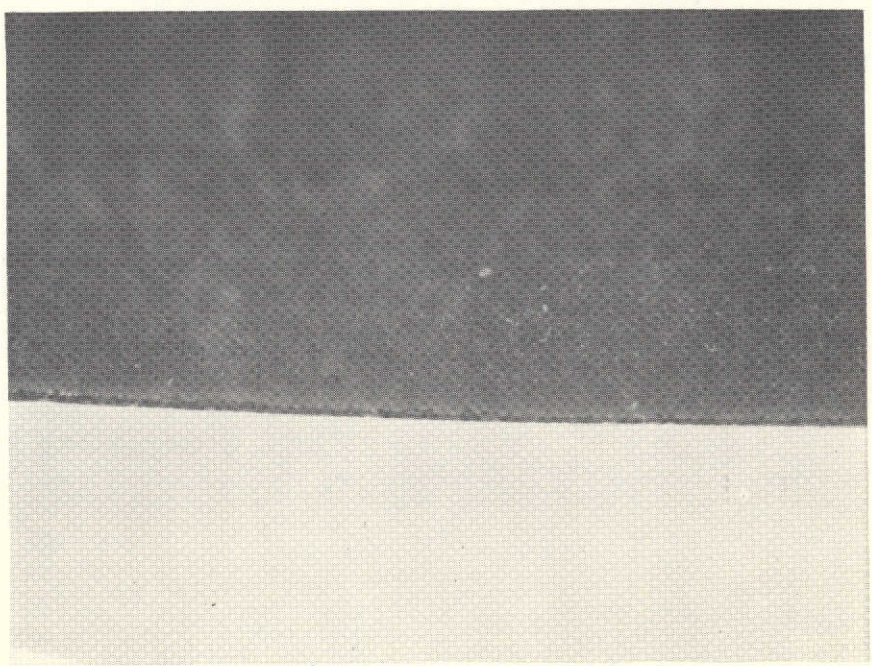

Figure 73. Type C Positive Plate - Bottom (Uncoined) Edge After Accelerated Testing 5X

C-2

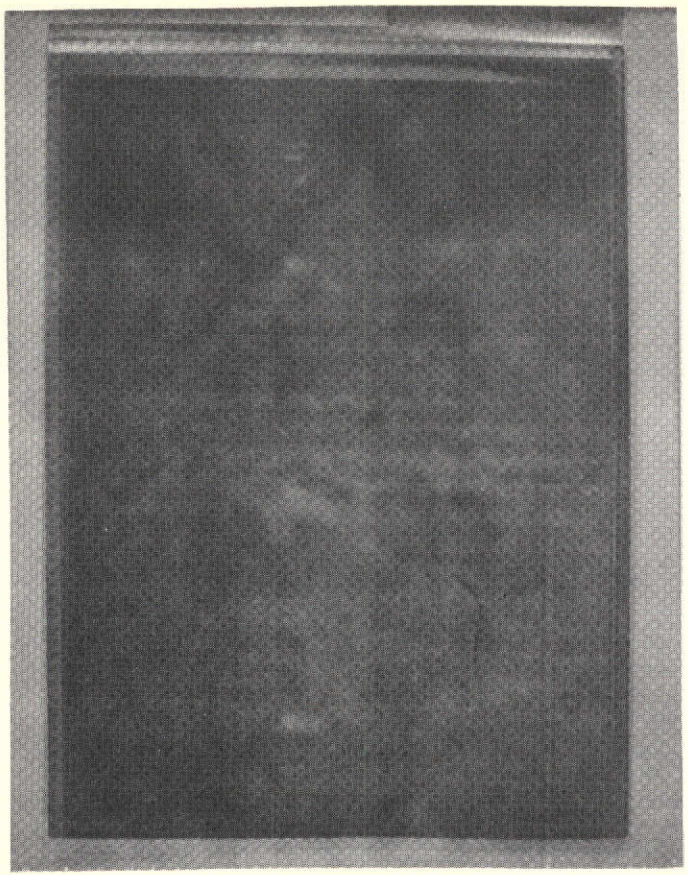

Figure 74. Type D Positive Plate After Accelerated Testing

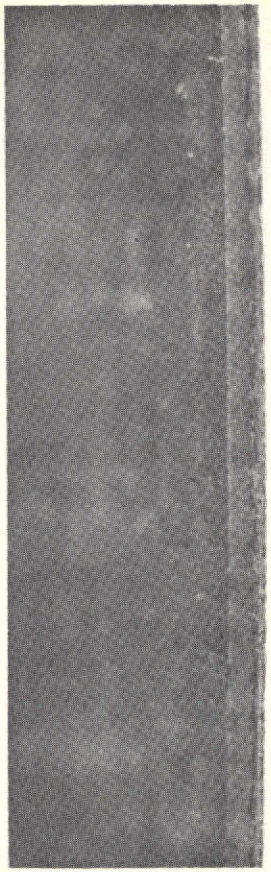

Figure 75. Type D Positive Plate - Coined Edge (Side) After Accelerated Testing 5X

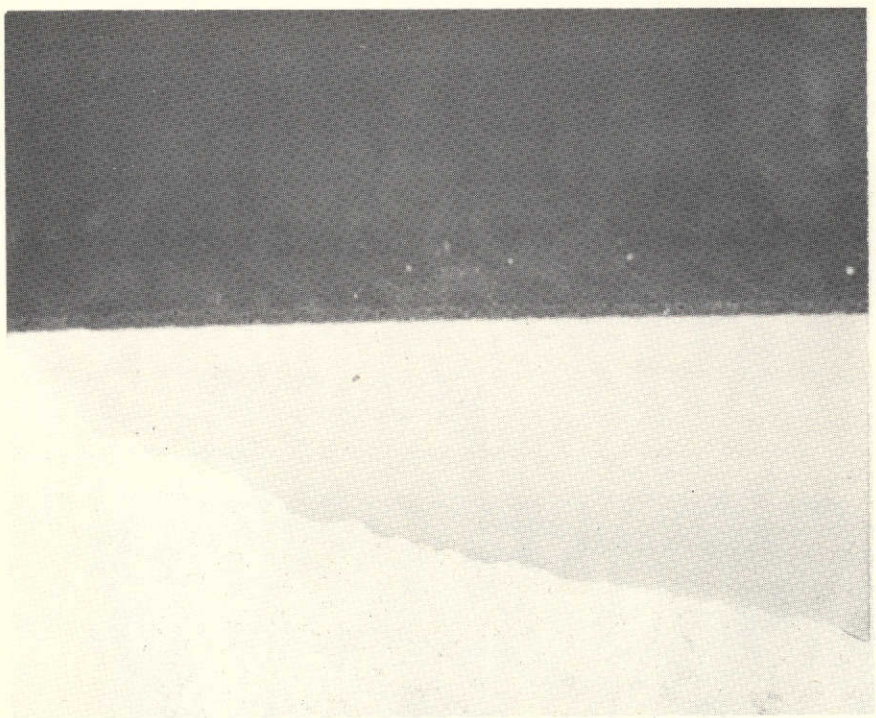

Figure 76. Type D Positive Plate - Bottom (Uncoined) Edge After Accelerated Testing 5X

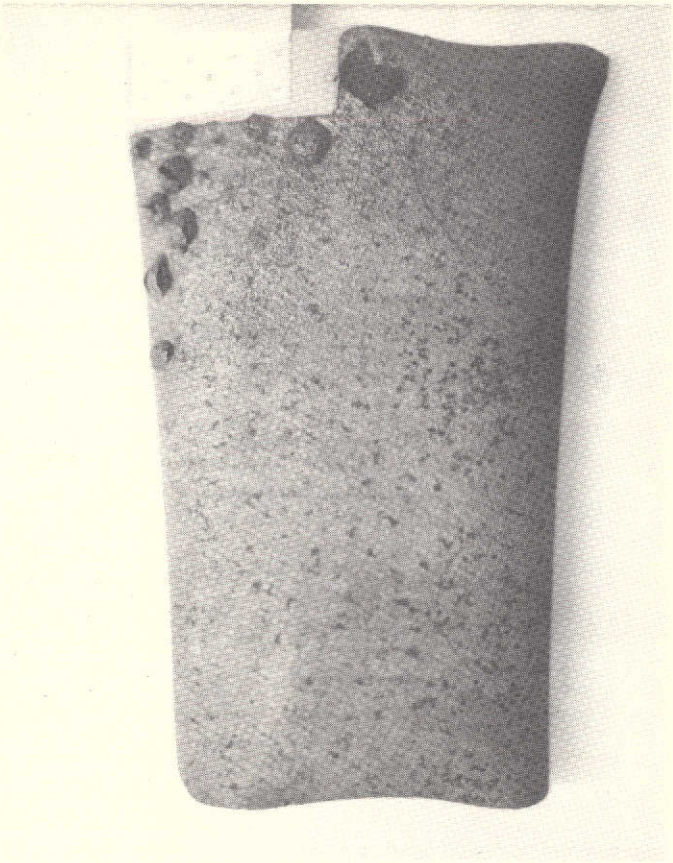

Figure 77. Type E Positive Plate After Accelerated Testing

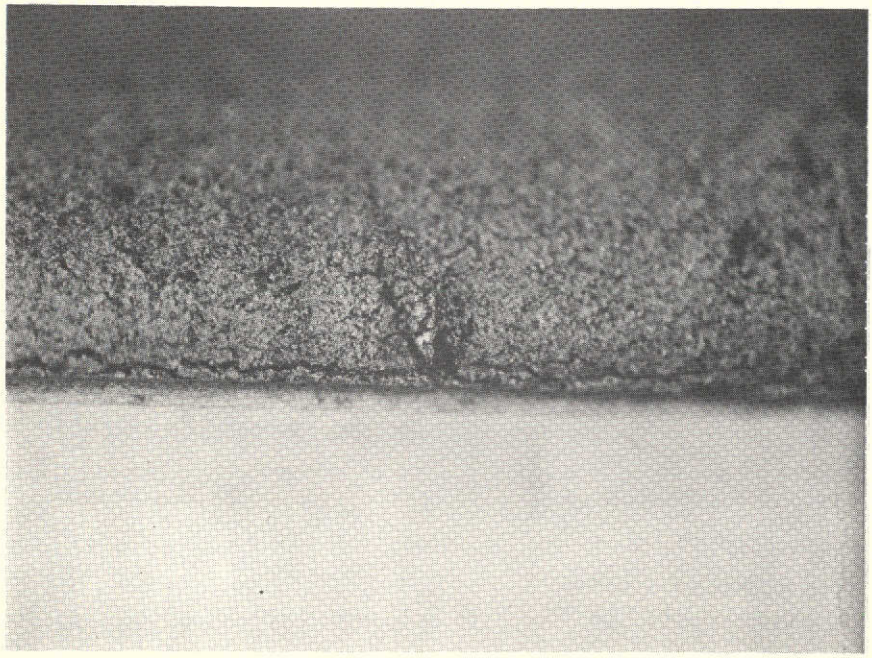

Figure 78. Type E Positive Plate - Coined Edge
After Accelerated Testing 5X

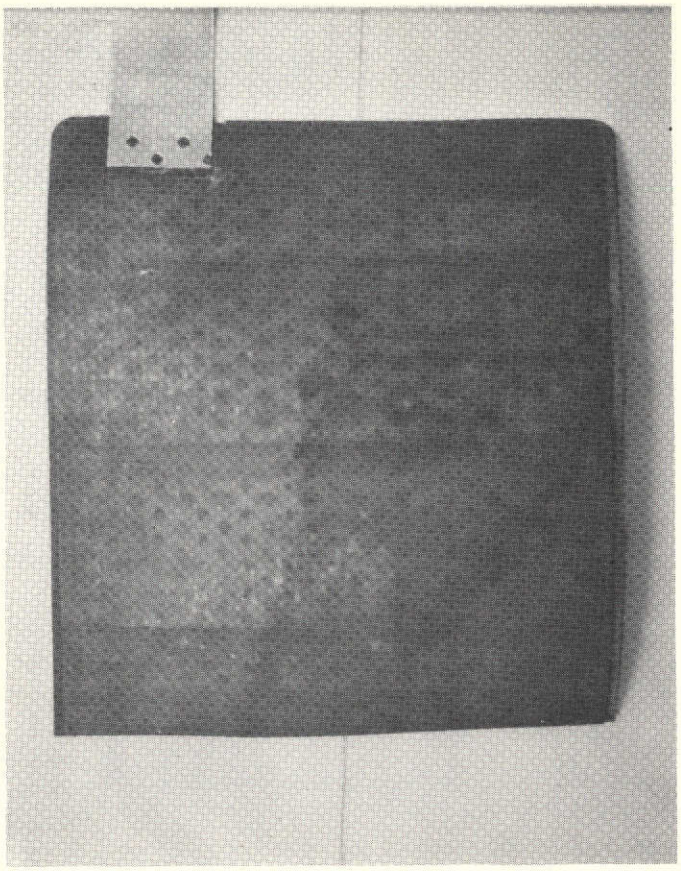

Figure 79. Type F Positive Plate After Accelerated Testing

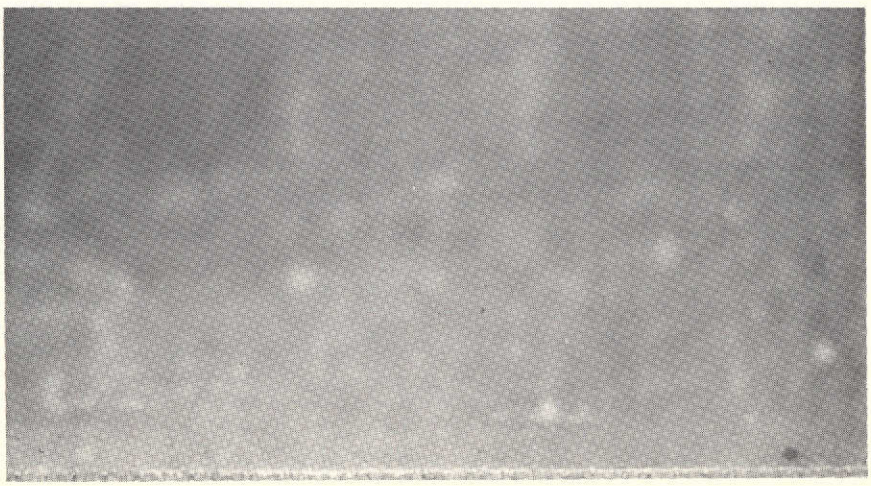

Figure 80. Type F Positive Plate - Uncoined Bottom Edge After Accelerated Testing 5X

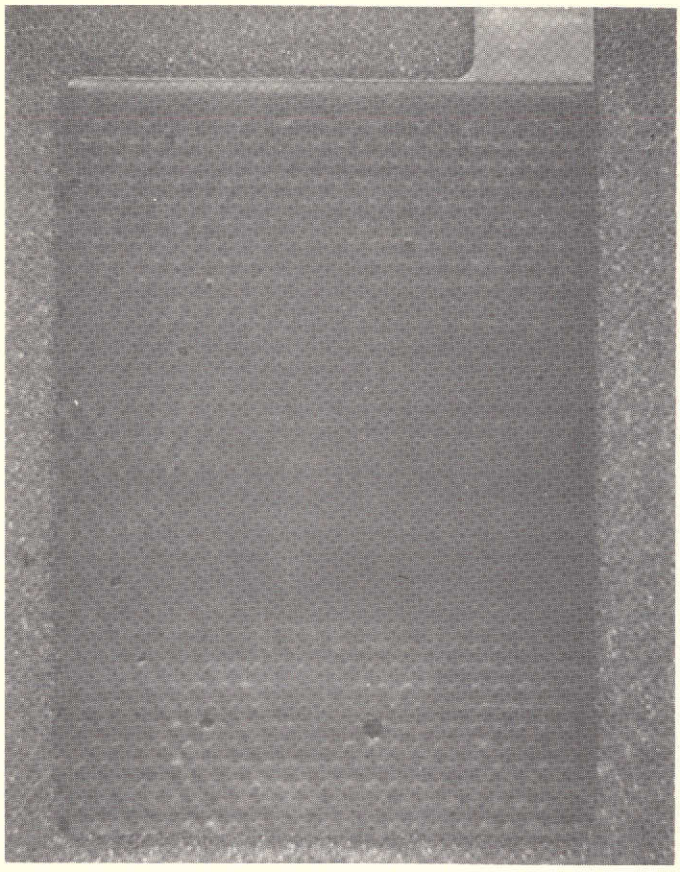

Figure 81. Type G Positive Plate ("Lot 3") After Accelerated Testing

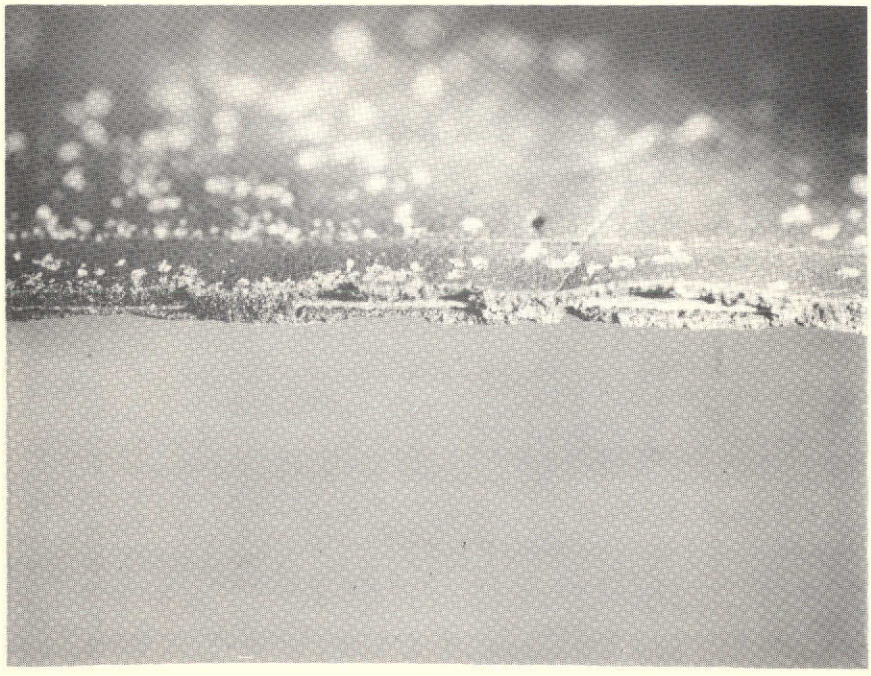

Figure 82. Type G Positive Plate ("Lot 3") Coined Edge Damage After Accelerated Testing 5X

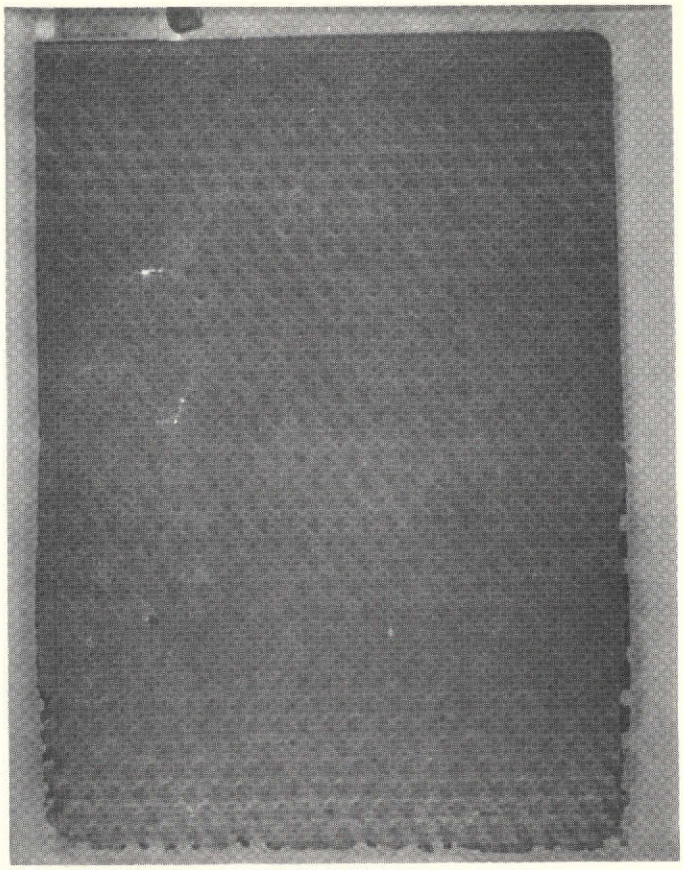

Figure 83. Type G Positive Plate ("Lot 4") After Accelerated Testing

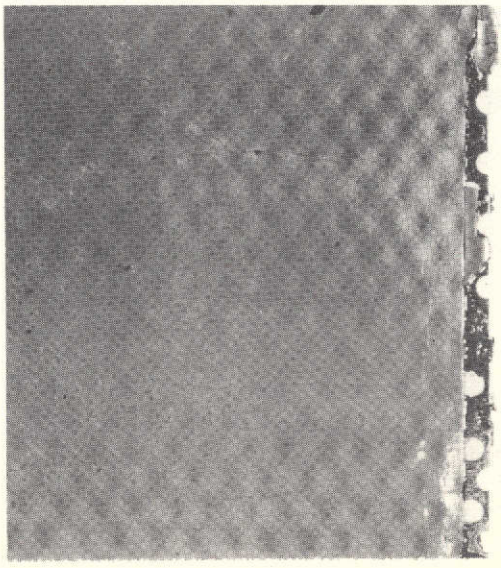

Figure 84. Type G Positive Plate ("Lot 4") Coined Edge Damage After Accelerated Testing (2X)

Figure 65 shows the sides of the two Type A plates that faced each other in the cell. The active (uncoined) area shows many tiny pits and blisters. The coined edges along the sides are in good condition. The uncoined edge at the bottom of the same plate, as shown in Figure 66, was disrupted by swelling and cracking. Figure 67 shows a more enlarged, edge-on view of another portion of the uncoined edge after testing, showing evidence of attack at the cut face.

The top coined edge of Type A plates (containing the tab) showed a special effect. The top edges of two different plates after testing are shown in Figures 68 and 69. Note that the sinter closest to the outer edge of the coined border has been disrupted, while that farther from the edge is in good condition. An investigation of this effect was made, the results of which are described in Section 6.1.5.

Photographs of a representative Type B (uncoined) plate after accelerated testing are shown in Figures 70 and 71. Note that the main area of the plate appears unchanged, but that the edges were attacked. The closeup edge view in Figure 71 illustrates the type of swelling and separation from the grid that occurred along the uncoined edges of this material.

Positive plate of Type C after testing is shown in Figures 72 and 73. This material appeared unchanged, as it did after the previous testing at a higher current density.

Positive plate of Type D after testing is shown in Figures 74 and 75. This material appeared unchanged, as before, but was somewhat warped by the effect of unequal current density on both sides of the plates during the test.

Type E positive plates after accelerated testing are shown in Figures 76, 77 and 78. These plates were badly curled, due to the fact that they are made with almost all the sinter on one side of the screen grid, and hence all the expansion takes place on that one side. Note the large blisters near the tab of one plate. The close-up view of a coined edge shows that although expansion and cracking of uncoined material

immediately adjacent to the coined border occurred, the coined border remained in good condition. The bottom, cut but uncoined edge was in fair condition, as seen in Figure 78.

Type F positive plates after testing are shown in Figures 79 and 80. These plates remained relatively flat, and the coined edges came through in good condition, although the sharp ends of grid wires were exposed at a number of points. Some small blisters formed on the (uncoined) body of the plate, and an apparently large amount of black powdery material was collected in the bottom of the test cell container. The uncoined edges were not visibly altered by the test, as shown in Figure 80.

Type G positive plates after testing are shown in Figures 81 through 84. The plate in Figures 81 and 82 are from one plate lot; the plate in Figures 83 and 84 are from another plate lot. Several blisters up to 0.5 cm in diameter had formed in the uncoined areas. Other than this the main active area of these plates appeared uncharged. The coined edges at the sides showed some degradation, as typified in Figure 82. On one plate the expected effect of coining was reversed, as shown in Figure 84, wherein the coined border was destroyed while the adjacent noncoined area was not. The thickness reduction was 10 percent in coined areas on those plates.

6.1.4 Plate Thickness Increases

In addition to the visual indication of structural changes to the positive plates produced by accelerated cycling, the thickness of the plates was remeasured after washing and drying the materials. The data for each plate type is shown in Table 9. Also shown is the difference (after minus before testing) and the percent change based on the original thickness. As before, a single value indicates an average of many single-point measurements where several points on each plate are measured (usually five) and more than one plate is measured. These measurements are averaged to a single value only if the spread is no more than a few percent. If the spread is 5 percent or more, the range is given.

Table 9. Thickness Changes Produced in Positive Plates by Accelerated Testing

Type	Thickness (mm)			Average Increase % of New Thickness
	New	After Accelerated Test	Increase	
A	.85	.90-1.00	.05-.15	12
B	.65	.70-.75	.05-.10	11
C	.88	.95-1.00	.07-.12	10
D	.77	.785	.015	2
E	.69	.85-.90	.16-.21	27
F	.71	.73-.78	.02-.07	5
G	.69	.74-.78	.05-.09	10

As can be seen from Table 9, all plates increased significantly in thickness during the test, as expected. Furthermore the variation in thickness from point to point increased by a factor of two to three in most cases. The range of percent increase observed was very large; from 2 percent for Type D to 36 percent for Type E. The latter figure may be higher than actual because of interference by blisters, but the thickness increase of this material was clearly much greater than that of the others tested.

6.1.5 Special Effects at the Top Edge of Plates

As mentioned above, the outer edge of the coined border at the top of Type A plates tended to behave differently than other coined areas under accelerated test conditions, in that this outer edge was often cracked and peeling as if it were not coined. A brief investigation to determine the reason why this edge behaved differently than the other coined edges was conducted. A number of new plates of this same type were examined closely under the microscope. It was evident that the border at the top on many of the plates tapered at the outside edge, whereas the coined borders on the other three sides were not tapered. On some top edges the taper was only slight. Examination of the tab area, shown in plan view in Figure 85, shows that these plates are die-cut to remove a thin line of sinter at the very edge of the originally sintered area of the strip as manufactured.

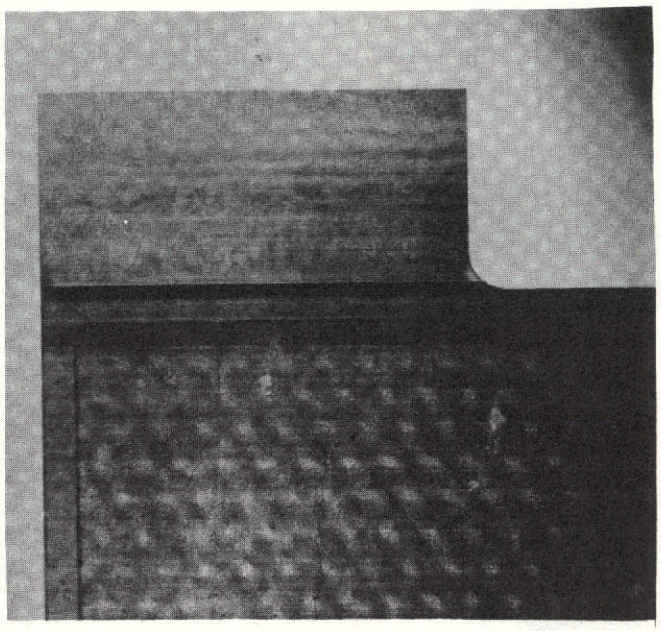

Figure 85. Type A Plate Tab Area 2X

A profile of the border between sintered and nonsintered areas (as on the tab) is shown for a Type A plate in Figure 86. This photo was taken looking at the edge of the plate at the tab side. The taper at the border is clearly shown. The same view of a Type G positive plate, Figure 87, shows an even longer taper. Both of these plates were nominally "coined" on all sides including the top.

Cross-sections taken through the top cut edge on two different Type A positive plates in the as-received condition are shown in Figures 88 and 89. Figure 88 shows no appreciable taper near the edge, while Figure 89 shows part of the original taper remaining at the edge. Note in Figure 88 that the coining indentation occurred on one side of the plate only.

It appears therefore, that an uncompressed, tapered-thickness border of sinter will remain when the plate is coined too near the edge of the sintered area of the strip, and/or where the reduction in thickness is too slight. These two variables interact, as illustrated in the drawing of Figure 90.

The type of coining and cutting that leaves a taper on the outside edge is shown as Coin A and Cut A. That portion of the original sinter edge taper between point P (at the cut) and point Q (where the compression actually ends) thus remains uncompressed and hence in the same condition of strength and porosity as the uncoined sinter in the body of the plate. It is assumed that the dimension W_c from the inside limit of the coined border to the die-cut edge is always the same.

Two other possible cases, either of which would eliminate the uncompressed outer rim, are shown in Figure 90. Coin B with Cut B brings the coined area entirely outside the original taper, and hence no taper is left outside of point R. Thickness reduction, $(t_0 - t_1)/t_0$, remains the same as for Coin A. Coin C and Cut C requires a greater thickness reduction $(t_0 - t_2)/t_0$ and brings the properly compressed area out to point P. Hence the Cut C at point P leaves no uncompressed taper. Coin B would require that the plate pattern be moved slightly toward the center of the sintered strip from current practice. This would result in a corresponding extension of the sintered area up the tap on the cut plate. An example of this type of cutting at the top of the plate was shown in Figure 23.

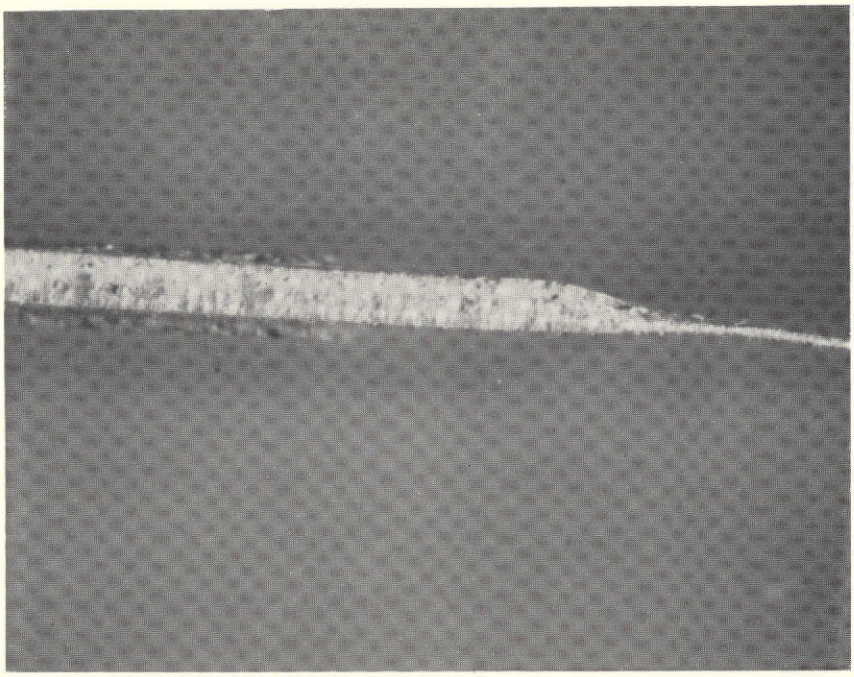

Figure 86. Type A Plate - Profile of Sinter to Nonsintered Border on Tab (10X)

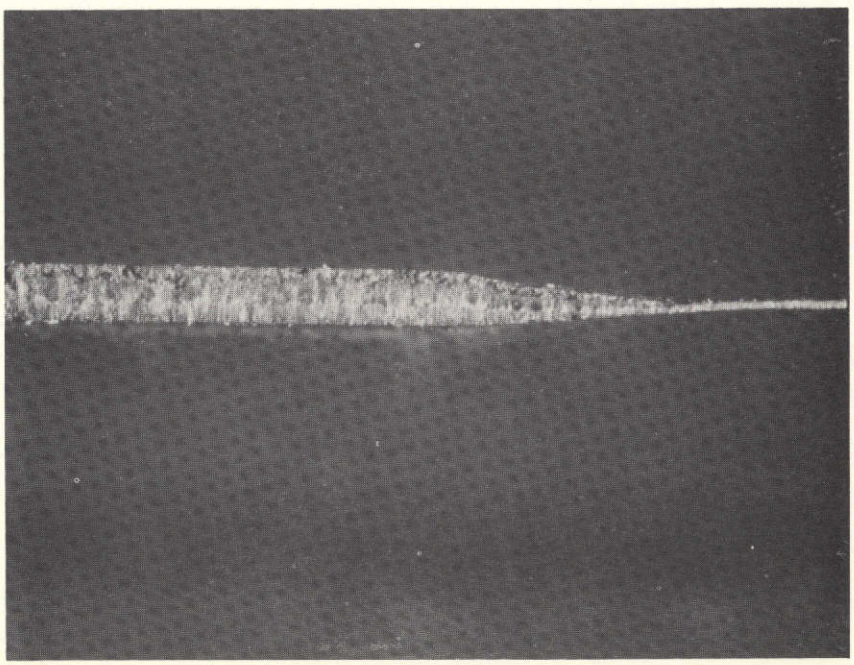

Figure 87. Type G Plate - Profile of Sinter to Nonsintered Border on Tab (10X)

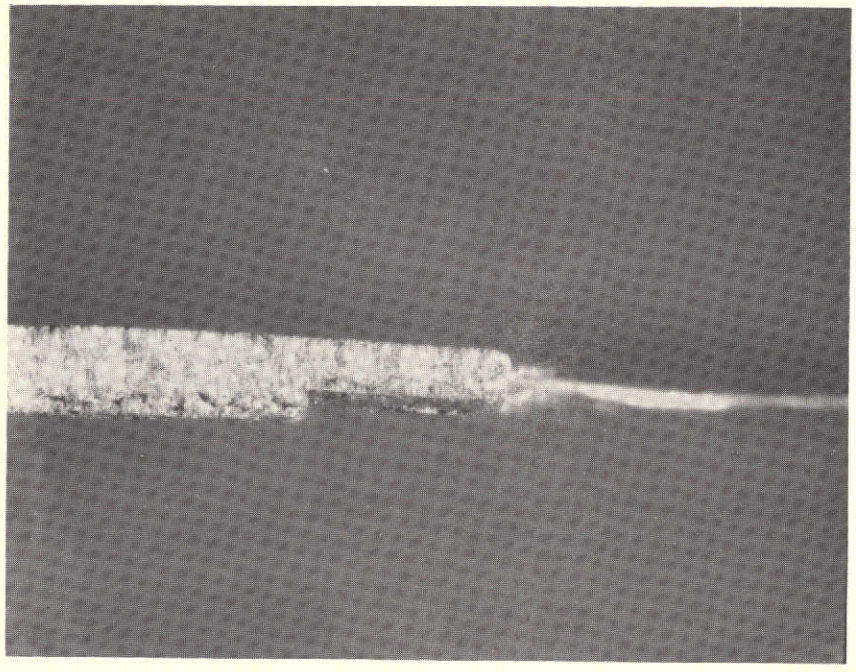

Figure 88. Type A Plate - Profile of Trimmed Coined Top Top Edge (Taper Removed) (10X)

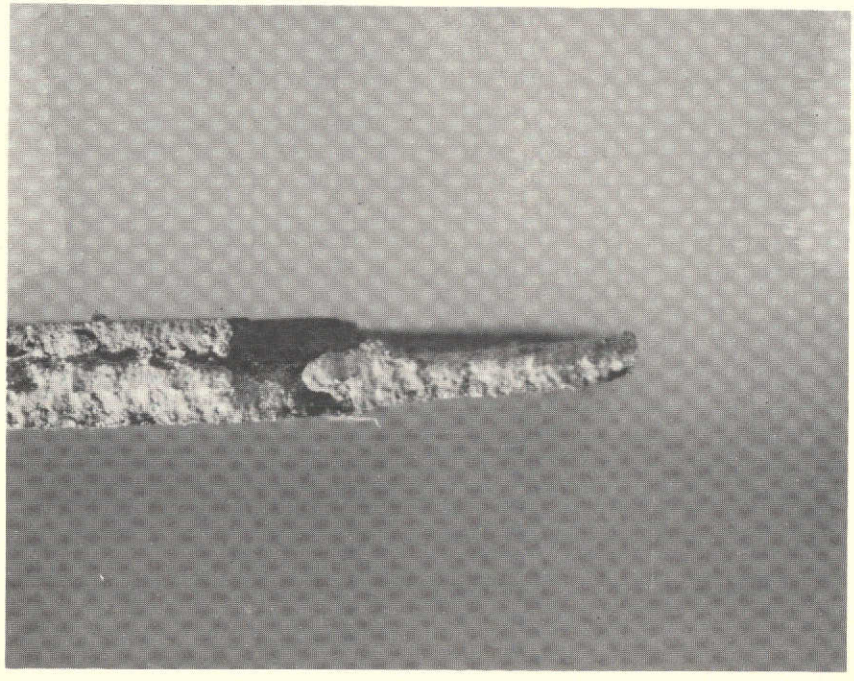

Figure 89. Type A Plate - Profile of Trimmed Coined Top Edge (Some Taper Remaining) (10X)

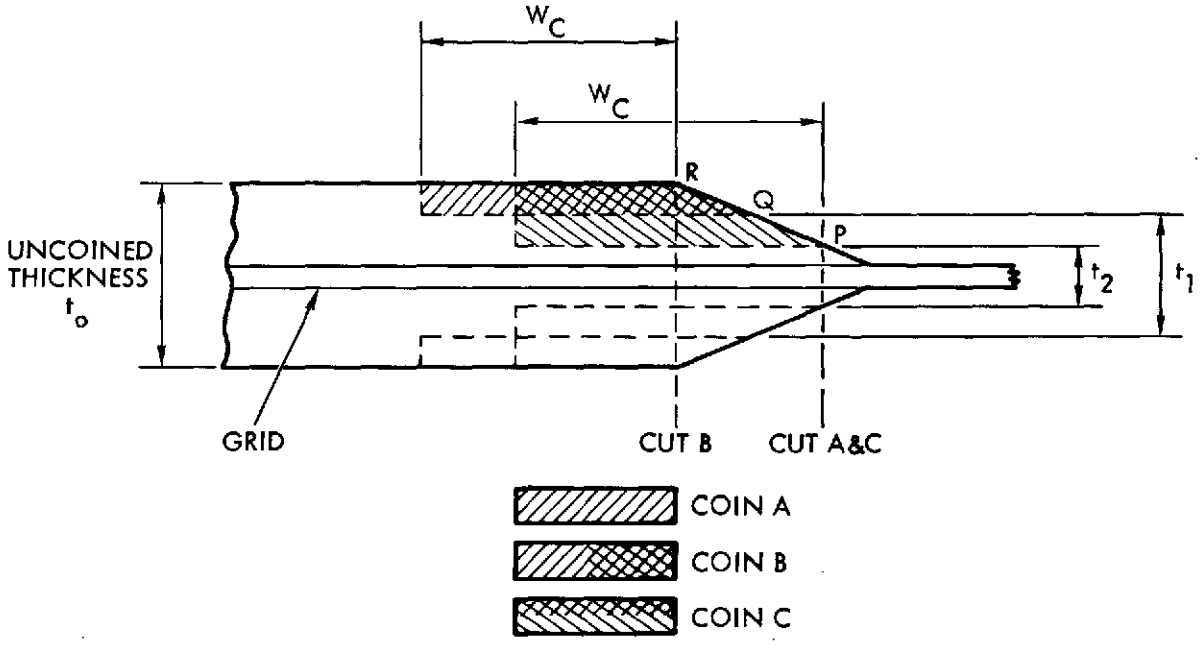

Figure 90. Diagram of Coining and Cutting Interaction With Tapered Border of Plate

6.2 ACCELERATED ELECTROCHEMICAL TESTING IN SEALED CELLS

6.2.1 Objectives

The objectives of this phase of the test program were to compare coined and uncoined edges of plates for resistance to cycling under conditions of actual sealed cells, and to correlate the results with those from the unsupported, flooded tests and with the physical and chemical properties of the plates.

6.2.2 Test Articles

This test was performed on the same cells that were used for cell vibration testing, as described in Section 5. Therefore, one cell each containing plates of Type A, B, C, D, E, and G were tested. Type F plate was not tested in sealed cells because of the large loss of active material seen in prior tests and the poor condition of the grid wires along the edges.

After the plates were inspected following vibration, the same plates and separators were reassembled. Note that these plates were installed in the as-received condition, i.e., no open-cell formation cycling preceded the testing described below. Each of the plates had at least one uncoined edge exposed.

Electrolyte was added by first filling the cells to a level above the top of the plates (visible through the lucite faceplates used), charging, discharging, and charging in the flooded condition, then dumping all free liquid during overcharging. The amount of electrolyte retained was not measured. All cells had the same plate area, and all were cycled at the same current in a series circuit.

6.2.3 Test Conditions

Following the initial conditioning cycles, the cells were tested continuously on a cycle consisting of a 5A charge for 2.5 hours and a 5A discharge for 2 hours. This continued for 14 days on all the cells except for that containing Type A plates. The discharge capacity of the latter cell decreased rapidly over the first two days of cycling, and on the third day the cell was inadvertently overdischarged to a negative voltage several times. A few cycles after this condition had been corrected the cell

shorted internally and was taken off test. Teardown inspection of this cell revealed that a small mass of black appearing active material had penetrated the separator and had bridged between a positive and a negative plate. The positive plates showed irregular black spots distributed over the surfaces. No appreciable damage to the edges, coined or uncoined, had occurred.

6.2.4 Test Results

After the remaining five cells had completed two weeks cycling, they were disassembled and the plates and separators were inspected. Typical features observed are shown photographically in Figures 91 through 104.

Most of the edges of the Type B plates (all edges uncoined), Figures 91 and 92, were in good condition. One edge of a positive plate had cracked and fallen off into the separator, Figure 94.

All the Type C plates and separators appeared in excellent condition. As seen in Figures 95 and 96 both coined (sides and top) and uncoined (bottom) edges were undamaged. There were only traces of black particles in the bottom fold of the separators.

All the Type D plates appeared in good condition, as seen in Figures 97 and 98. However, cadmium active material was deposited on the surface of some of the separators in contact with the negative plates.

The Type E plates were generally in good condition, Figure 99, including the uncoined edge at the bottom. No appreciable material was seen in the separators. Several of the negative plates had relatively large cracks, near the top and bottom edges running parallel to these edges, as shown in Figure 100. The nature of these cracks was different from those produced in positive plates by cycling, and it is postulated that they occurred when the negative plates, being somewhat warped when received, were compressed and flattened during cell assembly.

The coined edges at the sides of the Type G plates were in good condition, as shown for a positive plate in Figure 101, but the uncoined botton edge of the positive plates were degraded. Figure 102 is a close-up of the

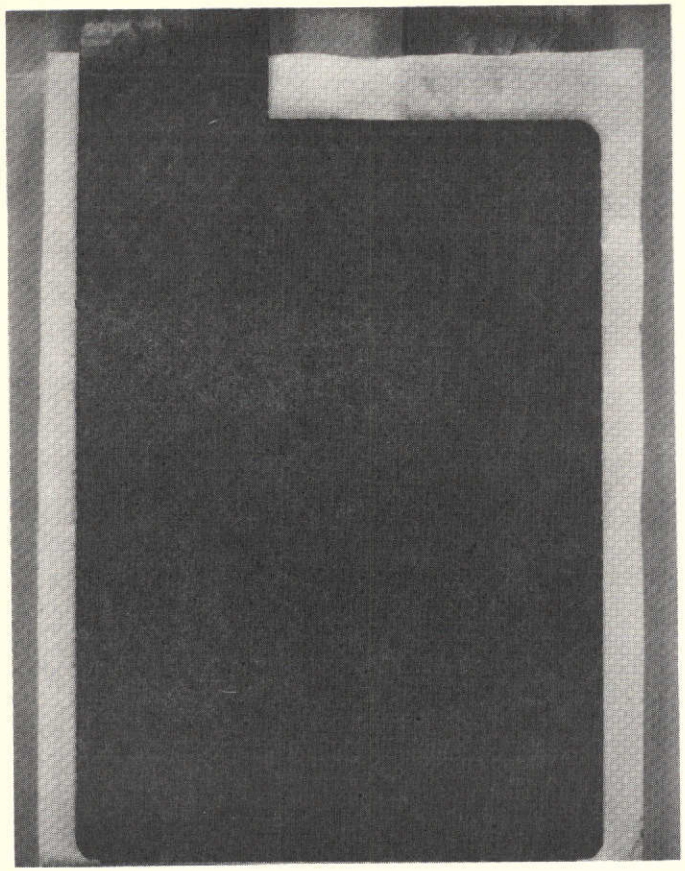

Figure 91. Type B Positive Plate After Sealed Cell Test

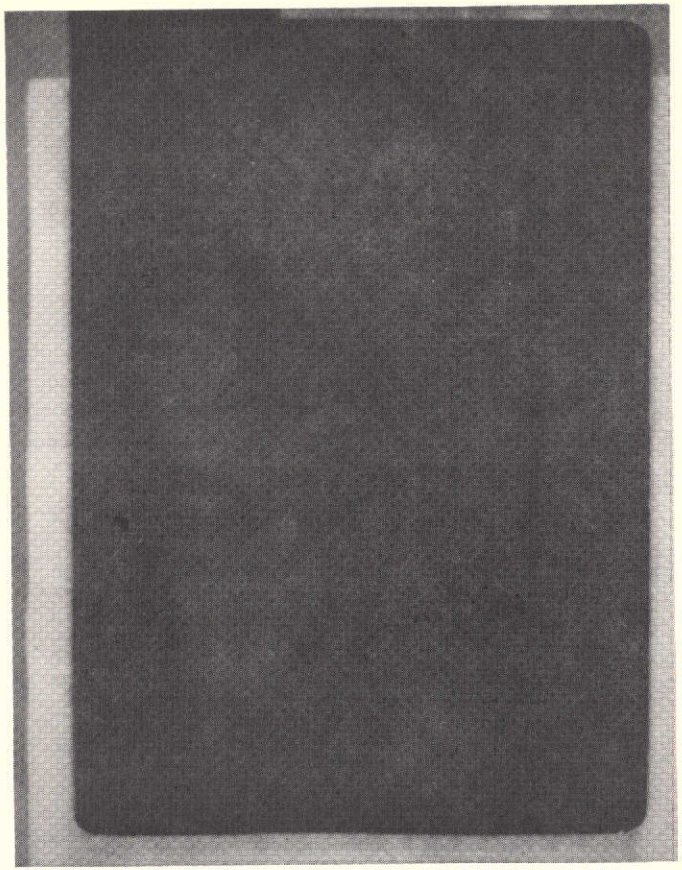

Figure 92. Type B Negative Plate After Sealed Cell Test

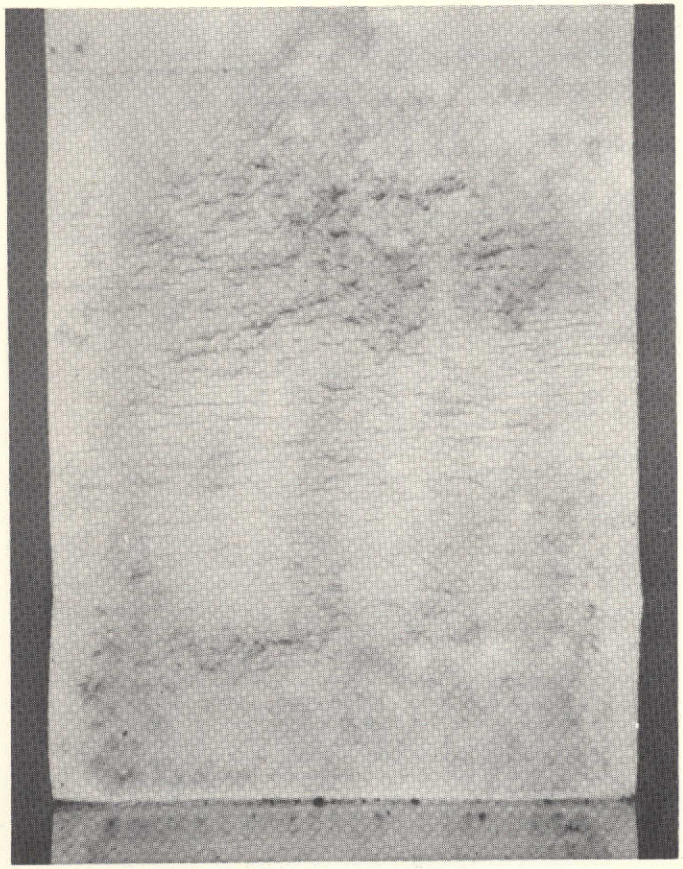

Figure 93. Separator From Type B Sealed Cell - Side Facing Positive Plate

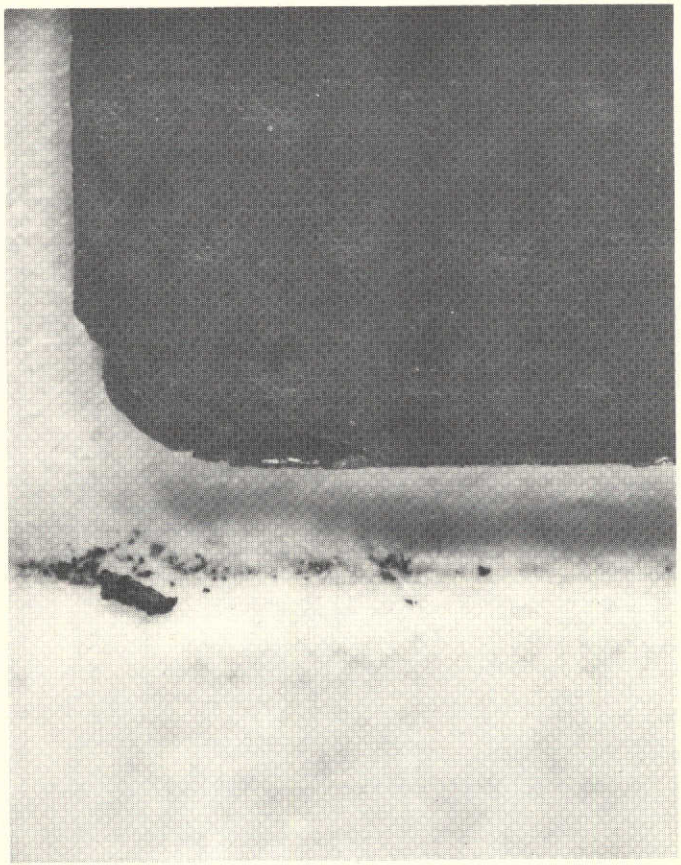

Figure 94. Type B Positive Plate Lower Corner After Sealed Cell Test

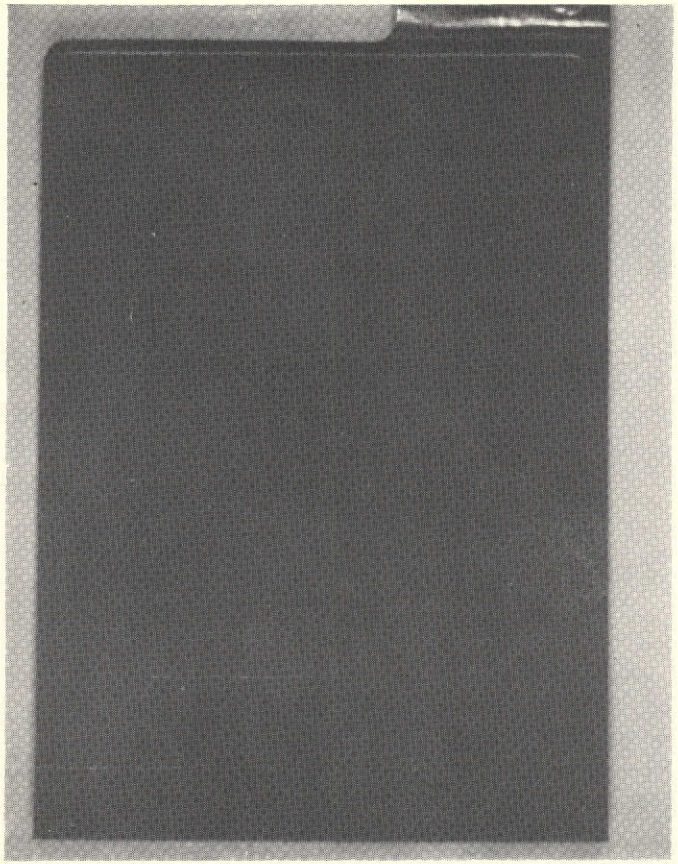

Figure 95. Type C Positive Plate
After Sealed Cell Test

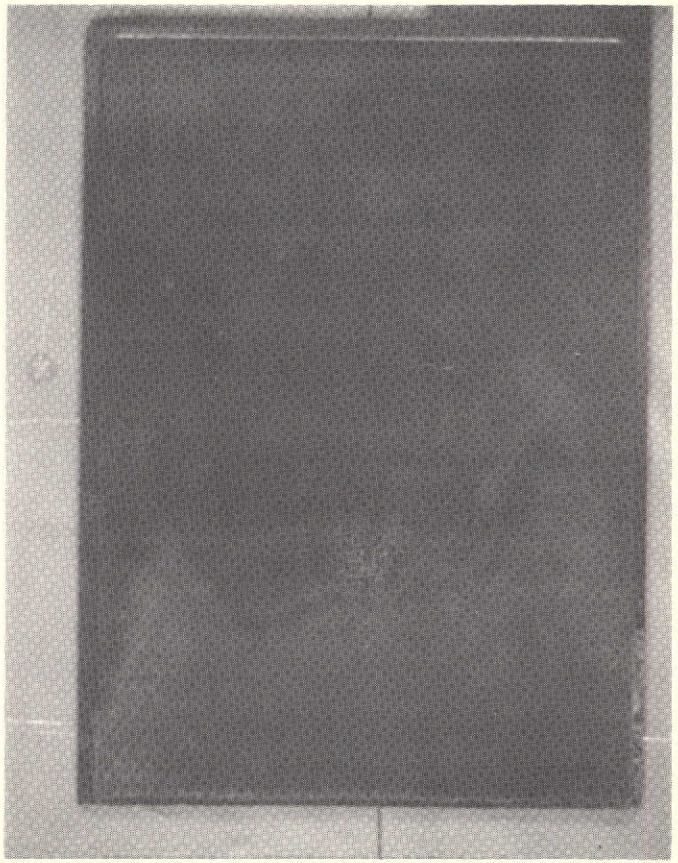

Figure 96. Type C Negative Plate
After Sealed Cell Test

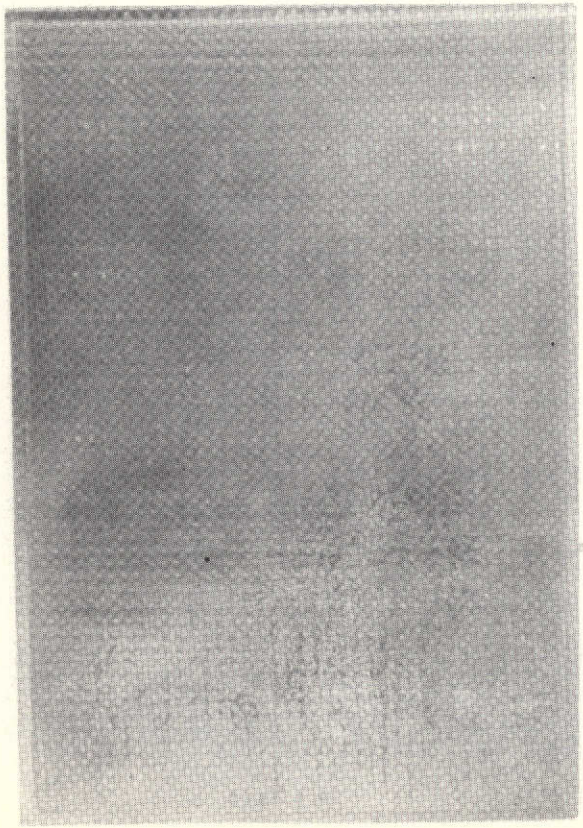

Figure 97. Type D Positive Plate
After Sealed Cell Test

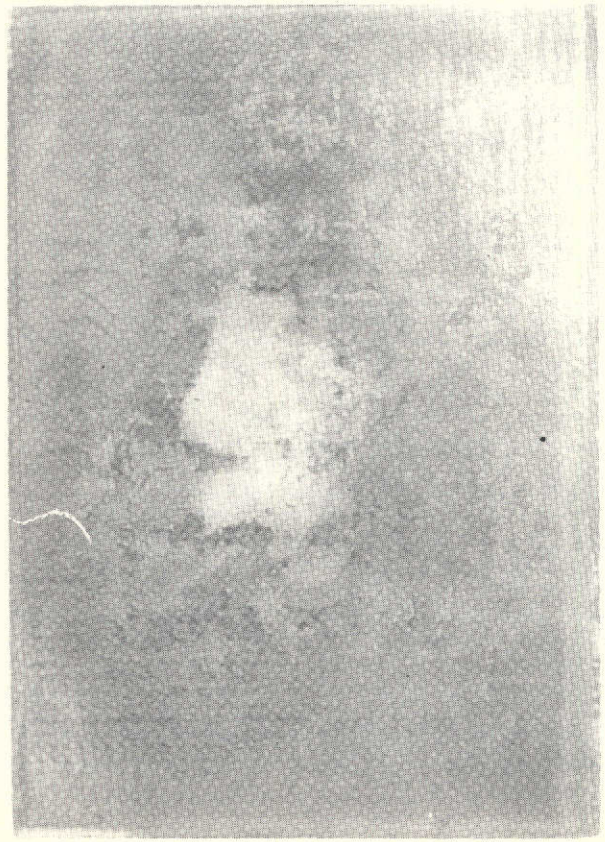

Figure 98. Type D Negative Plate
After Sealed Cell Test

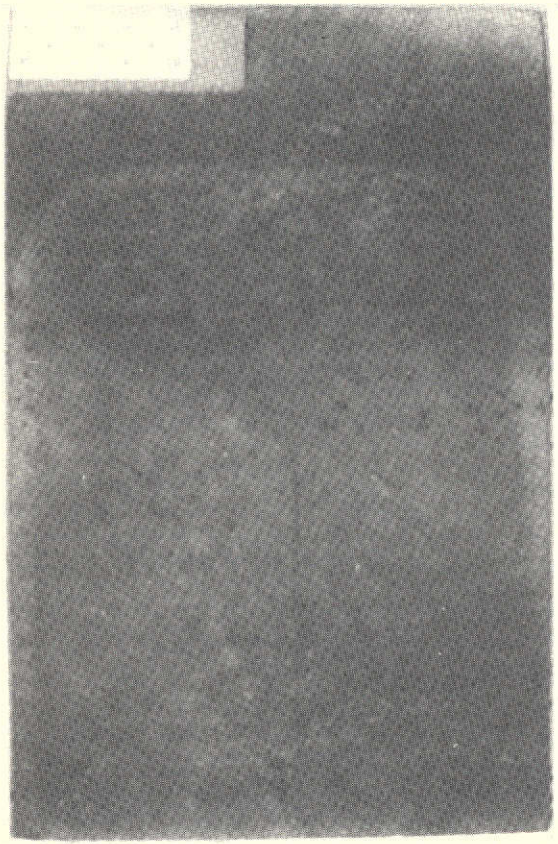

Figure 99. Type E Positive Plate After Sealed Cell Test

Figure 100. Type E Positive Plate Crack Near Edge (5X)

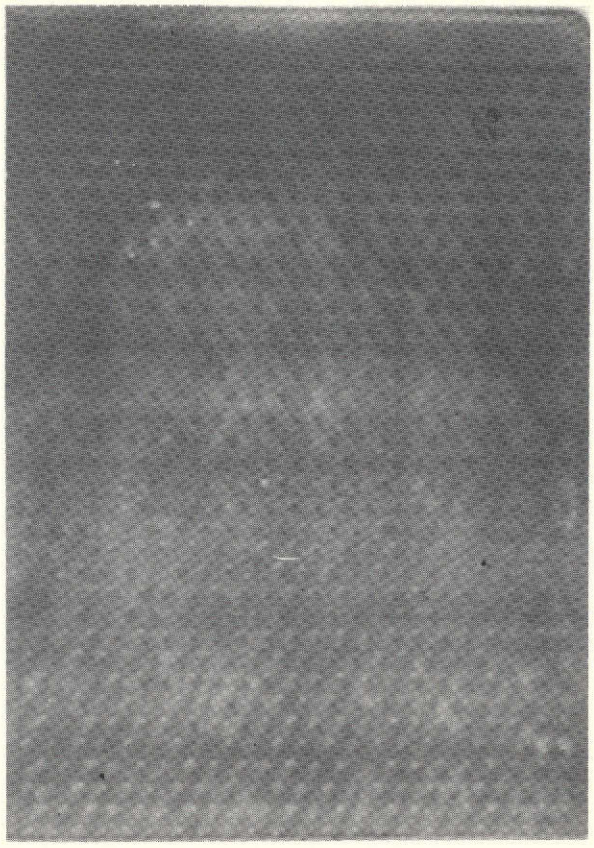

Figure 101. Type G Positive Plate After Sealed Cell Test

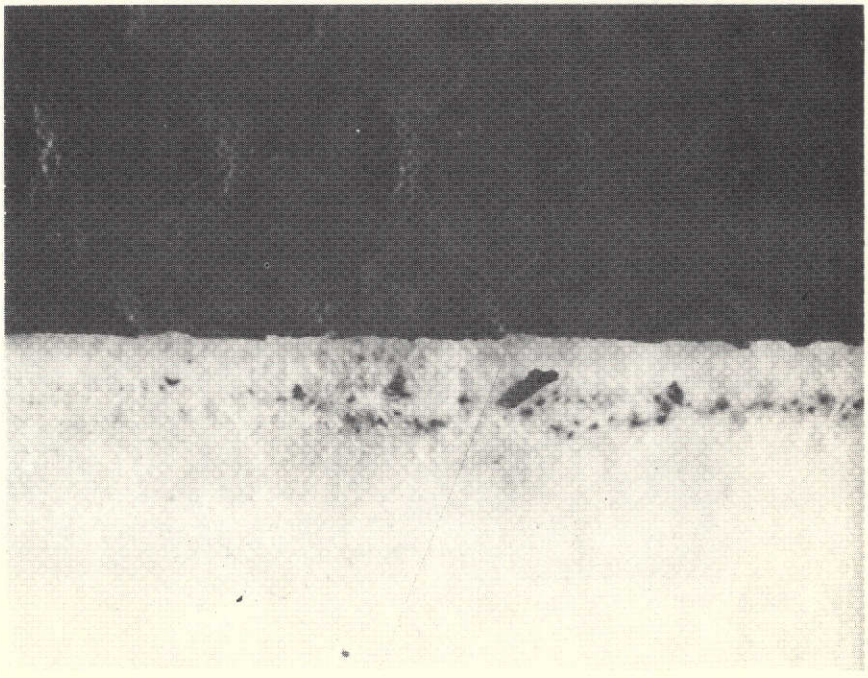

Figure 102. Type G Positive Plate Bottom Edge After Sealed Cell Test (10X)

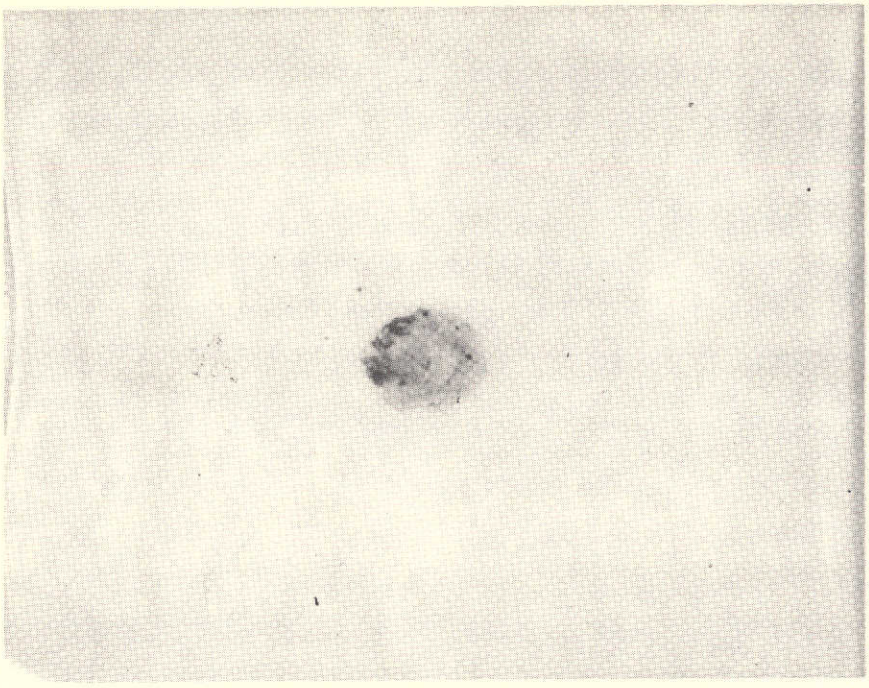

Figure 103. Separator from Type G Cell - Side Facing Positive Plate (10X)

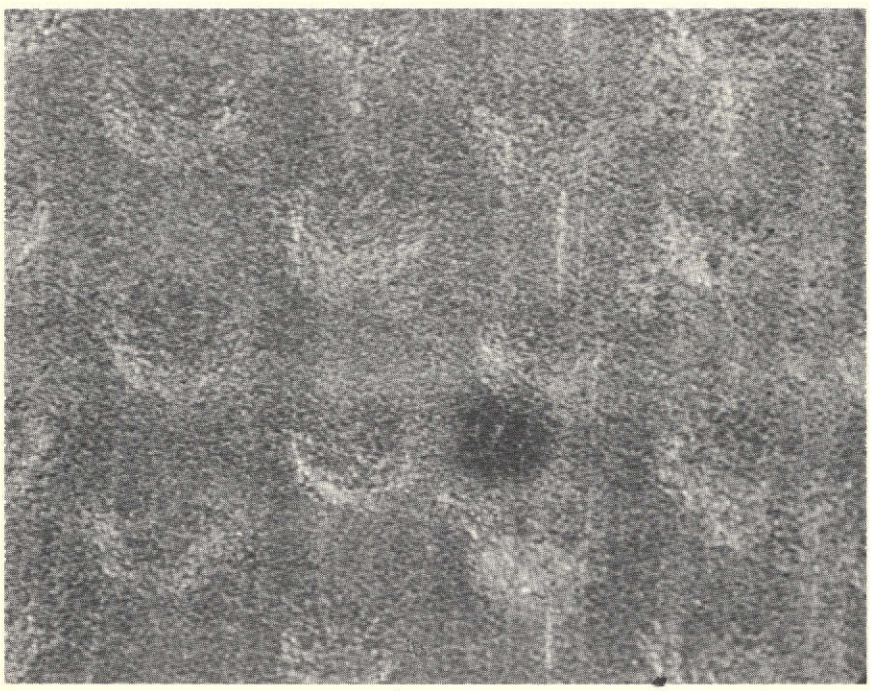

Figure 104. Type G Positive Plate Spot (10X)

bottom of one positive plate, showing cracking at and near the edge and loss of sinter particles of significant size to the separator. Figure 103 (at 10 x magnification) shows positive active material entering the separator in a well-defined spot near the center of a plate. The source of this occurrence is a small black spot on the adjacent positive plate surface, shown at 10 x Figure 104. The surrounding depressions are the locations of the perforations in the substrate.

6.2.5 Summary of Sealed-Cell Accelerated Testing

Cycling of plates with both coined and uncoined edges under sealed cell conditions, where cycling was performed at the C/2 rate for charge and discharge, and the depth of discharge was close to 100 percent, and where 84 cycles were performed over a 14 day period, produced significantly more damage to uncoined edges than to coined edges in the weaker plate materials, but caused no significant damage to either coined or uncoined edges in the stronger materials. The degree of the effects observed was far less than produced by the flooded accelerated tests, as expected, due partially to the lesser degree of gassing required for satisfactory sealed cell operation.

6.3 LONG-TERM TESTING: PLATE MATERIALS ANALYSIS

6.3.1 Purpose and Scope

The purpose of this task was to perform (1) disassembly of a group of cells that had completed a test that extended over a period of 18 months; (2) inspection and analysis of the plates in these cells; and (3) analysis of the data to correlate electrical performance and plate degradation with changes in physical and chemical characteristics of the plates.

6.3.2 Cell Test Description

The broad objective of the cell test program was to provide improved technology for a significant increase in the usable energy density and reliability for five or more years of life of nickel-cadmium batteries. More specific objectives are to establish the underlying causes of loss of electrical output of the electrodes in the cell, and to translate this information into requirements for improved plate design and/or processing.

The approach taken is as follows: Cells were assembled using materials and procedures believed to be capable of resulting in the highest cell-to-cell uniformity and quality achievable at the present state of the art. All cells were made from the same plate materials. The plates were made by the General Electric Battery Products Section under a special arrangement under which extensive traceability, samples, and controls were obtained during platemaking. All positive plates used in the cells were from only one positive spiral and all negative plates were from only one negative spiral. All plates were uncoined. The plates designated as Type B in the report are from the same two spirals.

From those plates in these spirals not used for cells, samples were selected and subjected to tests and analyses to establish their inherent characteristics. The results of these tests on the new materials are reported in Section 4. The cells were assembled using the reusable all cases described in Section 5 of this report. The assembly of the plate stacks and final mechanical assembly of the cells was accomplished at TRW under close control and scrutiny, in order to attempt to avoid all early failures due to mechanical defects. These cells were then filled, formed,

and precharge adjusted using procedures recommended by the plate manufacturer. Two levels of precharge were used: 10 percent and 30 percent, based on positive capacity. Half the cells were set at each level.

A total of 36 cells were fabricated. Each cell was equipped with a pressure gauge and a nickel-oxide reference electrode. Twenty-four were tested by repetitive 80 percent depth of discharge cycling in an 8 to 12 hour cycle. The remaining twelve cells were kept on a continuous low-level trickel charge.

The electrical cell test program was performed with two imposed operating variables, each at two levels:

Temperature	5°C and 25°C
Discharge Rate	0.5C and 1C

Depth of discharge was the same for all cells, so discharge time was adjusted accordingly. A group of three cells was operated at each of the twelve combinations of the three variables (including precharge level). The test groups and parameters are summarized in Table 10.

Table 10. Long-Term Cell Test Matrix

Group Number	Operating Temperature (°C)	Precharge Level (% of Pos.)	Discharge Rate
1	5	10	C/2
2	5	30	C/2
3	5	10	C
4	5	30	C
5	5	10	Trickle Charge
6	5	30	Trickle Charge
7	25	10	C/2
8	25	30	C/2
9	25	10	C
10	25	30	C
11	25	10	Trickle Charge
12	25	30	Trickle Charge

The total active positive plate area of these cells (7 positive plates @ 0.69 dm^2 per plate) was 4.82 dm^2. When new, the capacity delivered to 1 volt was 13.5 + 0.25 ampere hours when discharged at 6 amperes. Charge current was nominally 1.5 amperes during cycling. Each group of three cells was operated as a series unit with a separate charge and discharge control circuit. The controller imposed a charge voltage limit, at which point the 3-cell unit went into a constant voltage charge mode. The limit was initially set at 1.48 volts/cell at 25°C and 1.52 volts/cell at 0°C. A photograph of a group of these cells on test is shown in Figure 105.

At the end of electrical testing, most of the cells had completed a total of 515 cycles over a period of 18 months. Periods of continuous cycling were interspersed with periods of trickle charging varying from two days to 170 days. The number of successive cycles in any cycle period varied from six cycles to 109 cycles. The first 445 cycles were 8 hour cycles; the last 70 were 12 hour cycles.

6.3.3 Electrical Test Results

Of the twenty-four cells that began the test in the cycle mode, four did not complete 500 cycles. One of these leaked early in the test and was not tested further. The other three discharged to zero volts before the end of the prescribed discharge time before reaching 500 cycles. There was one such cell in each of three of the three-cell test groups. Of these, one failure was predicted due to the fact that too much electrobyte had been lost during vent charging. The reason for the remaining two failures was not apparent.

End of discharge voltage (EODV) data for all the cycled cells at the beginning of the test and at the end of the electrical test phase, and the differences between these two values, are shown in Table 11. Note that, with few exceptions, the EODV of at least two of the three cells in each original group was fairly close together at the end of the test, although some were well below 1 volt. The voltage of these cells was purposely allowed to go down as far as 0 volts before cut-off, in order that relatively large changes in the structure of the plates might be available to measure after tear-down.

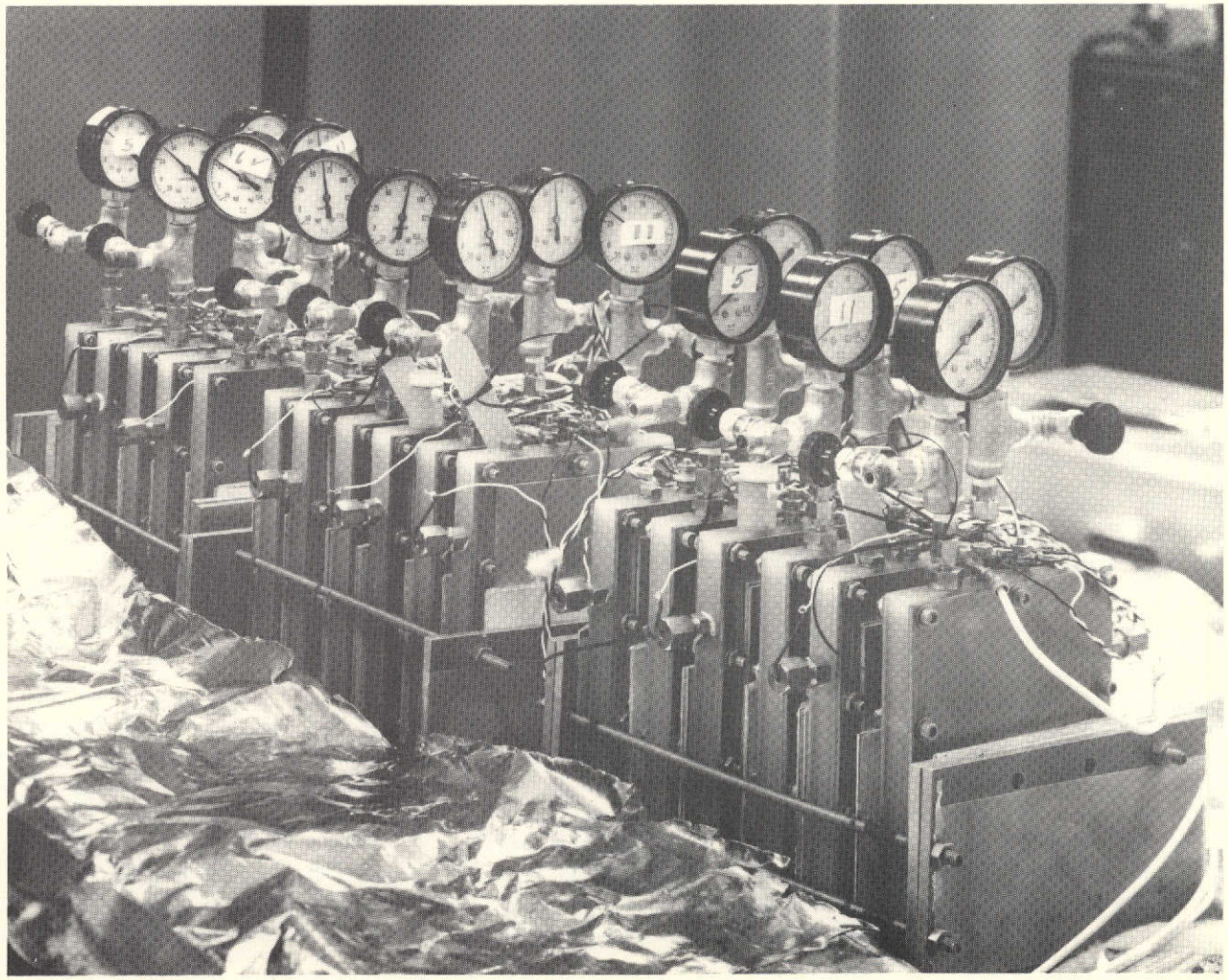

Figure 105. Reusable Cells on Test

Table 11. Cell Voltage Data from Long-Term Test

Group Number	Cell S.N.	End of Discharge Voltage		
		Beginning of Test	End of Test	End of Test-Beginning of Test
1	1	1.17	-	(Leaker)
	3	1.18	1.15	0.03
	22	1.17	1.09	.08
2	2	1.15	< 0	>1.15
	4	1.18	1.11	0.07
	8	1.17	1.10	0.07
3	5	1.13	0.8 est	0.33
	9	1.14	1.01	.13
	10	1.13	0.47	.66
4	11	1.14	1.04	.10
	13	1.13	0.8 est	.33
	14	1.08	< 0	>1.08
7	19	1.17	0.72	.45
	20	1.17	0.07	1.10
	34	1.17	0.64	.53
8	7	1.17	1.03	.14
	21	1.17	0.97	.20
	23	1.18	1.02	.16
9	7	1.17	1.03	.14
	21	1.17	0.97	.20
	23	1.18	1.02	.16
10	24	1.11	< 0	>1.11
	28	1.13	0.8 est	.33
	35	1.14	0.8 est	.34

6.3.4 Cell Disassembly and Inspection

Of the twelve groups shown in Table 10, eight groups were torn down, namely numbers 3, 4, 7, 8, 9, 10, 11, and 12. The remaining groups were diverted to other tests. Of the twenty-four cells opened, only eighteen cells, from groups 3, 4, 7, 8, 9, and 10, were examined in detail. These form the basis for the data reported below.

As the positive plates were removed from the separator bags, the lower separator seam was checked for particles indicating crumbling of the positive plate. Some particles were found with every plate; the range is illustrated by the photographs of Figure 106. Most of the plates of the same polarity looked alike as removed. Photographs of two representative positive plates as removed are shown in Figure 107. Negatives are shown in Figure 108. The narrow border around the edge seen in these photographs is the polystyrene edge coating.

Although difficult to see clearly in the photographs, there were extensive deposits of active materials on the surface of certain areas on many of the positive and negative plates. These areas appear relatively black in Figures 107 and 108. These deposits were hard and strongly adherent. Although such surface deposits are observed frequently in older cells on the negative (cadmium) plates, the degree and frequency of this phenomenon on the positive (nickel oxide) plates is considered unusual.

Although a large percentage of the total edge length of most of the plates was in good condition, a high percentage of the positive plates inspected had at least one spot where the edge was broken. A close-up of a typical degraded edge is shown in Figure 109. By far the most frequent location of an edge breakdown was a lower corner, as shown enlarged in Figure 110.

There was only slight sticking of separators to the negative plates, and this only in the driest cells. Visible deposits on the separator surfaces facing the negative plates were light and distributed randomly among the cells in any group and among the different cell groups. Two of the most heavily coated separators seen are shown in Figure 111.

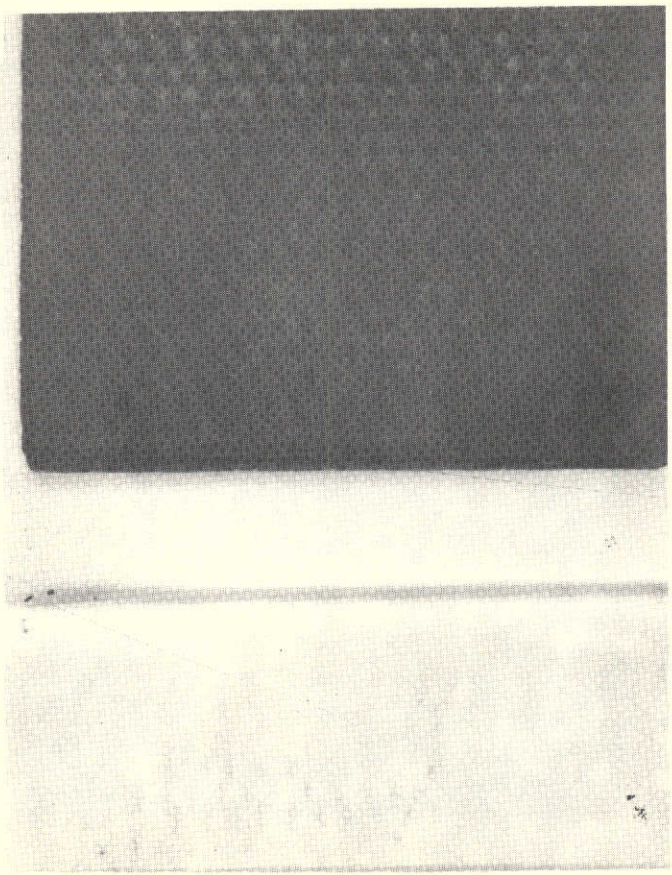

A. Lower Limit

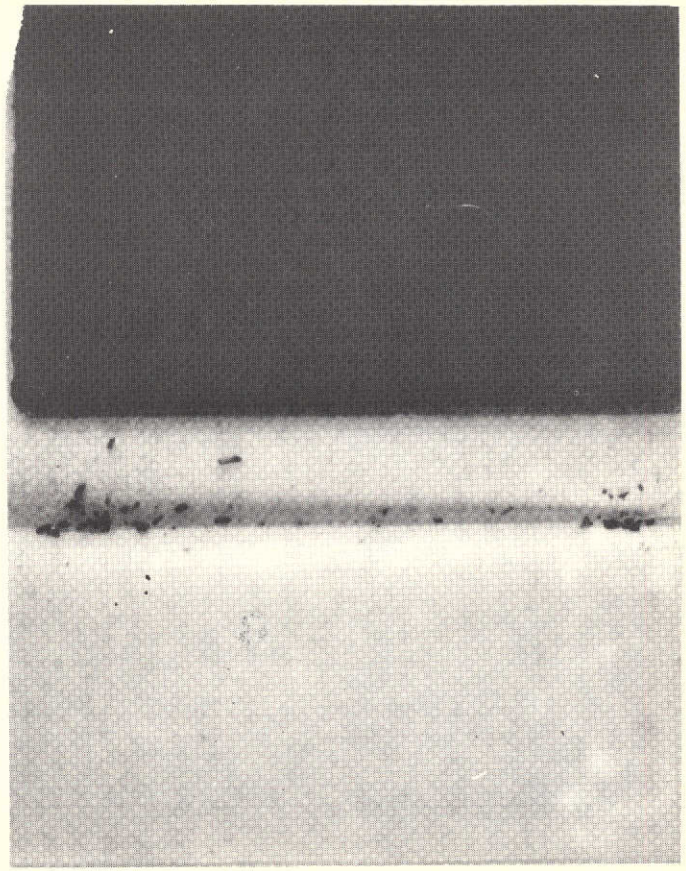

B. Upper Limit

Figure 106. Residue in Separators from Reusable Cells

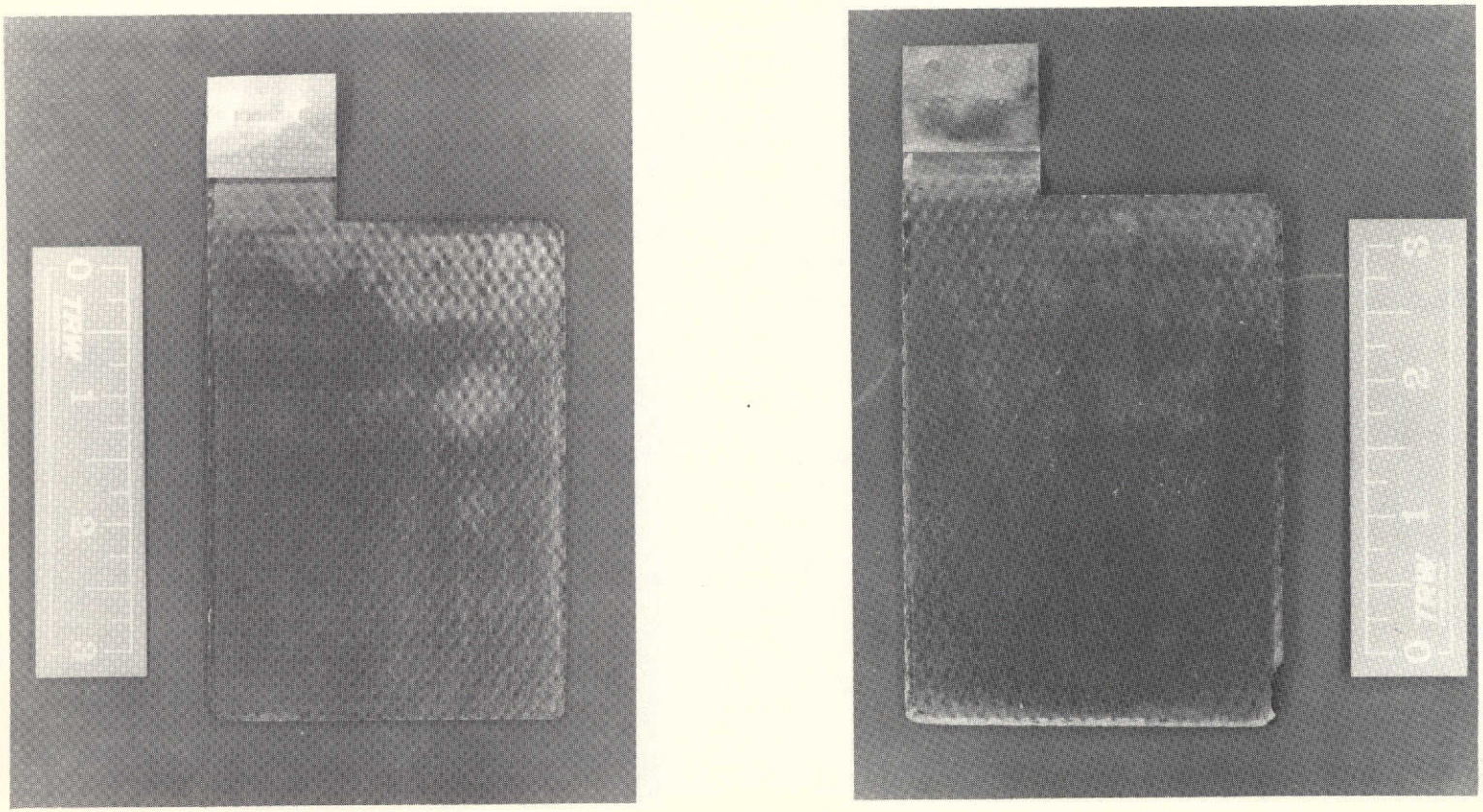

A. Cell SN09

B. Cell SN34

Figure 107. Typical Positive Plates from Long Term Cell Test

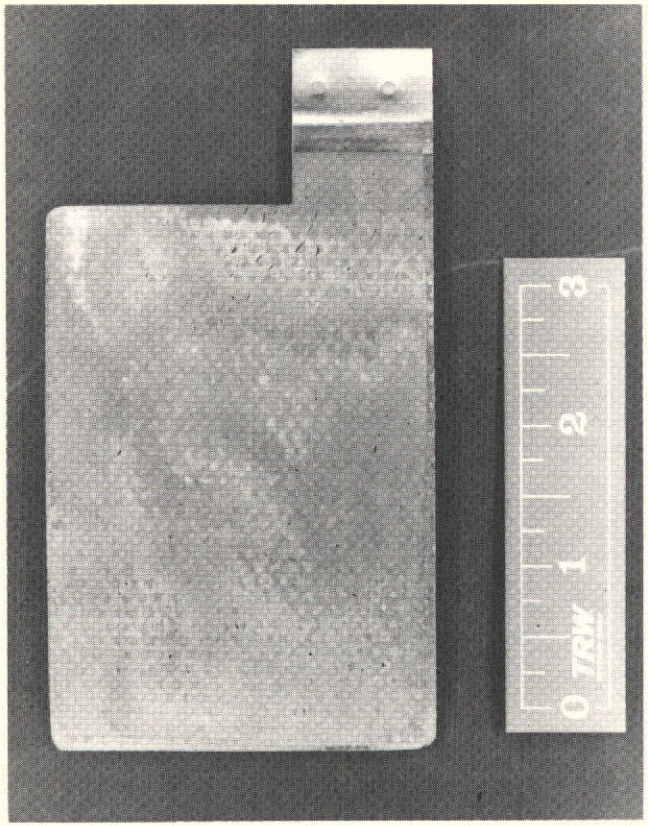

A. Cell SN05

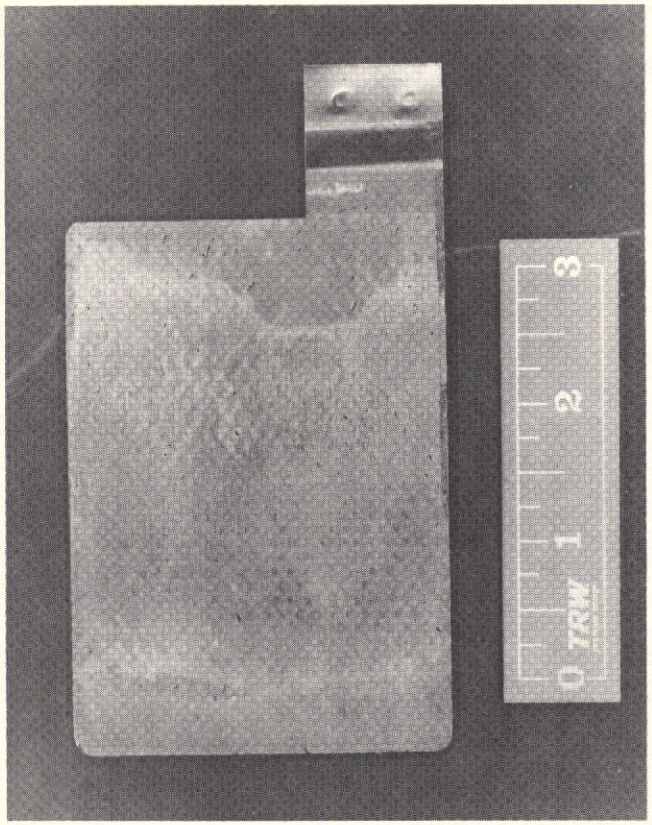

B. Cell SN23

Figure 108. Typical Negative - Plates from Long-Term Cell Test

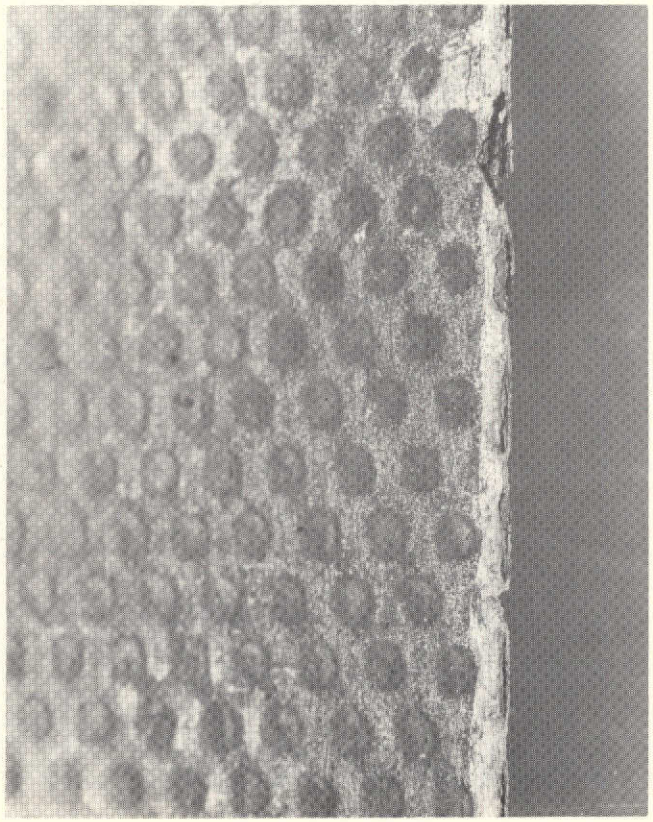

Figure 109. Closeup of Degraded Edge of Positive Plate After Long-Term Testing

Figure 110. Closeup of Broken Corner of Positive Plate

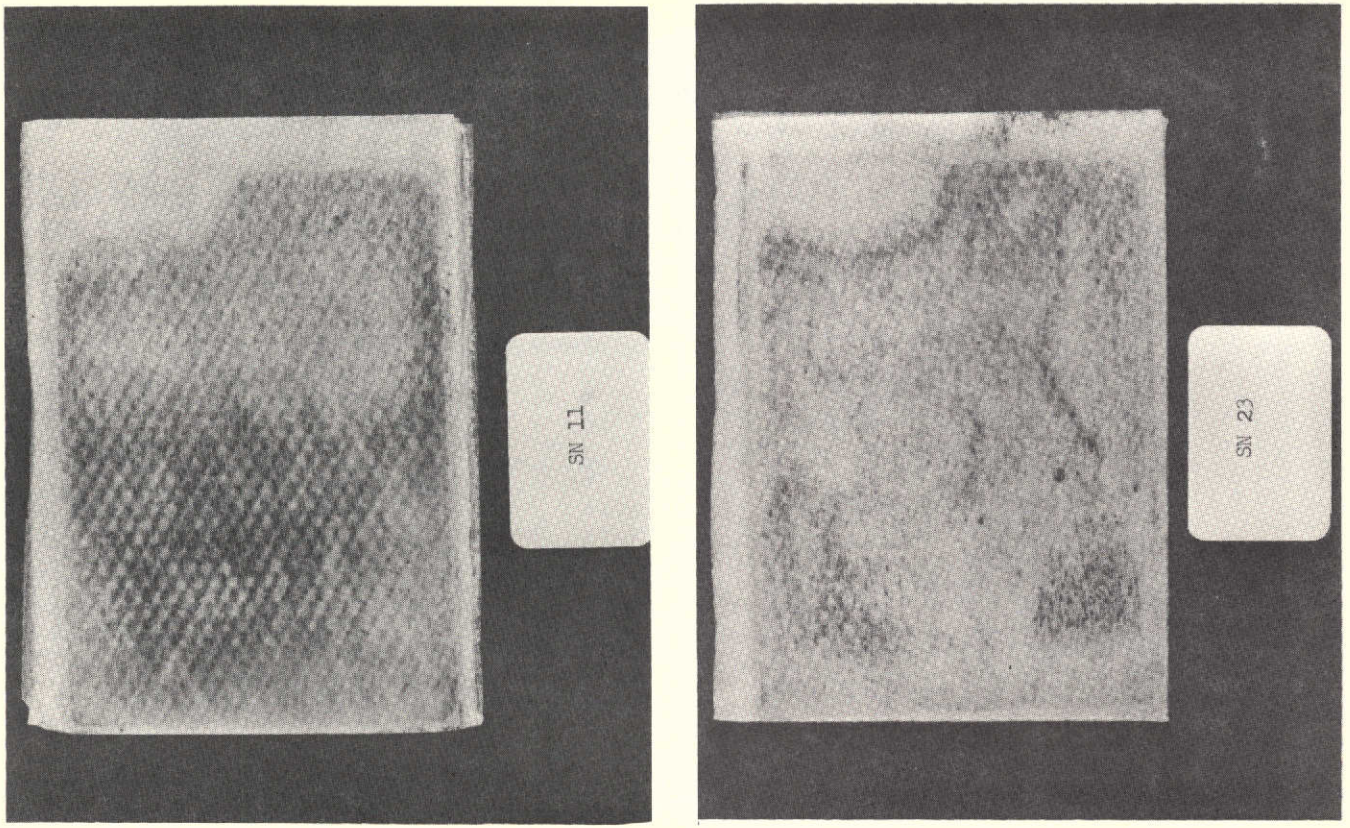

A. Cell SN11

B. Cell SN23

Figure 111. Polypropylene Separators After Long-Term Testing

6.3.5 Cycled Plate Testing and Analysis

Two sample positive and two sample negative plates were taken from each cell for testing and analysis. Thickness, compression strength, and resistivity (for positive plates) was determined on each plate as a whole as removed. After that, plates were sectioned for other tests. Charged nickel was determined on samples without prior removal of residual electrolyte, by the method described below. Density, void fraction, and active material content were determined after washing and drying in a nitrogen gas stream.

The method used for determination of charged nickel compounds (Ni^{+3} and higher valence states) in positive plates is one suggested by Tuomi* and modified in these laboratories. The sample is immersed in a solution containing a known quantity of aresenious oxide in concentrated (34 percent) KOH and allowed to stand until reaction is complete. The residual aresenious material is then determined iodimetrically. The other measurements are made as described in Section 4. The results are presented in Tables 12 and 13. Thickness values are averages of six or more point measurements, three or more from each of two plates. Resistance values are averages of four individual measurements, one on each side of two plates. Density, void fraction, total active content, and charged material content are averages of two determinations, one from each of two plates.

6.3.6 Long-Term Testing Data Summary

From consideration of the overall long-term cell test results shown in Table 11, the following effects of the primary test variables are deduced:

a) Operation at the lower temperature (5° vs. 25°C) resulted in higher discharge voltages at the end of the test at a given discharge rate. The effect of temperature was greatest at the higher discharge rate.

b) The higher rate of discharge gave the lower end of discharge voltages at the end of the test.

c) The higher precharge level gave the higher discharge voltages at both discharge rates. The effect of the higher precharge level was greater at the higher temperature.

*D. Tuomi, J. Electrochem, Soc. 112, 1 (1965).

Table 12. Cycled Positive Plate Characteristics

Group Number	Cell SN	Thickness (mm)	Resistance (mΩ)	Density (g/cm^3)	Void Fraction (%)	$Ni(OH)_2$ (g/cm^2)	Residual Charged Nickel (%)
3	5	.76	1.73	3.42	22-25	0.112	15
	9	.75	1.76	3.20	18.7	0.118	16
	10	.77	1.75	3.06	17-21	0.112	14
4	11	.74	1.84	3.37	22.1	0.125	15
	13	.75	1.79	3.11	19.7	0.116	18
	14	.78	1.82	3.00	16.2	-	9
7	19	.77	1.80	3.2-3.6	15-20	-	17
	20	.78	1.92	3.2-3.5	16.8	-	18
	34	.77	1.83	2.7-3.3	17.4	-	17
8	7	.77	1.87	2.7-3.3	16.9	-	16
	21	.77	1.85	3.19	18.3	-	16
	23	.765	1.73	3.34	18.8	-	15
9	25	-	1.91	3.39	20.4	0.125	28
	26	.77	1.91	3.11	20.1	0.122	17
	27	.80	1.84	3.06	21.2	-	18
10	24	.76	1.84	3.13	19.6	0.113	14
	28	.755	1.91	3.09	17-22	0.118	22
	35	.79	1.91	3.07	17.5	-	12

Table 13. Cycled Negative Plate Characteristics

Group Number	Cell SN	Thickness (mm)	Density (g/cm^3)	Void Fraction (%)	$Cd(OH)_2$ (g/cm^2)	Residual Charged Cadmium (g/cm^2)
3	5	.945	3.46	36.6	-	-
	9	.915	3.57	36.5	-	-
	10	.91	3.57	35.0	-	-
4	11	.915	3.59	35.1	-	-
	13	.90	3.61	35.2	-	-
	14	.935	3.44	31.2	-	-
7	19	.86	4.03	22-29	-	-
	20	.86	3.2-4.1	30-35	-	-
	34	.865	3.93	20.5	-	-
8	7	.91	3.72	21-25	-	-
	21	.845	3.2-3.8	34-44	-	-
	23	.86	3.91	20-30	-	-
9	25	.90	3.47	33-37	.144	.011
	26	.88	3.61	37.7	.122	.013
	27	.90	3.53	38.1	.103	.024
10	24	.94	3.33	37.7	.126	.021
	28	.89	3.45	30-36	.119	.012
	35	.92	3.54	33.1	.141	.022

There were about the same number and degree of cell "failures" at each temperature level, but more at the higher discharge rate, as expected. The "failures" were all of the type wherein the end of discharge voltage (EODV) dropped gradually to zero before the end of the test. There were no shorts or open-circuit failures.

Cell disassembly showed that there was no appreciable degradation of the polypropylene separators used, and very little cadmium material was adhering to separator surfaces. There was a considerable range of "wetness" apparent in the separators and plates of cells opened. Titration of sample separators with acid showed that the drier appearing separators had less total alkalinity ($OH + CO_3$) than wetter ones.

The data in Table 12 show that several properties of the positive plates changed significantly during the cycle testing. Plates from all cells increased in thickness by an average of about 15 percent from the new value of 0.67 mm. This is about the same degree of thickness increase as produced by the accelerated test described earlier.

Plate resistance increased by different amounts from the original average of 1.70 milliohms. The increases were greater at the higher temperature, and slightly greater at the higher discharge rate. Although these differences are small, they represent a much larger change in the resistivity of the sinter itself.

Compressive strength was also determined on a sample of positive plates selected at random from those removed from cycled cells. A composite plot of these data is shown in Figure 112. The horizontal bars indicate the range of values of penetration measured at each pressure. The curve at the left for new plate is shown for comparison.

As can be seen, the penetration of the cycled plate at each pressure is 4 to 6 times that for uncycled material. There was no perceptible correlation between the degree of change and the test conditions (i.e., temperature, discharge rate, etc.). Also, there was about as much variation from point to point on any one plate as there was in the average from plate to plate.

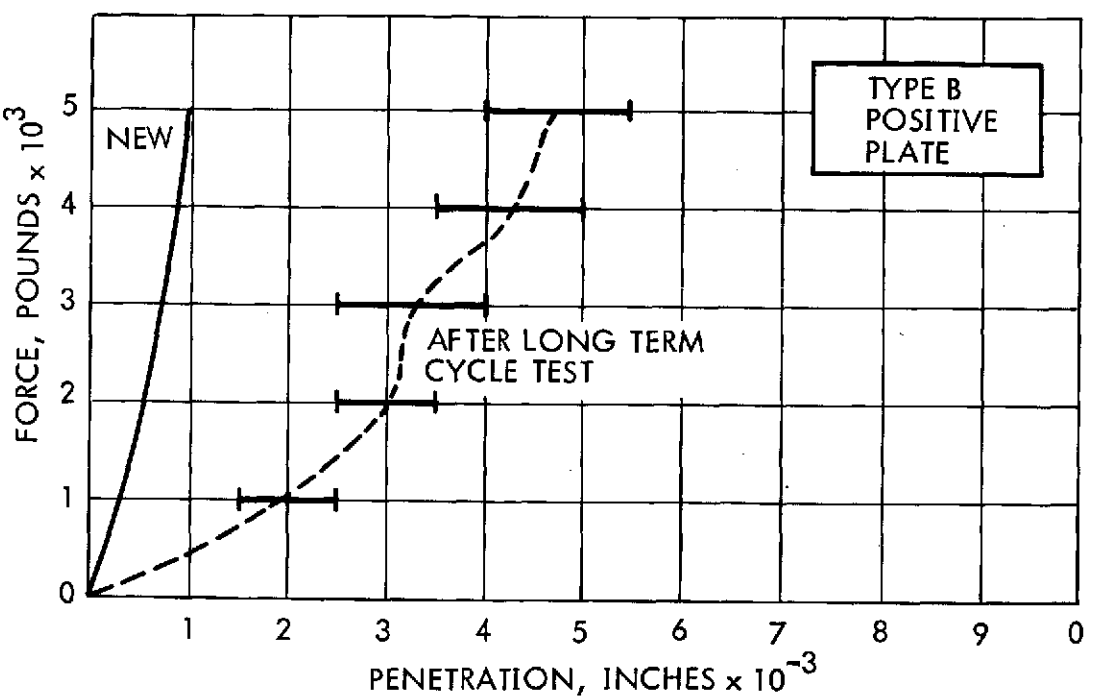

Figure 112. Composite Compression Strength Diagram for Cycled Positive Plates

The decreases in density (from an initial average value of 3.80 g/cm^3) are in most samples about what would be expected for the increase in thickness shown, assuming that there was no change in mass per unit area. This is believed to be the case as nickel compounds are essentially insolveable in the electrolyte and no appreciable loss of particulate matter from the positive plates was observed. A number of densities are well below the expected values, however. The reason for this is not known.

The void fractions, as shown in Table 12, have decreased substantially from the average of 24 percent for new positive plate. Most of the decreases observed may be explained if it is assumed that the internal void volume remains constant as the thickness of the plate increases. This assumption appears reasonable. It has been reported* that the pore size at the surface of positive plates decreases during cycling. Pore size was not measured during the study. This occurrence seems likely in view of the accumulation of material seen on the surface. The resulting decrease in accessibility of electrolyte to the active material internal to the plate would contribute to the general decline in discharge voltage during the test. Note that two of the failed cells have the lowest residual void fractions on the list. Other than that, correlation for individual cells is poor.

The values shown for active material content (expressed as equivalent $Ni(OH)_2$) are all much lower than the 0.18 - 0.25 g/cm^2 range for new plates. As no significant amount of active material was apparently lost by the plates during cycling, the low results shown must be due to a deficiency in the analytical method. This possibility was investigated briefly but no satisfactory reason for the low results was found in the application of the method.

The last column in Table 12 shows that the residual charged nickel active content, expressed as a percentage of the new content of $Ni(OH)_2$, was relatively high, in spite of the fact that all these cells had been discharged to zero volts and then shorted out prior to opening. This much "inactive" charged material, if permanently inactive, would result in a one-for-one loss of usable capacity. It is postulated without proof at

*Private communication - G. Halpert, NASA Goddard Space Flight Center, Greenbelt, Maryland.

this writing that this residual inactive material does not respond to the extraction step of the analysis as does the more active material. Resources did not permit testing this postulate.

Some of the changes shown for negative plates in Table 13 are also significant. Contrary to the popular belief that the negatives do not swell, there was a 10 percent increase in the thickness of the negative plates during the long-term test. This resulted in the decrease in density shown (from the original average of 4.0 g/cm^3). The void fraction data show that there was a significant decrease below that expected from the thickness increase, for cells discharged at the c/2 rate, but a real increase in void volume at the C rate.

The values for cadmium active material in the negative plates are well below those expected. Very few visible cadmium deposits were found outside the plates leading to the assumption that for positive plates, improved procedures may be needed for use with plate materials subjected to heavy and/or long-term cycling.

Thus, the results of a long-term cell test in which over 500 cycles at 80 percent depth of discharge were performed show that a number of changes in the physical characteristics and chemical composition of both positive and negative plates occurred as a result of the cycling. These changes appear to correlate with the general decrease in discharge voltage that occurred during cycling. Many of these changes, such as thickening (expansion of the sinter structure) and decrease in strength, are also those which lead to or are associated with blistering in the body of the plate and disintegration at the edges.

The plate data do not in themselves indicate why certain cells had much lower end of discharge voltages than others at the end of the cycling. The low voltage cells were generally drier than the others, however. The reason for this difference in wetness was not apparent from the data available, except for one cell (Serial No. 14) which began the test with a shortage of electrolyte. Further pursuit of the electrolyte question was beyond the scope of the present program. Investigation of the effect of electrolyte volume and distribution on cell performance is a promising area for further study.

It was originally planned to perform a more detailed analysis of the data such as shown in Tables 11, 12, and 13, to develop more quantitative relationships between the electrical output and the physical and chemical properties. However, such an analysis was not done because the materials analysis task proved more difficult and time-consuming than expected, and the resulting data were sufficiently scattered and uncertain to require further refinement before a mathematical correlation is justified.

7. DISCUSSION

7.1 CHARACTERISTICS OF NEW PLATES

The industry survey made indicated that there was little agreement between different cell manufacturers as to the benefits of, and need for, coining of sintered nickel oxide and cadmium plates for spacecraft cells. This situation may be explained by the great variety of properties and performance characteristics, found during the present study, of commercially available and other state-of-the-art plate materials as received.

For example, the thickness reduction in coined areas on positive places ranged from 10 to 65 percent, uncoined densities ranged from 3.11 to 3.80 g/cm^3, and void fractions from 25 to 39 percent. Similarly, the thickness reductions on negative plates ranged from 18 to 63 percent, uncoined densities from 3.15 to 4.00 g/cm^3, and void fractions from 32 to 51 percent. Relative resistance of plates ranged from 1.03 to 2.20 milliohms for positives and from 0.85 to 2.40 milliohms for negatives.

Another parameter showing great variety is the property referred to herein as compressive strength, and is defined in Section 4.3. As shown in Figures 3 through 9, these data, presented as continuous curves of applied force (actually pressure) versus penetration below the plate surface, provide an easy-to-perceive "picture" of the hardness and ductility of the plate structure near the surface. A gradual slope represents a soft material, while a steep slope represents a hard, unyielding material.

All of the unimpregnated materials were very soft up to penetrations beyond 0.01 inch, as expected. The wide range of slopes and shapes of the curves for positive plates is illuminating. The curve for Type D plate, for example, may indicate that the active material is deposited relatively deep in the pores, leaving the porosity near the surface open. By contrast, the curve for Type B plate suggests that a high concentration of active material is located just below the surface. A more detailed interpretation of the physical properties data presented is beyond the scope of this report. However, it is obvious that no two plate materials are alike, and hence the cells made from these plates

should not be expected to behave the same, especially over a large number of cycles or over a long time period

Less variation is seen in the active chemical content of plates than in their physical properties. The relatively low values of loading obtained for Types D, E, andF may be a function of the analytical method used, as the theoretical capacities per unit area calculated from these data, shown in Table 6, are less than the measured flooded values shown in Table 8. It appears that no one analytical method for determination of active material content of plates is wholly reliable for all types of plates. This suggests a need for further analytical method development if industry-wide standards are to be established and enforced.

The plan view photographs in Figures 10 through 16 are shown mainly to familiarize the reader with the outline and visible surface appearance of the different plates tested. Those aspects visible to the unaided eye are in no way adequate to characterize a plate in a useful manner. In this lies the weakness of relying only on visual inspection of plate material prior to cell assembly in the production of spacecraft cells.

The Scanning Electron Microscope (SEM) shows all plaque to look similar except in some details. The regular distribution of large pores in the Type D material is interesting, and may result from the use of a pore - former during manufacture.

The main difference seen by SEM between SAFT or SAFT-type plates (Types A, B, C, and G) and the others is the presence of apparently flattened peaks of sinter on the former materials caused by compressing and/or wire brushing the material during manufacture. Types D, E, and F plates are not compressed or wire-brushed to the knowledge of this writer.

7.2 MECHANICAL TESTS

The bend test as performed (the results of which are illustrated in Figure 49 through 56) may appear to be excessively severe, but it can be seen that some types of plate tested were able to retain all the sinter material, even though it was traversed with a great many cracks. On the other extreme some materials lost sinter the first time the specimen

was bent out of a plane. The results of compression strength testing and of electrochemical testing correlated strongly with the results of this test, and it is clear that the more pliable, more adherent materials are to be preferred, other things being equal. Thus this test is believed to be meaningful and useful for comparing plate materials for brittleness and adherance.

The tests for brittleness of the sinter and adhesion of sinter to the grid performed show that plate materials made with all-nickel grids are superior in these respects to those made with nickel-plated steel grids. This is particularly the case for adhesion. Although the same degree of cracking of the sinter per se may have occurred in each case for some plates under severe bending conditions, little appreciable detachment occurred from all-nickel grids relative to that which occurred from plated steel. It is suggested that the bond between the plating and the mild steel may be breaking in the latter materials; this interface does not exist in the former type.

7.3 VIBRATION TESTING

The complete lack of mechanical damage visible after vibrating cells in the direction perpendicular to the plane of the plates, even on the more brittle plate materials available, indicates that the separators are able to support and restrain the plates when properly installed and compressed. However, it is conceivable that if the plates are too loose they could undergo higher amplitude vibration and be damaged. On the other hand, if the separators are too tightly compressed, certain high points on adjacent plates may be forced so close together that they touch intermittantly during vibration. If such a cell were charged an arc would be drawn which could quickly burn a hole through the separator, leading to further degradation. Thus it is important to assure that cells are designed and assembled so that the proper balance of separator characteristics are obtained.

7.4 ACCELERATED ELECTROCHEMICAL TESTING

Distinct and repeatable differences correlating with differences in certain physical properties were observed in the degree of edge and other surface damage produced on different types of plates using the

accelerated cycle test developed under this contract. The conditions are quite severe, but a full range of response, from no detectable effect to severe disruption of uncoined edges and blistering was observed on the different materials tested. Those materials that had the greatest surface hardness by the compressive strength test and which were the most brittle by the bend test (Types A, B, and G) showed the most damage at uncoined edges after cycling. The coined edges of Type G positive plate were still attacked to some degree. This is attributed to the fact that the thickness reduction (T.R.) on this plate was only 10 percent. Type A positive plate, with similar physical and chemical properties, but with a T.R. of 34 percent in the coined border, showed no appreciable attack on the edges. Thus it appeared that some minimum T.R. was necessary to achieve the desired degree of protection.

This premise was tested using some older plate material from the supplier of Type G, which had a T.R. of 16 percent in the coined areas. Figure 113 shows a corner of a positive plate of this type after accelerated testing. This area has a coined edge on one side and a non-coined edge along the other side of the corner. The condition of this coined edge was not perfect, but was distinctly better than that of coined edges having only a 10 percent T.R. on this plate.

It is noted that several positive plate materials showed no visible damage from accelerated testing even on an uncoined cut edge. This behavior correlated with the physical properties of greater ductility and adherence to the grid. Thus the need for coining appears not to be absolute, but to depend on the characteristics of the plate. If a sinter is strong yet not brittle, and is strongly adherent to the grid, it may not need coining to have stable edges. Whether or not this is the case cannot be determined a priori, and not by normal inspection methods. Instead, it should be determined by means of a set of tests such as used in the work reported here.

The data in Table 9 show that all positive plate materials tested thickened significantly during accelerated testing. Type E, which thickened the most, was not among the worst showing edge damage, however. Types B and G, which showed the most edge damage, show a percentage

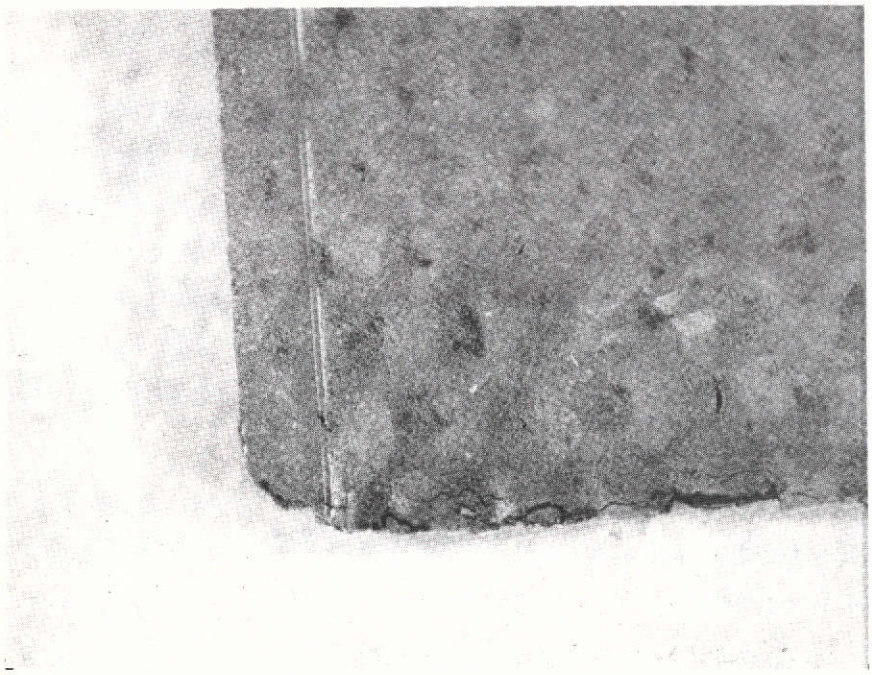

Figure 113. Type G Positive Plate with 16 Percent Thickness Reduction in Coined Edges

thickening that is five times that shown by Type D, for example, that showed no damage. The degree of thickening shown by some of these materials is of concern in another respect, namely, whether such plates will grow to unduly compress the separator in real cells.

7.5 ACCELERATED TESTING OF PLATES IN SEALED CELLS

The affects produced on the plates by two weeks of cycling in sealed cells under "starved" electrolyte conditions were much less severe than from the flooded test, as expected. Three factors are responsible: (1) the amount of electrolyte available is less in the starved cells, thus less is absorbed to promote swelling of positive plates; (2) the plates are confined by the force of compression of the separators; and (3) the degree of gassing was much less.

The lower volume of electrolyte reduces the amount of active material exercised, and also reduces the maximum pressure that builds up in the pores that contributes to expansion of the sinter. The effect of the separators is apparent, but the reason for the effect is not obvious. It would seem that the forces involved in expansion of the sinter structure would be much greater than the restraining forces that could be exerted by the separator, and so the separator should have little effect. This question requires further investigation.

In spite of the differences observed, the different positive plate materials exhibited the same order of susceptibility to attack at the edges as seen in the more rapid, high-rate test.

Testing in sealed cells was not pursued further under this study. It is suggested that a variation on the sealed cell test, wherein the plates would be cycled under normal compression by separators, but under flooded conditions with the cell vented, would produce more rapid yet meaningful results.

7.6 MECHANISM OF PLATE DISINTEGRATION AND SHORTING

The results reported in Section 6 indicate that the mechanism of loss of electrical output in cells may have much in common with the mechanism of disintegration of the sinter structure of plates. More to the point, all these phenomena appear to be part of one overall process of aging of plate material under cyclic stress.

The mechanism of the "growth" and thickening of the positive plate involves the stresses produced by the change in specific volume of the active material between the charged and discharged state. Ultimately these cyclic stresses weaken and begin to break the bonds between adjacent sinter particles in the plate. The deeper the depth of discharge, the more active material charges in volume, and hence the more severe the effects will be.

When this process occurs near the center of the plate area, dimensional changes are minimized by the surrounding structure. When the process occurs at the edge of the plate, there is no restraining force on one side, and excessive expansion and rupture can result. Coining reduces the concentration of active material and the access by electrolyte to the pores in coined areas. The level of electrochemical activity is thereby reduced, and with it the stresses generated.

Shorting of a cell does not occure automatically when sinter breaks off of a plate. It is possible, in fact, for large amounts of loose sinter particles to remain lodged indefinitely in the separator folds outside the boundary of the plate stack without causing a short. However, such particles must come off the extreme outer edges of the plates where they can fall away freely once detatched.

If, on the other hand, a sinter particle becomes loose where it cannot fall away, it will remain wedged between the plates. As the separation distance in most spacecraft nickel-cadmium cells is not more than 0.008 inch, any particle having any diameter greater than this can potentially penetrated the separator and produce a short. As the plates become thicker with use, and they undergo small but significant cyclic dimensional changes during electrical cycling, any loose particle compressed between plates is liable to work its way between the fibers of a non-woven separator layer. Similarly, any non-detatched portion of sinter that is thrust up above the normal surface contour, as by a blister, will exert great pressure on the contacted area of separator, tending toward penetration of the separator layer. Whereas this process can be controlled along the edge of plates by coining, other measures must be used on the plate as a whole. Thus coining should not be considered as a reliable substitute for plate materials that are inherently capable of withstanding the effects of considerable cyclic stress without disintegration.

CONCLUSIONS

Based on the results of the work performed in this study, the following conclusions are made:

1. Coining of sintered nickel and cadmium plates provides edges that are strong and more resistant to damage during handling and more resistant to electrochemical attack than are uncoined edges. The benefits to be derived from coining are much greater on positive than on negative plates, and are much greater on weakly adherent, brittle plate materials.

2. Edge coating (cementing) can provide temporary improvement for handling plates during cell assembly, but is not a reliable substitute for coining for long life or high cycle life applications.

3. Cracking of sinter along cut edges can be greatly reduced by proper coining prior to cutting and cutting only in coined areas. This is particularly important when plates are die-cut by automatic machinery. Although it is less true for hand-cutting, tools must be kept sharp, clean, and finely adjusted to prevent cracking when uncoined plate is cut.

4. The problem of edge damage produced by cutting is minimized when plates are cut to final size before impregnation, and not cut thereafter. This approach is not practical for mass-production however.

5. Not all plate materials need to be coined. The need for coining can be established by short-term accelerated testing in lieu of real time life test experience. A test developed under this study can serve as the basis for a decision to coin or not to coin.

6. A reduction in thickness of at least 33 percent of the uncompressed value appears necessary for adequate protection against mechanical and electrochemical damage of positive plates.

7. If plaque is coined too close to the edge of the coated (sintered) portion of the strip, compression of the outer edge at the top of the plate may not be sufficient to prevent subsequent edge damage due to cycling.

8. Coining and/or edge coating should not be used to "fix" inherently poorly adherent, brittle plate material. Minimum standards for the physical characteristics of the basic plate material should be enforced.

9. Commercially available plate materials are characterized by a relatively high degree of variability in certain key properties. This variability interferes with a uniform approach to control of degradation by mechanical and electrochemical action.

10. Improved methods for analyzing heavily cycled plates for active material content are needed. Presently available methods appear to be inadequate.

11. Positive plates impregnated using the electrochemical deposition process are significantly stronger and resistant to degradation than are plates impregnated by the more conventional acid-immersion/caustic precipitation process.

RECOMMENDATIONS

From the results of this study and the conclusions presented, the following recommendations are made:

1. Plate materials for use in nickle-cadmium spacecraft cells for critical applications should be qualified by testing for strength, self-adhesion, and resistance to disintegration under cyclic electrochemical stress. Mechanical tests involving significant deformation, and electrochemical tests involving multiple cycling and rapid gas evoltuion, are recommended

2. Performance of plate material on qualification tests should be used to determine whether or not plates should be coined.

3. Plate material showing high strength and resistance to cycling need not be coined; however, coining is recommended for extra insurance apainst edge damage. Plate material showing low strength and resistance should be used only after due assessment of risk, and should be coined on all edges.

4. Thickness reduction by coining should be not less than 33 percent of the original uncoined thickness at all points.

5. Positive plates should not be cut on uncoined areas after final formation cycling.

6. All edges should be edge coated prior to formation cycling and again after final drying following formation.

7. More adherent, longer-lasting edge-coating materials and improved coating processes should be developed.

8. Further work on test methods for plate materials should be done to improve the practicability and reliability of the tests.

9. Improved methods for analyzing cycled plates for active material content should be developed.

10. Increased emphasis should be placed on development and commercialization of the electrochemical impregnation process for plates for spacecraft cells.